GEOMORPHOLOGY OF THE HUECO BOLSON IN THE VICINITY OF THE PROPOSED LOW-LEVEL RADIOACTIVE WASTE DISPOSAL SITE, HUDSPETH COUNTY, TEXAS

by

Robert W. Baumgardner, Jr.

Assisted by

Arten J. Avakian

Final Contract Report

Prepared for

Texas Low-Level Radioactive Waste Disposal Authority
under Interagency Contract Number IAC(90-91)0268

by

Bureau of Economic Geology
W. L. Fisher, Director
The University of Texas at Austin
Austin, TX 78713

February 1990

CONTENTS

Figures

Tables

Plates (in pocket)

ABSTRACT

The Fort Hancock study area is located 40 mi (65 km) southeast of El Paso, Texas, in the Hueco Bolson on an alluvial slope between the Diablo Plateau and the Rio Grande. The study area spans the drainage divide between Alamo and Camp Rice Arroyos. Since deposition of bolson fill ceased, the arroyos have incised, cutting down to expose the Fort Hancock and Camp Rice Formations in their floors and valley walls.

Quaternary strata younger than the Camp Rice Formation underlying the study area can be divided into four units: a basal gravel, a middle sand, a petrocalcic horizon (Stage IV), and an upper sand. The petrocalcic horizon is interpreted to be the upper surface of the Madden Gravel, and, on the basis of its dense, laminated character, took 25,000 to 75,000 yr to form. These Quaternary sediments range in thickness from 20 to 60 ft (6 to 18 m), thinning to the southwest across the study area and toward the edges of arroyos.

The general trend of incision of arroyos has been interrupted periodically by alluviation. At present, remnants of weakly consolidated alluvial fill, 400 to 1,330 yr old, are being removed from the arroyos and their tributaries by headward migration of nickpoints. Rates of headcut retreat in alluvial fill during the last 1,330 yr vary from 0.1 to 5.2 ft/yr (0.04 to 1.6 m/yr). These long-term rates are much lower than modern rates of retreat (7.2 to 27.2 ft/yr [2.2 to 8.3 m/yr]), which are based on interpretation of aerial photographs covering a 44-yr period. For the same time, most headcuts on petrocalcic horizons have not retreated by a measurable amount. At one location where runoff is concentrated, the average rate of headcut retreat has been 3.3 ft/yr (1.0 m/yr), which is lower than all modern rates of retreat in alluvial fill in this study. Vertical accretion rates for the surface of the study area have averaged 0.009 inch/yr (0.24 mm/yr) for the last 1,440 yr. Prior to 7,000 yr ago, accretion rates were about 10 times faster. This change in accretion rates coincides roughly with the onset of drier climatic conditions about 8,000 yr ago. The mean value of data from erosion pins (0.04 inch [1 mm] deposition) shows that the ground surface was largely

1

unchanged during the study. Most sediment transport is a result of runoff from intense rainfall, which occurs infrequently. The most intense storm recorded during the study was a 0.5-hr, 1.3-inch (34-mm) storm with a 25-yr recurrence interval. Archeological evidence indicates that parts of the surface of the study area have been stable for at least 900 yr.

The surface of the study area slopes toward the southwest at about a 1 percent grade. The surface is composed of several landforms, primarily low-relief interfluves between ephemeral stream channels. Coppice dunes are present locally, especially on the south half of the study area. Gravel-covered topographic highs and uplands compose a small part of the study area.

Three surface fissures have formed in the study area, and an inactive, relict fracture has been exposed in a 20-ft (6-m) deep excavation there. The fissures are composed of aligned surface-collapse features that are as much as 4.4 ft (135 cm) deep and 5.1 ft (157 cm) wide. The collapse features form via enlargement of tension fractures by erosion and piping. Uneroded tension fractures are typically 0.8 to 1.6 inches (2 to 4 cm) wide and filled with sediment. Locally, openings in fractures extend horizontally as much as 2 ft (60 cm), but most are less than 4 inches (10 cm) across. The origin of the fractures is unclear, but the tensional stress that causes them to form may result from differential compaction of unconsolidated sediments over bedrock irregularities or abrupt facies boundaries. Similar fissures, natural and man-induced, have been reported throughout the desert Southwest from California to Texas. There is no evidence of fault movement on fissures at the study area.

STRATIGRAPHY AND PALEOCLIMATE

The study area for a proposed low-level radioactive waste repository is located in the Hueco Bolson, a Basin and Range graben, about 40 mi (65 km) southeast of El Paso, Texas. The area is centered along the drainage divide between two arroyo basins that slope to the southwest from the Diablo Plateau to the Rio Grande (fig. 1). Until about 600,000 yr ago the Hueco Bolson was

filling with fine-grained sediment that composes the Tertiary Fort Hancock Formation and with coarser sediment of the Tertiary-Quaternary Camp Rice Formation.

Stratigraphy

The following description of strata underlying the Hudspeth County study area is based on outcrops along the valley walls of arroyos south and west of the study area (fig. 2), on several cores taken from boreholes at the proposed site (pl. 1 and 2), and on exposures in trenches on the proposed site (figs. 3 and 4). In most boreholes only cuttings were recovered from the uppermost 40 ft (12 m); hence, descriptions of these near-surface strata are less complete than those based on whole core. However, exposures in trenches in the study area and along arroyo valley walls provide substantial information about the composition of these strata.

Camp Rice and Fort Hancock Formations

Although the Camp Rice and Fort Hancock Formations have similar lithologic characteristics, they can be distinguished in the vicinity of the study area. The Fort Hancock Formation can be identified in outcrop and in core by its high silt and clay content (often greater than 80 percent) and dark reddish-brown color (5YR 3/4 to 5YR 4/3, dark reddish-brown to reddish-brown). Pedogenic slickensides on fractures are present in outcrop and in core. In outcrop the silty clay layers (fig. 2, units 9, 11 and 13) in the formation weather to form convex slopes between sandy interbeds (fig. 2, units 10 and 12). The clayey outcrops develop a crumbly "popcorn" texture as they weather. Hard carbonate nodules are found in the upper parts of most outcrops, and gypsum crystals are present locally on fracture surfaces (fig. 2, unit 7). The Camp Rice Formation is sandier than the Fort Hancock and lighter colored (typically 5YR 6/4 to 5YR 8/4, light reddish-brown to pink). Locally, it contains clean (less than 5 percent silt and clay), structureless, fine to very fine sand. Carbonate nodules in the Camp Rice Formation usually are not as well-developed

as those in the Fort Hancock Formation. The contact between the two formations is obscure in core where sandy and clayey strata are interbedded or in intervals where no core was recovered. In this study, the highest clay bed was selected as the top of the Fort Hancock Formation. The top of the formation is at about 4,024 ft (1,226 m) (fig. 2) to 4,077 ft (1,243 m) (pl. 2) elevation in the valley walls of Camp Rice Arroyo south of the study area, and at 4,048 ft (1,234 m) in the valley walls of Alamo Arroyo west of the study area (pl. 2). More detailed information about the stratigraphy and depositional systems of bolson sediments is available in Gustavson's (1990) report on these two formations.

The contact between the Camp Rice Formation and the overlying Quaternary sediments is recognized in outcrops as an eroded surface overlain by gravel (fig. 2). This surface is difficult to identify in core because recovery of gravel layers is commonly poor. Therefore, they probably are underrepresented in cores and cuttings. As a result, in this report the lowest layer composed of more than 50 percent gravel is defined as the base of Quaternary sediments younger than Camp Rice. By this definition, the base of Quaternary sediments is subparallel to the ground surface, and the Camp Rice Formation is truncated by erosion beneath the west half of the study area (pls. 1 and 2).

These observations are supported by outcrop studies. There are no sandy or gravelly strata of the Camp Rice Formation in Alamo Arroyo west of the study area (pl. 2), whereas there are almost 13 ft (4 m) of sand (Camp Rice Formation) overlying the Fort Hancock Formation in Camp Rice Arroyo, south of the study area (fig. 2).

Quaternary strata

Quaternary sediments at the study area are composed predominantly of silty, clayey sand. Where gravel was recovered in core, it was usually in layers less than 2 ft (30 cm) thick. Gravel layers are locally present throughout the Quaternary section, but in some cores gravel content decreases with depth (pl. 2, wells 77 and 79). In well 38 (pl. 1), near the north boundary of the

study area, gravel was recovered throughout a 46-ft (14-m) interval, but lithologies in zones of poor recovery are unknown. In outcrops along valley walls, sandy gravel layers as much as 6.6 ft (2 m) thick are common. In the walls of the trenches at fissure 1, the composite gravel layers are as much as 13 ft (4 m) thick and 130 ft (40 m) wide. These gravel layers are composed of many individual channel deposits, which are usually about 3.3 ft (1 m) thick and 8.2 ft (2.5 m) wide, and are interpreted as coarse channel-fill deposits of braided streams. Paleoflow directions of the gravel lenses in outcrop, indicated by pebble imbrication, vary from southwest in Camp Rice Arroyo to northwest in outcrops along Alamo Arroyo. These correspond roughly to the directions of flow in modern-day channels.

Near the northern edge of the study area (well 38, pl. 1), Quaternary alluvium overlying older bolson sediments is 59 ft (18 m) thick. Near the southern edge (fig. 2; pl. 1, well 72), these sediments are less than 20 ft (6 m) thick. Along an east-west line from well 78 to well 79 (pl. 2) the sediments are about 23 ft (7 m) thick. They thin to 10 ft (3 m) or less near the arroyos, and locally they are completely eroded along valley walls of Alamo Arroyo.

The Quaternary fluvial sediments exposed in outcrops can be divided into four parts: a basal gravel, a middle sand unit, a strongly cemented upper sand or gravel, and an uppermost layer (locally absent) of silty, clayey sand. Locally the fine-grained bolson sediments are eroded and covered with sandy gravel on an abrupt, irregular contact. The basal gravel layer ranges in thickness from about 1.6 to 7.9 ft (0.5 to 2.4 m). Gravel is predominantly gray limestone (Cretaceous Finlay Limestone), with uncommon cobbles of yellowish sandstone (Cretaceous Cox Sandstone) and some reworked carbonate nodules. The color of the limestone pebbles gives the outcrops a gray hue, but the sandy matrix can be lighter (5YR 8/4: pink). Sandy interbeds as much as 1.6 inches (4 cm) thick and 7.9 ft (2.4 m) wide are present locally in this unit. Sedimentary structures include low-angle trough crossbeds, tabular crossbeds, and horizontal beds. Gravel clasts measure as much as 10.6 inches (27 cm) in diameter, but most range from 0.4 to 1.2 inches (1 to 3 cm). Dimensions of channel-fill deposits and grain size of sediments seen in outcrop are similar to those found in present-day channels in the area.

The middle part of most Quaternary sections is a layer of silty sand, and the lower contact can be abrupt or gradual. Low-angle crossbeds are preserved locally. The sand is cemented with calcium carbonate, which ranges from being dispersed throughout the horizon to being concentrated in indurated nodules. Color ranges from 5YR 3/4 to 5YR 6/4 (dark reddish-brown to light reddish-brown).

A strongly cemented silty sand or gravel overlies the middle sand. The color of the sand is lightened by the carbonate cement to white (5YR 8/1). Locally, two carbonate-cemented (petrocalcic) horizons are present within 16.4 ft (5 m) of the surface (fig. 3; pl. 3). Carbonate cement decreases downward from the top of both units, which are eroded and overlain by sand and sandy gravel. In upper parts of both cemented horizons, where they are sandy, the cement is horizontally laminated, with layers as much as 0.8 in (2 cm) thick containing individual laminae 0.008 in (0.2 mm) thick. The amount of carbonate cement in each horizon varies, but locally they are indurated and dense, and vertical faces and fractures are coated with carbonate. These characteristics of cementation typify a Stage IV pedogenic calcrete (Machete, 1985).

These calcretes, separated by sand and gravel deposits that were laid down by streams, represent two different periods of landscape stability. These periods, represented by the well-developed calcretes, are separated by sediments that were deposited during an interval when streamflow on this surface probably was more frequent. The upper petrocalcic horizon is interpreted to be the Madden Gravel surface on the basis of its degree of development, its apparent lateral continuity across the study area, and its topographic position higher than other gravel-capped surfaces along the major arroyos. This horizon has been cut out locally by streams, which are represented by coarse-grained gravel deposits (fig. 4).

The upper calcrete is overlain by unconsolidated sediments of variable thickness. Throughout most of the study area, these sediments are less than a meter thick. The relatively shallow depth of burial on this surface, which slopes more than 230 ft (70 m) over a distance of 5.4 mi (8.8 km) northeast to southwest across the study area, indicates that the carbonate-rich horizon formed on a land surface subparallel to the current one.

These unconsolidated near-surface sediments compose the fourth and youngest component of the Quaternary sequence at the study area. They are best exposed in trenches that were excavated near the center of the study area (fig. 3). On the basis of texture and sedimentary structures, the sediments overlying the uppermost calcrete can be divided into three subunits:

(1) The lowest is a layer of massive, gravelly, muddy sand that overlies the petrocalcic horizon. Its upper contact is abrupt and relatively flat (figs. 4 and 5).

(2) Overlying the lowest subunit is a layer of sandy silt to silty sand, with small-scale, low-angle trough crossbeds. Its upper contact is gradual and irregular and cannot be traced uniformly throughout the exposures in the trenches. The contact is marked by an upward decrease in the number and lateral extent of crossbeds.

(3) The third subunit has no crossbeds and is slightly finer grained than either of the two underlying subunits. It is predominantly sandy mud or sandy silt with some slightly gravelly, muddy sand locally.

These strata have radiocarbon ages ranging from 1,440±80 yr B.P. about 10.6 inches (27 cm) below the surface to 7,510±100 yr B.P. (all corrected for $\delta^{13}C$) at about 20 inches (50 cm) above the petrocalcic horizon (fig. 6). Details of the technique used for dating are available in White and Valastro (1984) and Haas and others (1986). These are bulk samples of organic residues from the sediments; consequently, they represent the average age of organic matter in each sample. The horizon that is dated 1,440±80 yr B.P. is covered with only 10.6 inches (27 cm) of younger sediment. Apparently, the ground surface at this location has been aggrading slowly for about the last 1,400 yr.

A snail shell was collected 5.6 ft (1.7 m) below the ground surface in the southeast wall of trench 4, from the fine sandy crossbedded unit that overlies massive gravelly sand (fig. 5). It is a *Hawaiia neomexicana* (identified by Dr. Raymond Neck, Texas Parks and Wildlife Department). Snails of this species are extant in the region today (Metcalf, 1984), and their shells have been collected from the surface at the study area. They are adapted to protected sites with reduced

desiccation stress, such as decaying leaf litter or the underside of rocks or wood (Raymond Neck, written communication, 1989).

On the basis of similarities in radiocarbon ages from this and the Organ geomorphic surface in southern New Mexico, and on similarities in their positions relative to other geomorphic surfaces, the study area is interpreted to be on the Organ geomorphic surface. This is the youngest major depositional surface of the post-Camp Rice sequence (Gile and others, 1981). The bulk of Organ alluvium accumulated between 6,400 yr B.P. and 2,200 yr B.P. (Gile and others, 1981). Similarly, most alluvium above the petrocalcic horizon at the study area accumulated between about 7,510 yr B.P. and 1,440 yr B.P. (fig. 6).

Accretion rates of the sediments that overlie the petrocalcic horizon have been calculated on the basis of these radiocarbon dates (table 1). Accretion rates range from 0.007 to 0.08 in/yr (0.18 to 2.08 mm/yr). There is a marked change to lower rates after 7,010±200 yr B.P. (table 1). Only one data point is available for the older materials, but the decrease in accretion rate is borne out by the presence of primary sedimentary structures in the oldest dated horizon (fig. 6). These sediments accumulated and were buried rapidly enough to protect the sedimentary structures from bioturbation. Younger deposits accumulated more slowly. During periods of landscape stability these fine-grained materials were burrowed, penetrated by roots, and probably reworked by eolian processes. The decrease in accretion rate may be a function of change in climate toward drier conditions, which occurred about 8,000 yr ago (Van Devender and Spaulding, 1979).

Paleoclimate

During the Wisconsinan Full-Glacial Period, about 25,000 to 14,000 yr ago, the climate of the southwestern United States was cooler and moister than it is now (Hall, 1985). In the Late Glacial Period, 14,000 to 10,000 yr ago, climatic conditions became warmer and drier (Hall, 1985), and a transition from glacial to post-glacial vegetation occurred throughout the Southwest. Xeric woodlands of juniper or juniper and oak persisted until about 8,000 yr ago in the deserts of

the Southwest (Van Devender and Spaulding, 1979). By then, however, woodland species in the lowlands were replaced by grass (Van Devender and Spaulding, 1979). Woodlands still existed in the Hueco Bolson east of El Paso from 8,000 to 4,000 yr ago, when they were replaced by grass (Horowitz and others, 1981).

According to Van Devender and Spaulding (1979), the present-day climate and vegetation of the southwestern United States, with short-lived variations, have been established since about 8,000 yr ago. However, Markgraf and others (1984) set 5,000 years ago for the establishment of the modern climate in the San Agustin Plains of New Mexico, about 150 mi (250 km) northwest of El Paso.

From about 4,500 to 3,000 yr ago the climate in the study area was moister than it is today (Horowitz and others, 1981; Hall, 1985). Freeman (1972) studied pollen in the Organ alluvium in Dona Ana County, New Mexico, 30 mi (50 km) north of El Paso. He described a transition from desert shrub to grass that began between 5,000 and 4,000 yr ago. This represented an increase in available soil moisture. Grassland and shrubland alternately dominated in the Hueco Bolson east of El Paso (Horowitz and others, 1981). The climate began to dry again about 2,200 yr ago (Freeman, 1972) after a cooler, mesic interval 2,500 yr ago (Bryant and Holloway, 1985). Between 1,700 and 1,500 yr ago, soils were eroded and desert shrub was established in the northern Chihuahuan Desert, which includes the study area (Van Devender and Spaulding, 1979). According to Van Devender and Spaulding (1979), this is the most recent major vegetational change in the Southwest induced by climate. This period of soil erosion may be represented in the study area by the sharp contact at the base of a soil horizon that has a radiocarbon age of 1,440±80 yr (fig. 6).

From 1,000 to 500 yr ago, climate in the Hueco Bolson east of El Paso was moister than at present (Horowitz and others, 1981). Since then, the climate has become drier, except for a brief period of above-average tree growth and luxuriant grass cover lasting from about A.D. 1610 to 1660 (Horowitz and others, 1981).

The oldest dated sediments overlying the petrocalcic horizon in the study area have a radiocarbon age of 7,510±100 yr (table 1). This age corresponds approximately to the establishment of modern climatic conditions about 8,000 yr ago, as reported by Van Devender and Spaulding (1979). These data indicate that most of the Quaternary sediments overlying the petrocalcic horizon at the study area have accumulated within the last 7,500 yr under climatic (and probably hydrologic) conditions similar to those that currently prevail. However, the sediments did not accumulate uniformly or without interruption. The gravelly channel-fill deposits that are cut into these strata (fig. 4) and into the petrocalcic horizon below are evidence that deposition and erosion occurred episodically throughout this period on this surface.

At present, alluvial-fill deposits in arroyos near the study area are being eroded. Two of these deposits have been radiocarbon-dated (fig. 7). The ages of these terrace deposits (920±70 and 1,330±60 yr B.P.) bracket the age (1,130±90 yr B.P.) of wood found at the base of a gully fill in southern Jornada del Muerto Basin, New Mexico (Freeman, 1972). This suggests that filling of gullies and arroyos occurred throughout the Rio Grande valley in western Texas and southern New Mexico from about 1,330 to 920 yr B.P. Since then these alluvial deposits have been incised.

Determining whether incision in the study area is related to changes in climate in the last 900 yr, to changes in land use in the last 100 yr, or to some other cause is beyond the scope of this study. It has been established that a period of pronounced arroyo development began in the southwestern United States in the second half of the 19th century (Bryan, 1928; Antevs, 1952), but the causes for this period of regionwide incision are not completely understood. Several conditions have been proposed, which have been arranged into three groups: random frequency-magnitude variations, secular climatic changes, and human land-use changes (Cooke and Reeves, 1976). Short-term changes in climate and vegetation, and changes in land use that affect valley-floor soils, can contribute to arroyo development, but the relative importance of these conditions varies from place to place. Concluding their summary of the extensive literature on arroyos, Cooke and Reeves (1976, p. 189) succinctly observed that "similar arroyos can be formed in different areas as a result of different combinations of initial conditions and environmental changes." The

evidence of recent vegetation and land-use change in the study area is presented in the following section.

GEOMORPHIC HISTORY

Since the end of Camp Rice deposition in middle Pleistocene time, the Rio Grande has incised the bolson fill, possibly in response to a drop in base level due to climatic changes related to global glacial cycles (Gile and others, 1981). The evidence of cyclic stability and incision by the Rio Grande is the "stepped sequence of graded surfaces located between the valley floors and the...piedmont slopes" in southern New Mexico (Gile and others, 1981, p. 48). In the study area, surfaces probably equivalent to those described in southern New Mexico are found within the valleys of the major arroyos (Collins and Raney, 1990). Thus, these arroyo basins began to develop soon after the first cycle of incision on the Rio Grande.

During the filling of the Hueco Bolson and the period of cyclic downcutting on the Rio Grande, normal fault movement was occurring on the Campo Grande fault (fig. 1) (Collins and Raney, 1990). This fault is subparallel to the axis of the Rio Grande valley and is approximately perpendicular to the axes of the major arroyos that drain the northeastern side of the bolson near the study area. The fault bisects the arroyo basins about halfway between the Rio Grande and the Diablo Plateau. During normal fault movement the southwest side of the fault moves down relative to the northeast side.

Incision by the Rio Grande and movement on the Campo Grande fault enhanced downcutting in these arroyos. Fault movement would have enhanced incision only upslope from the fault as streams adjusted to the newly steepened topographic slope at the fault by downcutting upstream. However, base-level change on the Rio Grande would have affected the entire arroyo basin. Dropping base level on the river would have caused episodes of incision, thus reestablishing new profiles on the arroyos that were graded to the new, lower base level. The amount of incision on the arroyos that can be attributed specifically either to fault movement or to downcutting on the Rio

11

Grande is not known. However, because older stream terraces along the arroyos can be correlated upstream and downstream from the fault, downcutting on the Rio Grande probably is more important than fault movement in controlling major episodes of incision and terrace development on the arroyos. Fault movement probably initiated localized and/or short-lived episodes of downcutting.

According to Gile and others (1981, p. 48), the evolution of the Rio Grande valley in southern New Mexico and western Texas includes the following stages: (1) excavation of the axial valley and at least the lower segments of tributary valleys during waxing and full-glacial intervals; (2) deposition during waning glacial and early interglacial times; and (3) relative stability during the remainder of a given interglacial interval. According to this scenario, the Rio Grande is now in a period of relative stability, which should persist until the onset of a climatic change to wetter conditions, when valley excavation will recur and the arroyos will probably incise again. However, within that context of relative stability the arroyos may undergo geomorphic changes that are unrelated to base-level change on the Rio Grande or to faulting. Natural processes of meander cutoff, stream capture, and oversteepening due to deposition can cause changes in erosion and deposition. Furthermore, dam construction or destruction and changes in land use and sediment yield affect stream behavior. The record of some of these processes is partially preserved in the terrace deposits along the arroyos. These deposits and channel networks, evidence of past geomorphic activity, are described next.

Erosion and Deposition in Arroyos

Three major arroyos are present near the study area on the northeast side of the Rio Grande (fig. 1). In general, the recent history of the arroyos upstream from Campo Grande fault has been one of continual downcutting interrupted by short periods of alluviation, as shown by (1) unpaired, low terraces overlying the Fort Hancock Formation along the arroyos, (2) exposure of the Fort Hancock Formation in the floor of Alamo Arroyo and its tributaries upstream from the

fault, and (3) ongoing removal of alluvial fill in the upper reaches of Alamo and Camp Rice Arroyos by upstream migration of headcuts.

Typical of these deposits is a cross profile in the Alamo Arroyo basin 0.5 mi (0.8 km) upstream from the Campo Grande fault (fig. 8), which depicts three unpaired, low terraces. All three terraces are thought to be relatively young because of their low height above the stream and the absence of well-developed calcic horizons that are characteristic of higher, older terraces. The three terrace levels are at unequal heights (unpaired) above the present stream. The fluvially deposited sediments are less than 6.6 ft (2 m) thick and lie unconformably on top of the Fort Hancock Formation, not on older alluvial fill. This arrangement of relatively thin sediments directly overlying much older bolson sediments at heights that alternate across the stream is the result of downcutting by the stream as it meandered several times across its valley, leaving overbank and channel deposits behind. This mode of terrace development is significant because it suggests that during the recent geologic past, downcutting has been the dominant stream process in this basin. Two other observations support this conclusion: exposure of Fort Hancock strata and removal of alluvial fill. The Fort Hancock Formation is exposed locally in channel floors throughout the Alamo Arroyo basin upstream from the Campo Grande fault. No thick layer of alluvial fill underlies the channel floor, indicating that the channel is at its lowest level of incision. Where alluvial fill is present, as in the upper reaches of Alamo and Camp Rice Arroyos and in some valley-side gullies, it is being eroded as nickpoints migrate headward.

These deposits accumulated during a brief period of alluviation that ended less than about 400 to 1,300 yr ago. This time for the end of alluviation is based on the ^{14}C ages of organic material in low terraces along tributaries of Alamo Arroyo. Carbonized wood from a 5.7-ft-high (1.75-m) terrace (fig. 7, location A) has been radiocarbon-dated at 920 ± 70 yr B.P. Alluvial fill from a 7.7-ft-high (2.35-m) terrace in the arroyo just west of the study area (fig. 7, location C) has been radiocarbon-dated at $1,330\pm60$ yr B.P., age-corrected for $\delta^{13}C$. The date was obtained on the humic acid fraction of the organic humates in a sandy, silty, clayey organic layer. The dating technique is described by White and Valastro (1984) and Haas and others (1986). This date is the

mean residence time of organic matter in the soil and indicates that organic matter in this deposit began to accumulate at least 1,330 yr ago. The time of onset of accumulation is not known; hence, the mean residence time is taken as the minimum age of deposition of this alluvium. The organic layer is part of the alluvial fill, 4.9 ft (1.5 m) thick locally, which unconformably overlies older bolson (Fort Hancock Formation) sediments. At present, the organic layer is exposed upstream and downstream for a total distance of about 130 ft (40 m) on both sides of the incised channel. The organic horizon accumulated on a relatively flat, gently sloping surface within the arroyo valley.

In this arroyo, as in others, alluvial deposits can be traced upstream along the arroyo onto the low-relief alluvial slope between the main arroyo valleys. There, the alluvial fill covers the bottoms of shallow swales where ephemeral streams flow across the alluvial slope. The alluvium probably was once a continuous deposit, extending from the alluvial slope down into the arroyo at an angle slightly greater than that of the present arroyo slope. Now this alluvial package is being excavated near the upper end of this arroyo where a 10-ft-high (3-m) nickpoint marks the eroding edge of the alluvial fill. Because alluvial fill throughout the study area is being incised by headward-advancing nickpoints, it is possible that climate is the cause of this widespread change from alluviation to incision.

Climate of the Hueco Bolson became increasingly drier beginning about 500 yr ago (Horowitz and others, 1981), and there is evidence in southern New Mexico of a severe, short-term drought that began about 500 yr ago and lasted about 50 yr (Hall, 1985). More recently, desert shrub vegetation expanded in the Hueco Bolson near El Paso between 1835 and 1905, reportedly as a result of drought and overgrazing (Horowitz and others, 1981). These shifts in climate may have induced erosion of the alluvial fill that had accumulated previously. It is not known to what extent livestock grazing in the study area has affected vegetation cover there.

Drainage Pattern Change

Stream capture may have enlarged Alamo Arroyo basin upstream from the Campo Grande fault at the expense of Camp Rice Arroyo. Alamo Arroyo is the widest of the three basins and has the largest drainage area upstream from the fault (fig. 1). The width of Alamo Arroyo basin increases about 4.5 times upstream from the fault, from 0.9 to 4 mi (1.4 to 6.4 km), with more than 75 percent of this expansion toward Camp Rice Arroyo. The main channel of Camp Rice Arroyo flows close to the drainage divide between the two arroyos, at one point less than 2,400 ft (730 m) away. This suggests that Pear Canyon (fig. 7), which is adjacent to Camp Rice Arroyo and now drains into Alamo Arroyo, previously may have been part of the Camp Rice Arroyo drainage system. The tributary from Pear Canyon that now flows into Alamo Arroyo makes a sharp 55-degree change in direction from S42°W to N83°W within 2,600 ft (790 m) of the drainage divide between the two arroyos. Further evidence of possible stream capture is furnished by short, relatively deep valleys between Alamo Arroyo and Camp Rice Arroyo (fig. 7). They are not currently connected to drainage networks upslope, but in the past they may have carried overland flow into Camp Rice Arroyo from Pear Canyon or from the area now lying between the two arroyos. They may have been beheaded by a tributary of Alamo Arroyo that migrated eastward and captured their headwaters.

The Campo Grande fault has affected basin development. The drainage networks of all three arroyos expand abruptly upslope at or near the Campo Grande fault (fig. 1) as a result of normal fault movement and readjustment of the drainage system in each arroyo. Nickpoints were created by surface rupture events where the fault crosses each arroyo. These nickpoints migrated upstream until new profiles were established. This headward advancement of erosion up the drainage network eventually reached the lower order streams. Extending upslope until they occupied the entire drainage basin, these lower order streams eliminated unintegrated areas between the basins.

Downslope from the fault, where the arroyo base level is unaffected by fault movement, arroyo basins are narrower, with fewer lower order tributaries (fig. 1). There are areas between the basins—mostly between 3,550 and 4,000 ft (1,082 and 1,220 m) elevation—that are still not integrated into the drainage system of the major arroyos. These interarroyo areas are underlain by the Camp Rice Formation and covered with coppice dunes. Upslope from the fault the interfluves are much narrower than they are downslope from the fault (fig. 9). Alamo Arroyo has cut the deepest valley at the fault, and more Fort Hancock Formation is exposed at the surface upstream from the fault due to faulting as well as to headward migration of tributaries directly up the alluvial slope toward the Diablo Plateau. In addition, gravity data show that throw on the Campo Grande fault is greater at Alamo Arroyo than farther to the southeast (Keller, 1990). This means that the base level of Alamo Arroyo may have been dropped by fault movement more than base levels of the other two arroyos were and that the Fort Hancock Formation may be closer to the surface of the footwall block here than farther to the southeast. Clay- and silt-rich outcrops in the Fort Hancock Formation are almost unvegetated, leaving surface materials unprotected during high-intensity rainfall. The fine-grained sediments are more coherent than sandy sediments in younger formations; therefore, more rills can form per unit area where Fort Hancock Formation is exposed. These precursors to low-order streams collect runoff and expand the drainage network, narrowing the undissected interarroyo drainage divides. This process eventually leads to higher drainage density.

Drainage Network Differences

Drainage density is a measure of the length of stream channels per unit area of land (Horton, 1932). For this study, drainage density was measured on the extended blue-line network of streams shown on 1:24,000-scale USGS topographic maps. The blue lines were extended upslope to the highest V-shaped topographic contour. The resulting network was then checked against larger scale (1:13,680) aerial photos, and drainage density was determined using the line-

16

intersection method described by Mark (1974). Because many variables affect drainage density, including climate, erodibility of substrate, basin relief, and vegetation cover (Gregory and Gardiner, 1975; Ritter, 1978), drainage density can be used to describe the interaction between these variables.

A previous study showed that mean drainage density and total stream length in a basin were highly positively correlated ($r\geq.96$, $p\leq.02$) with various measures of discharge in intermittent streams in northwestern Texas and northeastern New Mexico (Baumgardner, 1987). This relationship suggests that, under similar conditions, areas with higher drainage density will have higher discharge than areas with lower drainage density. This correlation is easily understood because in high-drainage-density areas, runoff travels shorter distances before being collected into channels and is therefore more quickly concentrated and moved downslope, resulting in higher discharge.

The arroyo basins near the study area can be divided into five zones on the basis of drainage density (fig. 10; table 2); from lowest to highest drainage density, these zones are Diablo Plateau, alluvial slope, scarp, area below the fault, and dissected surface above the fault. Drainage density varies from a low value of 2.9 mi/mi^2 (1.8 km/km^2) to a high value of 19.9 mi/mi^2 (12.3 km/km^2).

The relatively high drainage density and high local relief of the escarpment upslope from the alluvial slope indicate that rainfall on the escarpment will be collected in channels and conveyed downslope relatively quickly. As runoff reaches the alluvial slope, where channels are not deeply incised and where drainage density and slopes are lower, the volume of runoff from large storms may exceed the capacity of the channel network and spread out of the poorly defined ephemeral channels, covering wide areas of the alluvial slope with a thin sheet of water. Flooding potential of the study area is discussed in detail by Akhter and others (1990).

The study area is on the alluvial slope that lies between the Campo Grande fault and Diablo Plateau (fig. 10). The surface slopes away from the Diablo Plateau at about 55 to 65 ft/mi (10 to 12 m/km). The topographic contours on this surface are slightly convex in a downslope direction. Convex slopes tend to disperse overland flow, rather than concentrate it into channels, and as a

result, drainage density tends to remain low on these surfaces. Drainage density values on the alluvial slope are lower than anywhere else in the arroyo basins except on top of Diablo Plateau (fig. 10).

This measure of long-term interaction between substrate, climate (especially rainfall), basin relief, and vegetation cover, indicates that the alluvial slope where the study area is located is relatively inactive compared with other parts of the arroyo basins. As the dissected zone above the Campo Grande fault expands, the areal extent of the alluvial slope will be reduced. The rates at which drainage networks have grown headward in the historical and recent geological past provide an estimate for future rates. These rates and the variables that affect this expansion—substrate, climate, and vegetation—are discussed in subsequent sections of this report.

Landforms in the Study Area

The surface of the study area has nine types of natural landforms that can be distinguished by their shape, local relief, elevation and position relative to other landforms, vegetation cover, and grain size of surficial sediments (fig. 11; table 3). Landforms were mapped on aerial photographs at a scale of about 1:13,680, then checked in the field by describing the vegetation, surficial sediments, and local topography at surveyed locations in the study area.

The study area probably was once predominantly grassland (Horowitz and others, 1981). According to Branson (1985), the vegetation on much southwestern semidesert range has shifted from grass to brush since livestock ranching began there. Branson's conclusions are based on a survey of scientific literature about vegetation change on western rangelands. The primary invaders of grassland in this region are mesquite (*Prosopis glandulosa*) and creosote bush (*Larrea tridentata*). Their propagation is fostered by overgrazing (which disperses seeds and contributes to destruction of the A soil horizon), drought, and, possibly, a decrease in range fires. Some research cited by Branson showed that conversion of desert grassland to desert shrubland was "permanent" because of the loss of the A soil horizon (York and Dick-Peddie, 1969). In particular, invasion by

18

creosote bush was found to be preceded or accompanied by soil loss (Gardner, 1951). However, even in areas protected from grazing, woody species were reported to continue increasing, probably due to the reduction in range fires (Humphrey and Mehrhoff, 1958). Other workers cited a long-term temperature increase since 1900 and altitudinal shifts in xeric species to support their conclusion that vegetation changes resulted from climatic change and livestock grazing, not from a reduction in range fires (Hastings and Turner, 1965).

In the study area, creosote bush is present on all landforms and dominates in topographically high areas where soils are thin and stony (table 3). Mesquite is most common on coppice dunes but is also found on other landforms. These observations agree with results reported by Satterwhite and Ehlen (1982) for studies in southern New Mexico, where they found creosote bush on shallow soils overlying bedrock or petrocalcic horizons. Where eolian deposition was occurring, the plant community was dominated by mesquite. Mesquite was prevalent where soil depth was 6.6 ft (2 m) or more, whereas creosote bush was usually restricted to areas where soil depth was less than 1.6 ft (0.5 m). Potential soil-water-holding capacity controls plant distribution in this area. Tarbush (*Flourensia cernua*) and mesquite are less drought-tolerant than creosote bush (Satterwhite and Ehlen, 1982), hence, their greater abundance on drainageways.

Comparison of aerial photos of the study area taken in 1941 with those taken in 1985 showed that mesquite-colonized dunes were present in both vintages and that dunes did not change position appreciably during that period. Woody vegetation on arroyo floors increased during this period. Individual plants that can be seen in both vintages grew larger between 1941 and 1985. Vegetation cover on the interfluves also increased. Vegetated swales were larger and more individual shrubs were present on the interfluves in 1985 than in 1941. Thus, a trend toward increasing woody vegetation can be documented for this period. However, whether this trend is due to overgrazing or reduction of fires is not known.

The plants discussed below are not the only ones in the study area. These species were selected because their abundance is characteristic of some of the landforms described. Other

perennial plants are present, but most are not as common as those noted here. The letter in parentheses refers to features on the landform map (fig. 11).

Dunes (D): These are eolian deposits of silty fine sand as much as 5 ft (1.5 m) high and 33 ft (10 m) long. Most are about 3.3 ft (1 m) high and less than 16 ft (5 m) long. Dunes are distinctly topographically higher than their surroundings. They are more common and better developed in the southwestern corner of the study area than elsewhere (fig. 11). They are ridges, hummocky or branching in plan view on aerial photographs. Distance between individual dunes ranges from 20 to 65 ft (6 to 20 m). The dune surface is composed primarily of sand (50 to 90 percent) and gravel (as much as 50 percent, locally), which is brought to the surface by burrowing animals. Dunes are usually stabilized by woody plants (mesquite, *Prosopis glandulosa* or the xerophyte, creosote bush, *Larrea tridentata*). Grass is abundant seasonally, and mesquite (as much as 70 percent of all vegetation) is more common here than on any other landform (table 3). Lichen crusts are present locally on the soil surface.

Drainageway (Dr): This is the lowest mappable surface adjacent to a recognizable channel of an ephemeral stream. Channels are usually about 2 ft (60 cm) deep (range = 8 to 30 inches [20 to 75 cm]) and about 5 ft (1.5 m) wide (range = 1.6 to 10 ft [0.5 to 3.2 m]). Where no channel is present, other signs of concentrated overland flow are evident, such as meandering swales with thicker vegetation cover, or shallow, discontinuous swales. Gravel bars and channel lag gravels are present locally, covering as much as 20 percent of the ground surface. This landform is subject to inundation by overbank flow. Frequency and depth of inundation are not known. Roots of woody plants (creosote bush, tarbush) commonly are exposed by erosion. The soil cover and grass are stripped locally in zones 33 to 100 ft (10 to 30 m) wide on both sides of the channel. Underlying sediment is slightly compacted silty fine sand. Farther from the channel, where grass inhibits overland flow, clay drapes are common, with abundant desiccation cracks. Trash lines of plant debris deposited by overland flow are present, and lichen crusts are common. Vegetation is dominantly either creosote bush (as much as 95 percent) or grass (as much as 90 percent), except locally in swales. Tarbush (*Flourensia cernua*) is much more common here than elsewhere on this

or any other landform (table 3), comprising as much as 80 percent of all vegetation. Woody plants are more common where soil cover has not been stripped by overbank flow adjacent to ephemeral channels. Mesquite is locally common but usually accounts for less than 20 percent of all vegetation on this landform.

Floodplain (F): This landform is mapped only along the incised reach of Camp Rice Arroyo in the southeastern part of the study area (fig. 11). The floodplain there is a well-defined surface adjacent to the channel of Camp Rice Arroyo.

High, topographic (H): Gravel-covered topographic highs are usually about 1.6 ft (0.5 m) (range = 1.6 to 33 ft [0.5 to 1 m]) higher than the surrounding surface. They are 33 to 66 ft (10 to 20 m) wide and 66 to 165 ft (20 to 50 m) long. Most trend southwestward, subparallel to drainageways. They are higher than adjacent landforms but do not have as much local relief as uplands. These features probably develop into uplands through denudation and preferential erosion of finer grained sediments around them. Gravel composes 40 to 90 percent of the ground surface; the rest is silty fine sand. Only uplands have more gravel. No desiccation cracks are present. These landforms are usually sparsely covered by creosote bush (as much as 90 percent of vegetation present). Low coppice dunes are present locally.

Interdune (Id): This landform is adjacent to dunes but is topographically lower. The ground surface is composed primarily of silty fine to very fine sand (20 to 90 percent). Locally derived gravel (carbonate-cemented sand) is present (mostly less than 50 percent), brought to the surface by burrowing mammals. No channels or swales are visible on aerial photographs, although ephemeral channels less than 1.6 ft (0.5 m) wide and 1.6 ft (0.5 m) deep may be present between dunes. Vegetation is primarily creosote bush (75 to 90 percent) with some mesquite (10 to 20 percent) and grass in scattered clumps (5 to 10 percent).

Interfluve (If): This low-relief landform is the most common one in the study area. Constituting most of the land surface between drainageways, it is intermediate topographically between drainageways or terraces (lower) and topographic highs or uplands (higher). No evidence of concentrated overland flow, such as channels, swales, thicker vegetation cover, or exposed

21

roots of woody vegetation, exists on this surface. The surface may have sandy, clayey silt drapes over silty, very fine to medium sand. Gravel usually accounts for less than 30 percent of surface sediment, but local outcrops of 80 percent gravel are present. Most gravel is less than 1.2 inches (3 cm) in diameter and is mostly carbonate-cemented sand, which is derived from the petrocalcic horizon that underlies the ground surface. Desiccation cracks are common locally. Small (≤20 inches [50 cm] high and as much as 16.5 ft [5 m] long) coppice dunes may be present. Creosote bush is common, usually about 80 percent of vegetation present. Mesquite, grass and forbs, cactus and yucca, and tarbush (where present) each account for between 1 and 30 percent of all vegetation (table 3).

Slope (S): Identified mostly by its distinctly sloping surface, this landform lies between a higher surface, such as an upland, and a lower surface, such as a drainageway. It is covered with locally derived sediment. The ground surface is composed of fine to coarse silty sand (60 to 80 percent) and gravel (20 to 40 percent). Desiccation cracks are common and lichen crusts are present locally. Vegetation is predominantly creosote bush (as much as 90 percent), mesquite, cactus and yucca, and grass and forbs each composing as much as 5 percent of the vegetation. Vegetation cover is slightly thicker than on topographic highs.

Terrace (T): In the study area, these alluvial surfaces are found only along the incised reaches of Camp Rice Arroyo and a tributary to Alamo Arroyo (fig. 11). They slope downvalley and toward the stream channel. They are remnants of a former floodplain of the stream before it incised to its present level. Because they contain parts of former floodplains and drainageways, the surface sediments are similar to those seen on those landforms. The surface sediment is locally gravelly where small fans build up at the mouths of valley-side gullies that debouch onto the terrace surface. Creosote bush is the dominant perennial plant species.

Upland (U): These features have the highest local relief in the study area. They are distinguished from topographic highs on the study area by greater local relief. Uplands are as much as 10 ft (3 m) higher than adjacent landforms. Steepest slopes on their flanks are about 6 percent. These are the least common of the landforms described. All three are in the east-central part of the

study area, near the county road (fig. 11). Gravel covers the ground surface in greater concentration than anywhere else (70 to 95 percent). The rest of the surface is silty very fine to coarse sand. Desiccation cracks are not well-developed, indicating a lack of clay. Vegetation cover is mostly creosote bush (80 percent), with minor amounts of mesquite (10 percent), grass and forbs (5 percent), and cactus (5 percent). In aerial photographs, the texture of this landform appears smoother than that of others, probably because vegetation is less dense and plants are smaller. These are well-drained features, having less water available for plants than do drainageways; hence, the abundance of creosote bush and scarcity of mesquite. Uplands may be gravelly facies of alluvial debris derived by erosion from outcrops of limestone and sandstone along the Diablo Plateau escarpment.

One manmade feature (roads) in the study area has had an important impact on landforms. Because the topographic relief of the study area is low (slope = 1 percent) and ephemeral stream channels are shallow (usually less than 2 ft [60 cm]), the graded county roads, which are as much as 2 ft (60 cm) lower than the adjacent surface, capture streamflow wherever they intersect the natural drainage network. As a result, runoff is concentrated in the roads, and its erosive power is thereby increased. The effects of this process can be seen during and after high-intensity rainfall events, when roads fill with water and act, essentially, like manmade streams. After the water recedes, the effects of overland flow are plainly visible. The roadbed is locally scoured clean of fine-grained sediment, revealing the strongly cemented petrocalcic horizon underneath. The long-term effects of this drainage diversion could include accelerated retreat of headcuts in arroyos downstream from the roads, initiation of nickpoints on the upstream sides of the roads where they intersect natural channels, and transformation of the roads into incised gullies.

PRESENT-DAY PROCESSES

The most important geomorphic processes currently occurring in the study area result from rainfall and runoff. The nature of rainfall that typically occurs there, and its effect on erosion and

deposition, are described in the following section. The results of erosion and deposition are seen in the retreat of headcuts in arroyos and gullies and in the formation of surface-collapse features (fissures). Runoff is the primary agent forming these features.

Rainfall

To monitor rainfall at the study area and upstream from it, four continuously recording rain gauges were installed in July 1988 (fig. 12). These gauges measure rainfall in 0.2 mm increments, and are accurate to ±1 percent at rainfall intensities as much as 76 mm/hr (Meteorology Research, Inc., 1979). On the north side of the study area, a meteorologic station with a similar rain gauge has been operated by Texas A&M University since June 1988. That rain gauge measures precipitation in increments of 0.01 inches. Erosion pin fields were installed near each rain gauge in July and August 1988 to monitor erosion and deposition. Crest-stage gauges were installed near each pin field in October 1988 to monitor depth of overland flow. Finally, five rebar fields were set up in July 1989 to monitor headcut retreat on calcrete outcrops in gullies on the south and west sides of the study area.

The maximum 0.5-hr, 1-hr, and 24-hr rainfall events that occurred during this study and their recurrence intervals are shown in table 4. The largest 0.5-hr event recorded between July 15, 1988, and December 31, 1989, was 34 mm at the East rain gauge. On the basis of interpolation between isohyets on maps of rainfall recurrence intervals (Hershfield, 1961), this rainfall intensity has a 25-yr recurrence interval. As is common for convective-cell thunderstorms, this rainfall was limited in its areal extent. Precipitation amounts for the same storm at other rain gauges in the study area less than 2 mi (3 km) away were less than one-third the maximum (fig. 13). Maximum values of the 0.5-hr rainfall for other storms at other gauges did not exceed a 10-yr recurrence interval (table 4).

Maximum values of 1-hr and 24-hr rainfall amounts recorded during the monitoring period have recurrence intervals of 10 yr or less (table 4). None of the 1-hr or 24-hr events recorded

24

during the monitoring period equalled the maximum intensities of events that have been recorded in El Paso, which is about 40 mi (65 km) to the northwest.

The total rainfall for calendar year 1989 at the 5 rain gauges ranged from 5.2 to 9.3 inches (131 to 237 mm). Short data gaps in the records for Center and East gauges were filled by using a Thiessen network of polygons (Linsley and others, 1949). The polygons were formed by drawing perpendicular bisectors of lines connecting the gauges that had data for those dates. Rainfall amount at the gauge with data was assigned to the gauge in the same polygon that had a data gap. The mean annual rainfall from 1966 to 1987 at Fort Hancock was 11 inches (280 mm) (J. R. Scoggins, Texas A&M University, written communication, 1989). Assuming that during the same period, rainfall at the study area was approximately the same as that in Fort Hancock, which is about 11 mi (17 km) from the nearest gauge, then 1989 was a drier than average year at the study area.

Erosion and Deposition

Short-term

To monitor erosion and deposition in the study area, erosion pin fields were installed near each rain gauge. Erosion pins are nails that are 10 inches (25 cm) long and 0.4 inch (1 cm) in diameter that have been inserted through a metal washer. Initially, each pin was driven vertically about halfway into the ground and the washer rested on the ground. Pin-to-ground and pin-to-washer measurements were recorded. Pins were remeasured monthly if a single 1-hr rainfall event greater than 0.5 inch (12.5 mm) occurred during that time (table 5). Otherwise, they were measured about every 4 months. Cumulative pin-to-ground measurements for each pin are presented in figure 14. These values represent total change over the entire monitoring period. Some pins recorded erosion and deposition during this time, but only the cumulative result is presented here.

The effect of large runoff events is reflected in the data collected from erosion pins. Of the 23 pins that recorded more than 0.2 inch (0.5 cm) of cumulative erosion or deposition during the monitoring period (fig. 14), 17 are in pin fields adjacent to ephemeral stream channels, and 4 of those 17 are in the channels themselves. At 13 of these 23 pins most of the erosion or deposition occurred within the first month of the monitoring period, when two of the most intense rains of the entire study were recorded (July 19 and 29, 1988) (table 4). Two more pins recorded most of their deposition in August 1989, as a result of the second most intense 0.5-hr rainfall recorded at the study area (North gauge, table 4). In these pin fields, runoff resulting from intense rainfall is the principal agent transporting sediment. No measurable eolian transport has occurred.

Overland flow is the primary means of sediment transport, as shown by the numerous shallow rills that cross the pin fields and by the small (usually <2 cm high) piles of plant debris (trashlines) that remain behind after runoff has ceased. Some sediment is dislodged by rainsplash, as indicated by sand grains adhering to the sides of erosion pins and rain gauges after rainstorms. But, there has been no significant development of hoodoos (earth pillars) beneath the metal washers around each pin. This indicates that sediment removal by raindrop impact has been negligible. Furthermore, slopes in the pin fields are so low (mostly <3 degrees) that there is no net downslope transport of sediment by this mechanism.

Although there is a wide range in the amount of cumulative erosion and deposition measured by the erosion pins, nearly half of the pins recorded 0.04 inch (0.1 cm) or less of cumulative erosion or deposition between July 1988 and September 1989 (the last time pins were measured) (fig. 14). Thus, nearly half of the erosion pins are recording little or no change in the level of the ground surface. Several factors were examined to determine their effect on erosion and deposition. These included local setting (such as rill, channel, or slope), angle of local slope, percent bare surface, percent gravel, percent sand, silt and clay, and presence or absence of a lichenous soil crust. Linear and simultaneous regressions of several factors were performed using either erosion or deposition as the independent variable. Each of the environmental factors was the dependent variable. No simultaneous regression of more than one variable increased the level of significance

of those variables considered independently. Thus, there is no justification for considering the variables simultaneously.

Erosion is significantly positively correlated with absence of lichen crust ($r = .26$, $p = .05$) (fig. 15a) and with percent bare surface ($r = .26$, $p = .05$) (fig. 17), and, at a higher level of significance ($r = .43$, $p = .01$), with local setting (fig. 16). Deposition is significantly positively correlated with absence of a lichen crust ($r = .33$, $p = .01$) and with local setting ($r = .48$, $p = .01$) (figs. 15b and 16, respectively).

None of the other conditions that were examined have a significant effect on erosion or deposition. Slope angle does not significantly affect erosion or deposition. Neither does soil texture. The texture of surface materials at each pin was estimated by a point count conducted using a photograph taken about 4.3 ft (1.3 m) directly above each pin. The photograph was projected onto a grid and the texture at each grid intersection was tabulated. Gravel ranges from 0 to 64 percent, sand ranges from 0 to 91 percent, and silt and clay ranges from 4 to 100 percent. Percent gravel and percent sand, silt and clay are not significantly correlated with erosion pin measurements. Laboratory-derived particle-size data are not available for surface materials at every pin. However, a representative surface sample was collected at each pin field for laboratory analysis. Most samples were silty sand. Three, with small amounts of gravel (≤ 6 percent), were gravelly, muddy sand.

To determine if extreme values (outliers, which were identified as Studentized residuals) of erosion and deposition were significantly affecting their correlation with lichen presence (fig. 15) and percent bare surface (fig. 17), these extreme values were dropped and correlations were recalculated. Whereas this slightly increased the value of the correlation coefficients (r), it did not raise their significance (p). For example, dropping a single outlier (0.6 inch [1.6 cm]) from the regression of erosion versus the presence or absence of lichen (fig. 15a) raised r from .26 to .29, but the higher r value is still significant at the $p = .05$ level. Therefore, no justification exists for eliminating these outliers from the data set.

Thus, for the data available, only three environmental conditions that have been measured have a significant effect on erosion and deposition: absence of lichen crust (fig. 15), local setting (fig. 16), and percent bare surface (fig. 17). However, the r values are quite low ($\leq.48$), and the highest r value accounts for less than 25 percent of the variability in deposition observed. Clearly, other conditions are affecting sediment transport.

Both erosion and deposition are positively correlated with absence of lichen crust (fig. 15). The presence of a crust indicates a stable surface, undergoing neither erosion nor deposition. Absence of a lichen crust probably is an effect of erosion and deposition, not a cause of either one.

Erosion is positively correlated with percent bare surface (fig. 17), but deposition is not negatively correlated with percent bare surface. This suggests that vegetation protects the surface from erosion either by blocking direct raindrop impact or by inhibiting overland flow, but it does not promote deposition. Nevertheless, the correlation coefficient between erosion and percent bare surface is quite low ($r=.26$), indicating that other factors account for most of the variability in erosion.

Although the highest values of correlation coefficients are associated with setting, the effect of local setting on erosion or deposition is not straightforward (fig. 16). Highest values of deposition occur in rills and on channel floors. Highest values of erosion occur in flat areas, local lows, and rills. In general, these results suggest that rills are the most active environments, undergoing erosion and deposition. Channels are undergoing more deposition, locally, than erosion. Flat areas and local slopes are about equally affected by erosion and deposition. Local highs are characterized by low-magnitude erosion, and local lows commonly undergo deposition.

In summary, these results indicate that for the short period of observation (14 months) deposition is more common than erosion in the environments being monitored. Even in channels, where more sediment probably is being transported, deposition occurred more frequently than erosion. The mean and median values for all pins are close to zero. The monitoring period is too short to be the basis for any predictions about future surface stability. But, as expected, most sediment transport occurs as the result of runoff from high-intensity, low-frequency rainstorms.

Although most measures of the pin environment showed little or no effect on erosion or deposition during this study, these conditions may show some influence on sediment transport after more runoff events have occurred.

Long-term

The recent stability of the surface in the study area can be inferred from archeological evidence. A projectile point, a sherd of brownware pottery, and a uniface grinding stone (mano) were found together in the north part of the study area. These objects provide "minimal evidence" of the age of the archeological site where they were found (Gerald, 1988). The projectile point and ceramic sherd indicate that the site may have been occupied from about 4000 B.C. until A.D. 1100 (Gerald, 1988). The artifacts were found near hearths containing soil blackened with charcoal. If these objects are contemporaneous with the hearths, then the surface in their vicinity has been stable for at least 900 yr. The presence of a 1,400-yr-old soil horizon at fissure 1 within about 10 inches (25 cm) of the ground surface supports the conclusion that the surface of the study area has been relatively stable, aggrading and degrading locally, for several hundred years.

Rates of Arroyo-Fill (Gully) Erosion

Two methods were used to calculate rates and amounts of headcut retreat in alluvium in arroyos around the study area (table 6). First, radiocarbon ages of alluvial sediments were used to estimate long-term rates of erosion since alluvial sediments were deposited. Second, headcuts were located on aerial photos of different vintages. The distance between headcuts on the same arroyo on different vintages was divided by the time between vintages to yield a rate of headcut retreat.

29

Radiocarbon ages

The radiocarbon ages of sediment samples collected in the study area shed light on the history of erosion and deposition there. A piece of carbonized wood in an alluvial terrace west of the study area was radiocarbon-dated at 920±70 yr B.P. (fig. 7, location A). A sample was collected from a shallow soil horizon exposed in a gully wall at the western edge of the study area (fig. 7, location B). It has a radiocarbon age of 400±70 yr. A third sample was collected from a terrace in the tributary of Alamo Arroyo that drains the north half of the study area (fig. 7, location C). The organic matter in the soil has a radiocarbon age of 1,330±60 yr. All three deposits are now buried by younger sediments but are exposed in cutbanks. Apparently, within about the last 400 to 1,300 yr, accumulation of alluvial sediments at these locations has been interrupted by headcut retreat, which has exposed the buried horizons.

Assuming that (1) the organic material in these deposits was only a few years old when deposited, (2) the organic matter was deposited in the alluvium just before it began to be incised, (3) the headcut was just downstream when the organic matter was deposited, and (4) the alluvial fill was a continuous deposit upstream from the headcut, the rate of headward advance of the headcuts ranges from about 1.6 inches (4 cm) to 5.2 ft (1.6 m) per yr (table 6). Although these rates are high, they apply only to erosion of the unconsolidated alluvium in the arroyos. They do not apply to the older sediments underlying the study area that form the interfluves between arroyos. The variability in rates (more than an order of magnitude) is partly a function of the incomplete preservation of these deposits, which controls sampling location. For example, if a suitable outcrop of the soil horizon at location C had been exposed farther downstream, the distance and rate of retreat would have increased, approaching the values derived from the other locations.

The four assumptions used also affect the calculated retreat rates. Assumption 4, which tends to maximize the calculated rate, probably has the greatest impact. It proposes that the alluvial fill

between the dated deposit and the present headcut was removed by the advance of a single headcut. If the alluvial fill upstream from location A were originally discontinuous instead of continuous, as is assumed, then the calculated retreat distance and rate would be less than that shown (table 6a). There is some evidence for this possibility. There may have been several headcuts upstream from the dated deposit, as there are now on Camp Rice Arroyo, and the alluvium may have been removed in stair-step fashion. Conversely, assumption 3 tends to minimize the calculated rate. If the original headcut had been farther downstream than its assumed position near the dated deposit, the calculated distance and rate would be greater than that shown (table 6). Assumption 2 minimizes retreat rate by proposing that incision began soon after deposition. Likewise, assumption 1 minimizes retreat rate by proposing that the dated deposit is not contaminated with older, reworked organic matter. The opposing effects of assumptions 3 and 4 are about the same magnitude and cancel one another out, to some extent. Because the actual time of onset of incision is unknown, the magnitude of the effect of assumption 2 is unknown. Given the mode of deposition of the dated organic matter, assumption 1 is probably quite reasonable and therefore gives an accurate retreat rate.

Photointerpretation

Analysis of aerial photos taken in 1941, 1971, 1974, and 1985 shows that measurable headcut retreat has occurred within the last 50 yr on Alamo and Camp Rice Arroyos (table 6). Headcut retreat was observed on 103 separate headcuts around the study area, which is less than half of the headcuts that can be seen on arroyos and valley-side gullies at the area. The limit of resolution of measurable erosion indicated in the photographs is about 50 ft (15 m), or 0.04 inch (1 mm) as measured on the 1985 photographs (table 7). Headcut retreat less than 50 ft (15 m) cannot be reliably mapped because of the lower resolution of the 1941 photographs and because of differences in shadow orientation. Headcuts are easiest to see where they are accentuated by shadows. But shadows in the low-sun-angle photographs taken in 1985 are oblique to shadows in

31

the older vintages. Consequently, the headcut can appear to have moved when only the shadows are oriented differently. Nevertheless, it was possible to identify several headcuts that were unchanged from 1941 to 1985. Thus, a lower limit (no change) of headcut retreat was established.

Between 1941 and 1985 the amount and rate of headcut retreat in alluvial fill on the arroyos varied by a factor of about 4. The headcut in Camp Rice Arroyo (table 6b, location D) retreated almost four times as far as the headcut in Alamo Arroyo (table 6b, location C). The area of the drainage basin upstream from each headcut does not account for the differences in amounts and rates of headcut retreat (table 6b). Although headcut retreat occurs as a result of runoff, area cannot be used as a substitute for discharge for two reasons. First, runoff-producing storms in this region, as in most deserts, commonly cover only part of the drainage basin upstream from a given point (fig. 13). Second, in arid and semiarid regions, stream discharge tends to decrease downstream due to transmission losses into the streambed (Reid and Frostick, 1989).

It is also possible that this difference in retreat rate may result from a data record that is short relative to the recurrence interval of the erosive events, which is analogous to the erosion pin data discussed previously. Because runoff-producing storms occur episodically, one must conclude that headcuts retreat episodically. Hereford's (1987) study of erosion in a small (1.1 mi^2 [2.8 km^2]) basin in a similar climate (semiarid) showed that sediment was deposited in a reservoir only 21 times in 38 yr. Hence, it is possible that headcut retreat in the study area occurred only a few times during the 44 yr covered by aerial photographs, and that storms did not cover the areas upstream from each location in figure 7 equally. Furthermore, the period of observation is an arbitrary one, based solely on when the photographs were taken. As a result, retreat rates are artificially controlled by the coincidence of rainfall events with the photographs. For example, if a rare, high-magnitude rainfall event occurred a year before the first photographs were taken instead of a year after, the rate of headcut retreat would appear to be much different.

However, an important comparison can be made between locations that are close to one another on the same stream and, presumably, have the same rainfall-runoff history from 1941 to 1985. Locations C and E are only 1900 ft (580 m) apart on the tributary that drains the north part

of the study area (fig. 7). At location E the headcut in a Stage IV carbonate-cemented horizon has retreated only 150 ft (45 m) since 1941, at an average rate of about 3.3 ft/yr (1 m/yr) (table 6b). This rate of retreat is about half that of location C just downstream in alluvial fill, suggesting that the petrocalcic horizon may inhibit headward migration of nickpoints on streams in the area. Analysis of headcuts in valley-side gullies supports this conclusion. Few headcuts on carbonate-cemented outcrops in valley-side gullies were eroded a measurable amount between 1941 and 1985. But at the same time headcuts in alluvium in the valley-side gullies advanced an average of 490 ft (150 m) (table 6b).

An upstream-progressing wave of erosion does not appear to be moving systematically through valley-side gullies, as a result of headward movement of nickpoints on the main arroyos, past the junctions between the gullies and the arroyos. Incision in valley-side gullies does not appear to be a function of upstream drainage area of the gully. Some gullies have incised adjacent to others that have not, whose drainage area and slope are similar. Alluvium now being incised is in preexisting gullies. So, gullies eroded and filled before 1941, and eroded again between 1941 and 1985.

At the three locations with retreat rates based on photointerpretation and radiocarbon-dated material (fig. 7, locations A, B, and C), modern rates of retreat in alluvial fill are 4 to 55 times faster than those based on radiocarbon dates (table 6). This increase in retreat rates may occur partly because of changes in climate or vegetation cover that enhance runoff and headcut retreat and partly because the older rates are based on longer periods of time. In fact, the headcuts may have retreated at rates similar to the modern ones for brief periods, and been unchanged the rest of the time. Finally, as discussed, part of the apparent increase in modern rates probably is an artifact of the arbitrary 44-yr period used for calculating the modern rates.

Fissure Development

Introduction

The following discussion of fissures makes a distinction between the fissure at the ground surface and the subsurface fracture that underlies it. The underlying fracture is an extensional feature that localizes the formation of surface collapse structures composing the fissure. The fracture extends from the base of the shallow surface collapse feature to at least 20 ft (6 m) below the ground surface, and is usually between 0.8 and 1.6 inches (2 and 4 cm) wide. Typically it is filled with sediment; however, locally there are openings in the fracture fill. Opposite sides of the fracture commonly display mirror-image symmetry. The fissure is the surface feature composed of aligned holes and depressions that form when surficial sediments collapse into soil pipes or are washed into the underlying fracture. The widths and depths of the holes depend on the degree to which they have been eroded and filled with sediment. Widths and depths of 3.3 ft (1 m) of collapse features are common in fissures at the study area. In profile, the bottom of the fissure is at the highest point of the tension fracture where extensional opening predominates over collapse of sediment.

Fissures in the study area

Surface-collapse features. Three surface fissures ranging in length from 67 ft (20.5 m) (fissure 2) to 460 ft (140 m) (fissure 1) have been found at the study area (fig. 18). Shallow pits were dug by hand as deep as the petrocalcic horizon at all three fissures. Deeper trenches were excavated at fissure 1 (fig. 19); consequently, more detailed descriptions are available for this fissure and for the fracture beneath it. One relict fracture, with no fissure above it, has been exposed in the floor and walls of a 20-ft deep (6-m) trench at the study area (fig. 18). Because the fracture is filled with sediment, a fissure must have formed above it at some time. The fissure has

been obscured or removed by subsequent erosion and deposition on the surface above the fracture. The relict fracture is at least 100 ft (30 m) long, which is its exposure across the width of the trench. The surface fissures in the study area are composed of aligned surface-collapse and piping features, which are roughly wedge- to slot-shaped, narrowing downward in profile. Maximum depth of collapse features is 4.4 ft (135 cm); maximum width is 5.2 ft (157 cm). Both maxima were seen at the longest fissure (fissure 1). At fissures 2 and 3, collapse features are as deep as the top of the petrocalcic horizon, about 21.5 to 24 inches (55 to 60 cm). Most collapse features at fissure 1 are about a meter deep and less than a meter wide. Width/depth ratios of the fissures, which increase as the fissures are eroded and filled with sediment, range from 0.2 to 2.0 (table 8). The collapse features are discontinuous, separated by bridges of sediment over horizontal soil pipes. Locally, as much as 33 ft (10 m) of uncollapsed material lies between these holes (fig. 19), but spacing between them is more commonly 3.3 to 10 ft (1 to 3 m).

The widest and longest collapse features are near the middle of fissure 1. The smallest collapse features are near the northwest and southeast ends of the fissure (fig. 19). These observations suggest (1) that the largest collapse features are the oldest ones at this fissure because they have been eroded more by overland flow and (2) that the fissure has propagated laterally away from an origin near its center. Fissure 1 is composed of two, or possibly three, arcuate segments. The two principal segments overlap slightly between trenches 3 and 4 (fig. 19). The southeastern segment may be composed of two smaller segments that overlap a few meters southeast of trench 4.

All three fissures in the study area are located in topographic lows where vegetation is thicker than that in adjacent areas (fig. 18). Fissure 1 trends N55°W, oblique to local drainage. It lies in a topographic low that has about the same orientation. Fissure 2 is oriented about N50°W, subparallel to the topographic low in which it lies. Fissure 3 is a curvilinear feature that is roughly perpendicular to drainage. Its orientation, measured end-to-end, is N20°E. At fissures 1 and 3, leaf litter and branches have washed into the collapse features, evidence that the fissures are capturing runoff. There are small, uncommon accumulations of gravel in fissure 1, probably derived locally

35

from the ground surface or eroded from the fissure wall. Fissure 3 extends upslope beyond the topographic low where the vegetation cover is relatively thick. On the less-vegetated slope, grass and forbs are more common within 6.6 ft (2 m) of the fissure than farther away, indicating that moisture content of the soil near the fissure is high enough to enhance growth of annual plants. Runoff captured by the fissure in the topographic low probably moves laterally through the fissure system to points outside that low. The relict fracture has no fissure above it, nor is it in a topographic low. But, when it opened and was filled it may have intersected a topographic low that is no longer apparent.

Fractures and fracture fill. At the study area, all known fissures are underlain locally by a fracture that is subparallel to surface-collapse features. The fracture narrows downward at fissure 1 from a maximum of 2.6 inches (6.5 cm) at a depth of 12.5 ft (3.8 m) to 1 inch (2.5 cm) at a depth of 18.4 ft (5.6 m) (pl. 3). Maximum width of the fracture in the top of the petrocalcic horizon at fissure 2 is 2.8 inches (7 cm). Widths of 0.8 to 1.6 inches (2 to 4 cm) are typical of all fractures, including the relict one. The maximum widths may result from widening of the tensional fracture by local erosion and collapse of the walls. Where their walls have eroded little and display mirror-image symmetry, fractures are typically 1.2 to 1.8 inches (3 to 4.5 cm) wide.

The fracture below fissure 1 is at least 20 ft (6.2 m) deep, the maximum depth of trench 3 (pl. 3). The relict fracture is exposed to a similar depth. The fracture at fissure 1 may extend several meters deeper than this. If one assumes downward movement and storage within the fracture of all material missing from the widest collapse feature at the surface (which has a cross-sectional area of 9.7 ft^2 [9,000 cm^2]), a fracture 1 inch (2.5 cm) wide would have to be 116 ft (36 m) deep to accommodate the same amount of sediment. However, some of the sediment missing from the collapse feature may have been compacted by wetting or flushed out of the fracture and into porous gravel layers on either side of the fracture (pl. 3). If this has occurred, the fracture could be shallower than the 116 ft (36 m) estimated. Some evidence for a shallower depth exists. The fracture at fissure 1 branches at a 16.5-ft (5-m) depth, and each branch is smaller than the main fracture (pl. 3). The smaller branch dies out downward in the gravel layer at that depth.

Overburden pressure may cause the fracture to terminate at a depth shallower than that estimated by these areal calculations.

No movement of one side of the fracture parallel to the other, either horizontally or vertically, has occurred at fissure 1 or at the relict fracture. (The walls of the fracture below the petrocalcic horizon are not exposed at fissures 2 and 3.) Such movement would indicate fault movement. Opening of the fracture has occurred only by perpendicular movement of the fracture walls, the result of tensional cracking. Where the fracture walls are not eroded or modified by localized collapse, they display mirror-image symmetry. This indication of simple tensional separation of the fracture walls is common at fissure 1 and at the relict fracture. Locally, the fracture at fissure 1 branches and rejoins, enclosing pieces of silty sand and carbonate-cemented gravel (pl. 3, 18-ft [5.5-m] and 10-ft [3-m] depth). These have not rotated and therefore also demonstrate simple tensional cracking.

The subsurface fractures are filled with sediment ranging from slightly silty, very fine sand to sandy, silty clay. Pebbles are rarely present in the fracture below the base of the uppermost gravel layer (pl. 3, 11.2-ft [3.4-m] depth). Fracture fill locally contains more clay than surrounding material. The fracture fill contains laminae that locally are horizontal or concave upward. They probably represent individual depositional events when sediment was washed into the fracture by storm runoff. Layers of clay on the walls of the fractures and internal clay laminae (≤0.04 inch [1 mm] thick) within the fill are evidence of multiple episodes of filling and fracturing of the fill material. The internal clay laminae are subparallel to the subvertical fracture walls, although they branch and join on a scale of a few centimeters. These internal laminae probably mark events when the fill fractured because of desiccation of the fill or further tensional opening of the original fracture, which pulled the fracture fill apart. Presumably, after the fill fractured, clay was deposited on the walls of the new (internal) openings, either by settling out of downward percolating water or by adhering to the walls as water moved laterally out of the fracture and into the surrounding sediments. Similar features in fracture fill, described as "medial partings," were reported by Bull

(1972) in his study of fractures in Fresno County, California. He attributed their development to repeated periods of deposition of sediment carried down into the cracks by water.

The fractures conduct water more easily than surrounding sediments, as indicated by cementation along the fractures, presence of living woody roots in the fractures, and the results of a ponding test conducted in trench 3 (Scanlon, 1990). Carbonate cement less than 0.02 inch (0.5 mm) thick lines the walls of the fracture in the petrocalcic horizon at a depth of 14.1 ft (4.3 m) at fissure 1 (pl. 3). In addition, at a depth of 18.7 to 20.3 ft (5.7 to 6.2 m), gravel is weakly cemented by calcite in a 2.7-inch-wide (7-cm) zone adjacent to the fracture (pl. 3). The fractures are preferred pathways for roots through all strata, including the gravel layers. Live roots have been seen in fractures as deep as 20 ft (6.2 m) below the ground surface.

The fractures that underlie (trench 3) or bound (trench 4) fissure 1 are wider and are more often lined with gray clay or carbonate cement than are fractures farther from the fissure. These observations indicate that fractures near the fissure that have reached the surface are more likely to be preferred pathways for downward-moving water. Although many fractures (lined and unlined, filled and hairline) can be traced upward from fractures in the petrocalcic horizon (fig. 4), those outside a 10-ft-wide (3-m) zone parallel to the fissure and those beyond the ends of the fissure are not as wide ($\geq$0.4 inches [1 cm]) as those near the fissure.

Clay-lined cavities are present locally in the fracture below fissure 1. The horizontal dimensions of cavities exposed in trench walls range from 0.2 to 24 inches (4 mm to 60 cm). Most are less than 4 inches (10 cm) across. Total vertical extent of openings is about 5 percent of the exposed length of the fissure in the southeast wall of trench 3 (pl. 3). Some cavities at a depth of 9.2 ft (2.8 m) (2.3 ft [70 cm] below the top of the upper petrocalcic horizon) contain spiderwebs, indicating that they are connected to the ground surface via open cavities in or adjacent to the fissure. Some of the larger openings may be enlarged by or produced by animals burrowing near or along the fracture. Rodent fecal pellets are present in fissure fill near the ground surface where the fissure widens upward to form a collapse feature. Near the fissure, animal burrows in silty sand are present as deep as 6.6 ft (2 m) below the surface (fig. 5). Badger (*Taxidea taxus*) burrows

as deep as 7.5 ft (2.3 m) have been recorded in the western United States (Long and Killingley, 1983), and badgers have been seen at the study area.

At fissure 1 no cavities larger than 0.4 by 1.2 inches (1 by 3 cm) have been seen in the fracture deeper than 11.2 ft (3.4 m), the base of the uppermost gravel layer in trench 3 (pl. 3). A few small openings in fracture fill (mostly <0.2 inch [5 mm] wide) have been seen below the base of that gravel layer. This suggests that some collapse material may be dispersed into the matrix of the less-cemented, grain-supported gravel (pl. 3, 8.8- to 11.2-ft [2.7- to 3.4-m] depth), leaving open space in the fracture, locally.

At trench 4, which is between surface-collapse features (fig. 19), continuous fractures extend upward from a depth of 10 ft (3 m) to the base of the surface soil (12-inch [30-cm] depth), parallel to and flanking the interpolated trend of the fissure at about 0+06 SW and 0+12 SW (fig. 5). These fissure-bounding fractures are mostly less than 0.4 inch (1 cm) wide and narrow downward to a hairline crack lined with clay. These fractures are narrower than the fracture directly below collapse features at trench 3 (pl. 3), and they are the only ones in trench 4 with large (>0.4 × 1.6 inch [1 × 4 cm]) open spaces in unconsolidated sediments above the petrocalcic horizon (figs. 4 and 5). One of the fissure-bounding fractures in trench 4 branches and narrows abruptly at a depth of 7.5 ft (2.3 m) (fig. 5, 0+12 SW) to a 0.08-inch-wide (2-mm) filled fracture lined with gray clay. Orientation of the fracture changes from near vertical to sloping northeast about 60 degrees.

Numerous small, closed fractures between the fissure-bounding fractures are present in the crossbedded sandy unit above the massive gravelly sand (figs. 4 and 5, 4.9-ft [1.5-m] depth). These fractures branch upward, cutting the crossbeds, but there is no displacement across them. These are hairline to barely traceable, and all appear to be confined to this sedimentary unit.

Rubble zones bounded by fractures are present locally in the crossbedded sand (fig. 5). They are filled with structureless sediment that is siltier than the adjacent crossbedded silty, fine to medium sand. This structureless sediment contains small (<0.2-inch [5-mm]) fragments of clayey crossbedded material. These rubble zones may be tortuous collapse zones or burrows. Overlying sediments are continuous across these rubble zones. They appear to terminate abruptly in the

vertical wall of the trench, but in fact they probably continue up and down at some angle to the trench wall. Well-developed filled burrows are present near the rubble zones. A few fractures extend from rubble zones upward into the overlying massive unit to within 24 inches (60 cm) of the surface, but there is no offset across them.

Polygonal fractures in petrocalcic horizon. Vertical polygonal fractures in the petrocalcic horizon formed independently from the fissure. Such fractures are commonly observed in well-developed calcic horizons (Reeves, 1976; Gile and others, 1981; Machette, 1985). They are present at the study area, hundreds of meters away from the fissures, in outcrops of the petrocalcic horizon in the unpaved county road and along the channel floor of the tributary that drains the north half of the area. Most of these fractures are less than or equal to 0.3 inch (7 mm) wide and are lined with carbonate less than or equal to 0.04 inch (1 mm) thick. Some that are perpendicular to local slope in ditches along the county road and in the stream-channel floor are wider.

These polygonal fractures predate the surface fissure by several thousand years. All fractures greater than or equal to 0.08 inch (2 mm) wide in the petrocalcic horizon in trench 4 are at least partly coated with carbonate. Fractures as much as 3.1 inches (8 cm) wide in the petrocalcic horizon (trench 4) are lined with carbonate as much as 0.3 inch (7 mm) thick. These laminae are characteristic of a Stage IV pedogenic calcrete (Machette, 1985). Calcretes such as this near Las Cruces, New Mexico, are at least 25,000 yr old (Gile and others, 1981).

Polygonal cracks in the petrocalcic horizon near the fissure extend upward into overlying sediments, commonly to the base of the loose surface soil (fig. 4, 0+18 to 0+28 SW, 2-ft [30-cm] depth). This suggests that movement of the polygonal blocks in the petrocalcic horizon, possibly resulting from desiccation of underlying sediments, produces fractures in the overlying sediments. Fractures range from a hairline crack to 1.5 inches (37 mm) wide in the carbonate horizon. Most are less than 0.4 inch (10 mm) wide except in the vicinity of the fissure in trench 4. Fractures wider than 0.04 inch (1 mm) are lined with silt and clay locally. Hairline fractures are usually open and unlined above the carbonate horizon, indicating either that they have not been preferred pathways for water movement or that they formed during trenching. However, one of these has a

root growing in it (fig. 5, 0+1.5 SW, 3.3-ft [1-m] depth), suggesting that it predates trenching. Some fractures branch upward at the top of the massive, gravelly sand (fig. 4, 5.6-ft [1.7-m] depth).

Most of the fractures beyond the ends of fissure 1 (fig. 19, trenches 2 and 5) do not extend above the petrocalcic horizon. A few hairline fractures can be traced upward to the base of the surface soil (12-inch [30-cm] depth), but none are clay-lined. These are probably caused by trenching. The maximum width of fractures in the carbonate horizon is 0.8 inch (20 mm), narrower than the fractures near the fissure in trench 4.

Fractures in the petrocalcic horizon sometimes intersect local lows in the petrocalcic horizon exposed in trench walls. Most of these local lows are less than 10 inches (25 cm) wide and 4 inches (10 cm) deep, but a few are as long as 16 inches (40 cm) and as deep as 6 inches (15 cm). They appear to be dissolution pits or grooves in the upper surface of the carbonate horizon.

In summary, polygonal fractures are present everywhere in the petrocalcic horizon. Most are lined with carbonate, indicating relatively old age. Some have propagated upward into unconsolidated sediments. Some fractures in the overlying sediments appear to be caused by trenching. Others, lined with silt and clay, predate trenching. Those within a few meters of fissure 1 are wider and are more often lined with silt and clay. Fissure development appears to enhance formation of peripheral fractures that are preferred paths for water movement.

Quaternary stratigraphy in vicinity of fissure 1. The near-surface sediments in the vicinity of fissure 1 are composed of interbedded sand and gravel (fig. 3, pl. 3). In these sand and gravel deposits two petrocalcic horizons are preserved. One is at about 5 to 9 ft (1.5 to 2.7 m) in depth. The other is at about 14.1 to 17.7 ft (4.3 to 5.4 m) in depth, as seen in trench 3 (pl. 3). The carbonate-cemented horizons originally formed nearer the ground surface, probably at a depth of less than a meter (McFadden and Tinsley, 1985), and have since been covered by more sediment. These horizons have characteristics of Stages III and IV of calcium carbonate morphology in the classification of calcic soils and pedogenic calcretes by Machette (1985). Calcium carbonate is dispersed in the sandy matrix of the horizons (Stage III) and decreases downward from the top of

41

each one. Where the upper surfaces of the petrocalcic horizons are sandy, the carbonate cement is laminated, and locally there are carbonate laminae on fracture surfaces (Stage IV). The time required for development of such a soil in the desert Southwest is at least 25,000 yr (Gile and others, 1981). Except for the well-cemented petrocalcic horizons, all of these strata are weakly cemented and friable. However, all strata, at least to a depth of 20.3 ft (6.2 m), are competent enough for fractures to form and remain open (fig. 5; pl. 3).

Both petrocalcic horizons are eroded locally. The contact between these carbonate-cemented horizons and the sediments that overlie them is abrupt and locally irregular. In trench 4, a 13.1-ft-wide (4-m) gap in the upper petrocalcic horizon underlies the projection of fissure 1 (fig. 4, 0+02 NE to 0+12 SW). Similar irregular gaps also are present in the petrocalcic horizon near the relict fracture. However, a deeper channel is exposed in trench 5, where there is no fissure. Similarly, the petrocalcic horizon is cut out and overlain by gravel deposits at the northeast end of trench 4, where there is no fissure. Evidently, the presence or absence of the upper petrocalcic horizon does not control development of the fissure.

The strata overlying the upper petrocalcic horizon are predominantly silty or clayey sand (fig. 6). Calcium carbonate is dispersed throughout these sediments, which are only weakly cemented. The massive, gravelly sand overlying the upper petrocalcic horizon may be a poorly sorted sheetwash deposit or it may have been thoroughly bioturbated after deposition (figs. 4 and 5). No primary sedimentary structures are preserved in this unit.

Overlying the massive, gravelly sand is a layer of crossbedded silty sand. These are overbank deposits of relatively uniform thickness near fissure 1. This deposit has been radiocarbon-dated at 7,510±100 yr B.P. (fig. 6). The accretion rate for this unit is considerably greater than that of overlying sediments (table 1), which may explain why sedimentary structures in this unit are preserved. A rapid burial would have protected them from disturbance by shallow burrowing and root penetration or by reworking by wind and overland flow. This deposit contains snail fauna like that present in the area today, suggesting that climatic conditions at the time of deposition may have been similar to those now prevailing.

Over these crossbedded sediments is silty sand. The silty sand has no primary sedimentary structures, but blocky soil structure is weak to moderate (Sergent, Hauskins and Beckwith, 1989, their table 3.4c) (fig. 5). These sediments range in age from 7,010±200 yr B.P. to 1,440±80 yr B.P. (fig. 6). Accretion rate for these sediments is about one-tenth the rate for older sediments (table 1). A decrease in sedimentation rate would have allowed more time for soil development and bioturbation to occur, destroying whatever original sedimentary structures were present. Gravel lenses are relatively uncommon in the upper 5 ft (1.5 m) of the soil profile in the study area, on the basis of descriptions of cores and trenches. This suggests that streamflow decreased, possibly because of a decrease in runoff, during about the last 7,500 yr. The decrease in runoff may have resulted from a decrease in rainfall. The climate of this region became increasingly drier about 8,000 yr ago (Van Devender and Spaulding, 1979).

Near-surface strata (<20-ft [<6-m] depth) do not control development or location of fissure 1. In trench 4 the fissure can be interpolated over a local gap or channel cut in the petrocalcic horizon (fig. 4). But near its middle (trench 3) the fissure is located over an uneroded calcic horizon, which is composed largely of carbonate-cemented gravel that extends well beyond both sides of the fissure (fig. 3). A deep gap in the petrocalcic horizon is exposed in trench 5, where there is no fissure. Gravel lenses overlie the calcic horizon on the north side of the fissure, locally, but not on the south side (fig. 4).

Summary of fissure development at the study area. This summary begins with formation of the upper petrocalcic horizon, which is now covered by about 6.6 ft (2 m) of younger sediments (fig. 20, no. 1). The petrocalcic horizon formed in silty sand and sandy gravel, within about a meter of the paleo-ground surface. Carbonate-lined fractures (fig. 20, no. 2) formed as a normal part of calcrete development.

The soil above the petrocalcic horizon and the petrocalcic horizon itself were eroded locally, apparently by streamflow. Some fractures may have been widened by carbonate dissolution or erosion, analogous to the erosion of fractures by runoff in the ditches adjacent to the county road. There are channels or gaps in the carbonate-rich horizon in trenches 4 and 5.

Subsequently, gravelly, muddy sand was deposited on the exposed petrocalcic horizon (fig. 20, no. 3). This deposit may be a poorly sorted debris flow or sheetwash deposit, or it may have been bioturbated after deposition.

The gravelly sand was overlain by silty sand deposited about 7,500 yr ago (fig. 20, no. 4). It contains small-scale trough crossbeds, indicative of small channels carrying only fine-grained sediment. It is not heavily bioturbated, suggesting that it was buried rapidly or that root penetration and burrowing occurred only rarely after burial.

More sediment was deposited during the next 7,500 yr, probably as overbank deposits of ephemeral streams, or as eolian deposits (fig. 20, no. 5). There are no sedimentary structures to indicate the mode of deposition. Some channel gravels are present locally. Pedogenic processes produced blocky soil structure in the sandy sediments (fig. 4).

More recently, tension cracks formed (fig. 20, no. 6), and some became precursors to the fissure (fig. 20, no. 7). The source of this tension is unknown; there is no evidence of fault movement along the fissures.

Water introduced by overland flow eroded the tension crack at the surface, enlarging it and resulting in collapse of surface sediments into the fissure (fig. 20, no. 8). More tensional fracturing or desiccation of fill produced subvertical fractures in the fissure fill that were later lined with clay laminae (fig. 20, nos. 8 and 9). Aerial photographs taken in 1971 and 1985 reveal that collapse features at fissure 1 formed between those years. Collapse features at fissures 2 and 3 cannot be seen in the most recent photographs, so their age is undetermined. There are no surface collapse features at the relict fracture (fig. 18).

This summary describes the current state of development of fissure 1. Fissures 2 and 3 probably will follow similar patterns of development. In the future, overland flow will continue to enlarge the fissures until they fill with sediment—a process that may take many decades to complete. Fissures that were open in 1924 in Quitman Canyon, southeast of the study area, are still open today, and adjacent sediments are still collapsing into them.

Model of fissure development. In the model for fissure development proposed by Larson and Péwé (1986), the precursor of a fissure is a tension fracture (fig. 21, stage 1). The fracture forms in the shallow subsurface and is a preferred pathway for water moving downward from the surface. The fracture is enlarged by erosion until a soil pipe forms (fig. 21, stage 2). Sediments overlying the pipe collapse into the cavity, forming holes at the surface that directly capture surface runoff and sediment carried by surface runoff (fig. 21, stage 3). As the collapse features capture more runoff, they elongate and connect to form a laterally continuous fissure (fig. 21, stage 4). Eventually, the outlet of the soil pipe becomes plugged and the fissure begins to collect sediment (fig. 21, stage 5). Finally, the fissure fills with sediment. As long as it remains lower topographically than its surroundings, the fissure will preferentially collect and store moisture, providing better growing conditions for woody vegetation, especially deep-rooted phreatophytes such as mesquite (fig. 21, stage 6). At present, the surface fissures at the study area are at stage 3 or 4, as shown in figure 21. The relict fracture is beyond stage 6 because it is not marked by aligned vegetation or by a topographic low at the surface. The fissure there has been destroyed by subsequent erosion and deposition.

The principal mechanisms in the development of fissures are erosion of a preexisting crack at the surface and soil piping (fig. 21). According to Cooke and Warren (1973), it was Parker (1963) who identified four criteria that are necessary for piping to occur: (1) sufficient water to saturate part of the material above base level, (2) hydraulic head to permit subterranean water movement, (3) permeable and erodible soil above local base level, and (4) an outlet for flow. At the study area, surface water is present only after rain falls. No perennial streams or springs exist there. Thus, conditions 1 and 2 exist only locally and temporarily in ephemeral stream channels and other low areas, as a result of runoff-producing rainstorms. The third condition, permeable and erodible soil, is present everywhere in the study area. Local and temporary base level may be established at the base of this soil on top of the upper calcrete, which is 1.6 to 10 ft (0.5 to 3 m) below the ground surface. During and after heavy rains water could move down a preexisting tension fracture and collect on this surface either until it was removed by evapotranspiration or until it moved down

preexisting cracks in the petrocalcic horizon. The fourth condition needed for piping is an outlet for flow. Besides the deeper part of the fracture itself, the permeable grain-supported gravel that underlies the upper calcrete (fig. 3; pl. 3) may provide such an outlet. Thus, in the study area, conditions necessary for piping to occur along a fracture probably exist only locally, in topographic lows, and temporarily, during and after heavy rains.

Source of tensional stress. It is generally accepted that the fissure-controlling fractures are caused by tensional stress (Bull, 1972; Bouwer, 1977; Holzer and others, 1979; Jachens and Holzer, 1979, 1982; Bell, 1981; Larson and Péwé, 1986). Typically, the source of that stress is differential subsidence (Larson, 1986). Differential subsidence is most often attributed to withdrawal of ground water for agricultural or municipal use, which has produced declines in ground-water levels of 80 to 460 ft (25 to 140 m) in Arizona and California where fissures have developed (Holzer, 1977; Morton, 1977; Guacci, 1979; Bell, 1981; Holzer and Pampeyan, 1981; Boling, 1986; Larson, 1986; Larson and Péwé, 1986; Schumann and others, 1986). Other processes that can produce fractures, such as (1) tectonic movements, (2) desiccation of expansive clay soils, (3) hydrocompaction of low density sediments, and (4) horizontal seepage stress related to ground-water flow toward pumped areas, are less important than differential subsidence in desert basins of the southwestern United States (Larson and Péwé, 1986).

Differential subsidence and the fissures that result may be localized by different geological environments: (1) buried bedrock hills; (2) buried faults; (3) buried facies boundaries; and (4) the hinge line of subsiding areas (Larson and Péwé, 1986). Boling (1986) described the typical setting of earth fissures in south-central Arizona. They are located on alluvial plains between basin centers and basin-bounding mountains. The fissured sites overlie or are mountainward of inferred basin-boundary faults. The basins are underlain by thick, unconsolidated alluvium, anhydrite, and indurated conglomerate deposits, and they are bounded by fault-uplifted mountains. Depth to bedrock is 160 to 980 ft (50 to 300 m). Boling (1986, p. 760) asserted that "differential compaction of nonindurated sediments overlying irregular bedrock surfaces probably accounts for most of the major earth fissures seen at the surface."

46

Conditions similar to these prevail at the Fort Hancock study area, which is located on an alluvial plain between the center of the Hueco Bolson and the Diablo Plateau. It is upslope from the Campo Grande fault, which strikes parallel to the basin margin in the manner of basin-bounding faults. Depth to Cretaceous bedrock is about 560 to 720 ft (170 to 220 m), which is within the range of depths in the area studied by Boling (1986). However, despite these similarities, it is unknown whether relief on buried Cretaceous bedrock is affecting the development or location of the fissures in the study area.

Seismic reflection data were collected at the study area by Phillips and others (1986) and reinterpreted by scientists at the Department of Geological Sciences of the University of Texas at El Paso. Phillips and his coworkers (1986) inferred two high-angle faults in the study area. The more recent work infers two low-relief highs on Cretaceous bedrock at about the same locations (Diane Doser, University of Texas at El Paso, written communication to Jay Raney, 1990). Compaction of bolson sediments over these structures may cause the tension that is manifested at the surface by formation of fissures in a manner similar to that described by Larson and Péwé (1986). Those authors attributed formation of a surface fissure to differential compaction over a bedrock hill covered with 150 ft (45 m) of unconsolidated sediments. However, there are problems with this argument by analogy. First, the depth to Cretaceous bedrock in the vicinity of fissure 1, which is based on core from well LLW14 (2,600 ft [800 m] to the southeast), is about 660 ft (200 m), more than 500 ft (150 m) deeper than the bedrock hill studied by Larson and Péwé (1986). Second, the buried bedrock hill described by Larson and Péwé had local relief of about 100 ft (30 m). The bedrock high near fissure 1 has about half of that. Deeper burial of a smaller structure does not favor the argument for tensional fracturing at the surface in the study area. Third, fissures 1 and 3 and the relict fracture display no consistent orientation or position relative to these subsurface structures (fissure 2 is outside the area where seismic data were collected). Fourth, there has not been any significant drawdown of ground water at the Fort Hancock study area. At the Arizona site examined by Larson and Péwé, water-table levels had declined 300 ft (90 m).

In the Fort Hancock study area depth to ground water is 360 to 590 ft (110 to 180 m) (Mullican and Senger, 1990). No wells in the area have produced ground water in amounts sufficient to lower ground-water levels. Therefore, even though alluvial cover is thicker locally than depth to ground water, which provides the potential for compaction, it is unlikely that differential compaction has occurred, because no significant ground water withdrawal has occurred.

Because there has not been any large-scale withdrawal of ground water near the Fort Hancock study area, the fissures there must be attributed to natural phenomena. They may have formed as a result of naturally occurring differential compaction of weakly consolidated sediments over a bedrock high or a buried fault scarp, or they may be located at the hinge line of a subsiding area. More compressible, finer grained sediments nearer the center of the Hueco Bolson may have compacted more over geologic time than did the coarser grained proximal fan sediments near the basin margins (where the study area is). Similarly, the water table in bolson sediments has been lowered over geologic time by incision of the Rio Grande and dewatering of sediments above the lower base level. Incision of the arroyos, especially upstream from the Campo Grande fault, would have had a similar effect on the water table there. Eventually, compaction would have led to extensional stress at the point where curvature of the compacted surface changed: at the edges of the compacting sediments, where overlying materials are stretched over a noncompacting edge. There is not enough detailed stratigraphic information available from wells at the study area to determine whether there is a facies boundary such as this beneath the fissures (pl. 1). Alternatively, desiccation of clay-rich Quaternary sediments or the Fort Hancock Formation may be producing tensile stress in overlying sediments.

Similar hydrologic and geologic conditions may prevail in nearby drainage basins where there has been little pumping of ground water and where fissures have existed for as long as 60 yr. Sustained desiccation of surface sediments in some areas may explain the appearance of polygonal fractures. But the fissures at the study area are not polygonal, although they may be the first components of a polygonal system that is beginning to form.

Fissures in region

Other investigators have reported surface fissures in the Trans-Pecos region of Texas and in northeastern Chihuahua (fig. 22). In an early account, Baker (1927, p. 40), observed "deep, straight, and narrow cracks...[cutting]...the clays of the arroyo beds and the gravels of the benches" in the Green River valley. The valley of the Green River is west of the Van Horn Mountains, about 60 mi (100 km) southeast of the study area (fig. 22; table 8). Baker attributed the fissures to earthquakes and speculated that they may have formed in 1887 during the "great earthquake in northeastern Sonora." However, he provided no evidence for either the origin or the age of the fissures.

The cracks are not visible in aerial photographs taken in 1950 (Underwood and DeFord, 1975) or on photographs taken in 1957, but a 2,400-ft-long (740-m) fissure formed in the same area in May 1959 (Underwood and DeFord, 1975), cutting across a road. No fissure was seen near the locality studied by Baker (1927) when the Green River valley was visited in 1989.

Albritton and Smith (1965) reported "earthquake cracks" in alluvium near the center of Quitman Canyon, about 38 mi (60 km) from the study area (fig. 22). According to those authors (Albritton and Smith, 1965, p. 111), the cracks were "said to have formed" during the Valentine, Texas, earthquake (August 16, 1931), whose epicenter was 75 mi (120 km) to the east of Quitman Canyon. However, Albritton and Smith offer no evidence to support their contention, which is disputed by an eyewitness, R. H. Espy, a resident of Eagle Flat (fig. 22). Underwood and DeFord (1975) reported that Espy saw the fissures in Quitman Canyon during a cattle roundup in about 1924, 7 yr before the Valentine earthquake. Furthermore, Sellards (1932) reported that, other than in the town of Valentine, no ground disturbance was detected after the 1931 earthquake. He compiled observations from localities throughout the region where the earthquake was felt, including Sierra Blanca and Van Horn (fig. 22). The lack of reported "earthquake cracks" in the region may have resulted from a dearth of observers. Nevertheless, it is more reasonable to accept

Espy's account of the preexisting cracks in Quitman Canyon than the unsupported claim by Albritton and Smith (1965) of an earthquake-related origin.

The Quitman Canyon fissures are at the toe of a dissected alluvial fan, cutting Quaternary alluvium at the surface. The cracks are roughly orthogonal to one another, and they intersect to form polygons as wide as 1,280 ft (390 m) (on the 1957 photographs). The longer set trends N10°–25°W, parallel to topographic contours, to faults in the Quitman Mountains (about 3.8 mi [6 km] to the west-northwest), and to the valley axis. These fissures were as long as 2.6 mi (4.2 km) on aerial photographs taken in December 1957 (table 8). The shorter fissures trend N65°– 80°E. A calcic soil horizon composed of carbonate-cemented sand is present locally at the surface and is exposed in the fissure walls at depths of less than a meter. Ephemeral stream channels between fan remnants are perpendicular to the longest fissures. The major northwest-trending collapse features cut across drainage and intercept runoff. Woody vegetation (mesquite and tarbush) is more abundant within a few meters of the fissures than farther away, especially in a downslope direction. This suggests that the fissures capture all but the largest overland flows.

Locally, the fissures in Quitman Canyon showed evidence of recent collapse in 1989. One segment was 11.6 ft (3.55 m) deep but only 30 inches (75 cm) wide, deeper than any fissure at the study area. The width/depth ratio for this segment is very low (0.2) (table 8), indicating that it is still undergoing collapse. Fissure walls here were steep and unvegetated, showing that collapse had occurred recently. However, the fissures did not appear to be any longer (at the southern ends) than they were on photographs from 1957. Elsewhere, the fissures have filled with sediment washed in from upslope, and width/depth ratio has increased to 5 (table 8).

Another set of polygonal fissures was observed in 1957 aerial photographs of Quitman Canyon. The fissures are about 2.5 mi (4 km) south of those described previously and reported by Albritton and Smith (1965). The longest fissure was about 650 ft (200 m) long in 1957, about as long as those now at the study area.

A third set of fissures in Quitman Canyon was discovered in September 1985. In 1989 these fissures were reported to form a rectilinear pattern (Sergent, Hauskins and Beckwith, 1989). The fissures were as much as 1,000 ft (305 m) long, 6 ft (1.8 m) wide and 5 ft (1.5 m) deep.

Haenggi (1966) and Underwood and DeFord (1969) reported fissures in Bolson El Cuervo, northeastern Chihuahua (fig. 22), about 88 mi (140 km) south-southeast of the study area. Underwood and DeFord attributed formation of a new system of fissures in 1959 to drying of alluvium during a severe drought that lasted from 1950 to 1956. They observed that "torrential downpours" can widen fissures from an initial hairline crack to a width of 3 to 5 ft (1 to 1.5 m), and then fill them with sediment.

The same authors reported fissures at Eagle Flat (Underwood and DeFord, 1975), about 50 mi (80 km) southeast of the study area (fig. 22). According to R. H. Espy, the owner of the property where they were located, the fissures appeared in 1927 or 1928, 3 or 4 yr before the Valentine earthquake (Underwood and DeFord, 1975). They are visible in aerial photographs of the area taken in 1957. Underwood and DeFord (1975) reported that the longest fissure was about 2,500 ft (760 m) long and orthogonal fissures were about 590 to 790 ft (180 to 240 m) long, but in aerial photographs taken in 1957 the main fissure was about 3,000 ft (910 m) long. The main fissure is arcuate, convex toward the southeast and approximately perpendicular to local drainage.

The original fissure is currently degraded by overland flow. Locally, it is as much as 55 ft (17 m) wide and about 2 ft (60 cm) deep, and has the highest width/depth ratio (as much as 28) of any fissure seen during this study (table 8). Earthen dams less than 6 ft (2 m) high have been built across it, trapping sediment that was being transported along the fissure, which acts as an ephemeral stream channel. The surface immediately upslope from the fissure has aggraded, burying a fence with about a meter of sediment. A second fissure has developed upslope from the oldest fissure on this aggraded surface. It is as much as 5.5 ft (1.7 m) wide and 2.3 ft (70 cm) deep and has an intermediate width/depth ratio (as much as 2.7). It is nearly continuous, with few bridged-over segments. This fissure is subparallel to the oldest fissure and intersects it where small gullies have eroded upslope from the oldest fissure. A third fissure is now forming upslope from

the second fissure at a point about midway along the oldest fissure. It is only 210 ft (65 m) long, much shorter than either of the other two, and is composed of separate collapse features as much as 1.1 ft (35 cm) wide and 2.6 ft (80 cm) deep (width/depth ratio = 0.4). This fissure is similar to the one at the study area.

Apparently the fissure-collapse process is moving laterally upslope, subparallel to the oldest fissure. The tensional stress that causes the fissures to form is migrating laterally as well. The youngest collapse features still receive runoff from the drainage area upslope, unobstructed by the other fissures. The oldest fissure appears to be inactive and is gradually being infilled and degraded by surface processes. No collapse features currently exist at the south end of the main fissure, where they appeared in 1957 photographs.

Goetz (1977, 1985) described giant desiccation cracks in Salt Flat, in the Salt Basin Graben 60 mi (100 km) east of the study area (fig. 22). The cracks are located at the terminus of an alluvial fan. Smaller, shorter fissures connect the longest fissure and others parallel to it to form polygons. The longest fissure (2,600 ft [800 m]) is perpendicular to ephemeral stream channels flowing east-northeast. This fissure is slightly arcuate, concentric to a closed basin to the east. The longest fissures in the polygonal system of cracks trend roughly north-south.

The oldest known evidence of these fissures is their presence in aerial photos taken in 1946 (Goetz, 1977). The fractures may have existed for months or years before they appeared at the surface. According to Goetz (1977), the most important process contributing to the formation and growth of these cracks is desiccation of the surface and subsurface caused by prolonged drought and ground-water withdrawal. She also observed (Goetz, 1985) that the longest cracks are parallel to a nearby series of fault scarps that cut the alluvium, concluding that these dominant fissures probably represent the trace of a Holocene fault that is covered by bolson sediments. Goetz (1977, p. 89) speculated that the parallelism of primary fissures in separate groups of these orthogonal features may be the result of "uneven subsidence" across a buried fault. Further, she proposed that abrupt movement on this inferred fault during the Valentine earthquake may have caused failure of the alluvium, which was already undergoing brittle failure because of desiccation at depth.

However, she based her proposed earthquake origin on the similarity between these fissures and the description by Albritton and Smith (1965) of the "earthquake cracks" in Quitman Canyon. We have already noted that this proposed origin is contradicted by an eyewitness account. The orthogonal pattern of fracturing indicates that desiccation is the primary mechanism forming the fissures at Salt Flat.

Fissures in southwestern United States

Ground fissures have been reported in the southwestern United States, beginning as early as the 1920's (Baker, 1927; Leonard, 1929) from southern California to western Texas. Those most frequently studied are in the alluvial basins of Arizona, where ground-water withdrawal has led to differential compaction of alluvium over irregular bedrock surfaces, producing fissures at the ground surface.

Fissures in south-central Arizona (Boling, 1986) are linear and curvilinear features, generally segmented, in places forming en echelon patterns similar to that at fissure 1 (fig. 19). The fissures described in Arizona have several characteristics in common. They form in unconsolidated sediments, typically near margins of alluvial valleys or near outlying bedrock outcrops where ground-water levels have dropped 200 to 440 ft (60 to 135 m) (Larson and Péwé, 1986). Vertical offset is usually negligible, suggesting that fissures are of tensile origin. Simple horizontal separation of the blocks on either side of the fracture indicates that fractures are tensional breaks (Schumann and others, 1986). Vertical offset has been observed along a few fractures after the initial break occurred. Movement of blocks perpendicular to the crack surface shows that fractures are caused by tension and distinguishes fractures from faults where relative displacements are predominantly parallel to the failure zone (Holzer and others, 1979). Subsidence fractures propagate upwards and are usually exposed at the surface after surface sediments are eroded by heavy rainfall or by irrigation water (Larson and Péwé, 1986). Fissures are generally perpendicular to drainage, intercepting runoff that erodes the initial narrow crack to form a gully that can be

several meters wide (Larson and Péwé, 1986). Because the fissures act as local catchment basins for runoff, vegetative growth along them is more vigorous.

The fissures tend to connect and form linear fissure systems (Schumann and others, 1986). They are as much as 9 mi (15 km) long and may be as much as 50 ft (15 m) wide and 80 ft (25 m) deep (Boling, 1986; Slaff, 1989). Erosion at the surface enlarges them to form "fissure gullies" that are commonly 3 to 16 ft (1 to 5 m) wide, 3 to 13 ft (1 to 4 m) deep, and hundreds of feet long.

The Pixley, California, fissure (Guacci, 1979) was slightly arcuate and relatively continuous, 0.5 mi (0.8 km) long, 8 ft (2.4 m) wide, and 6 ft (1.8 m) deep. No vertical or lateral displacement was observed along the fissure. When described 5 yr after it appeared, cracks beneath the fissure extended to a depth of at least 55 ft (16.8 m), deeper than the water table (48 ft [14.6 m]). The cracks bifurcated and deflected toward one another. Opposite walls matched in many places, indicating no vertical offset had occurred on the fracture.

In several places within the fracture fill discontinuous, vertical strata or lensing near one crack wall was composed of a different soil type than near the opposite wall. Presence of vertical strata along fracture walls and in the center of the fracture fill and horizontal strata in the fracture fill suggest multiple periods of fracture filling (Guacci, 1979). Similar features were observed in the fracture fill at fissure 1 and at the relict fracture at the Fort Hancock study area.

Morton (1977) described fissures in the San Jacinto Valley, California. Most were linear and oriented parallel or subparallel to the Casa Loma fault, a basin-bounding fault on one side of the valley. Fissures adjacent to a bedrock hill were arcuate, and those nearest the hill conformed to the contact between alluvium and bedrock.

Overland flow contributes to formation and enlargement of collapse features that form the fissure at the surface. This process is recorded in reports on fissures in Arizona (Leonard, 1929; Holzer, 1976; Boling, 1986), California (Morton, 1977; Guacci, 1979), Texas (Underwood and DeFord, 1975), and with the model proposed by Larson and Péwé (1986). In Arizona, where fissures have been described extensively, many of them are nearly perpendicular to drainage. The

Pixley fissure appeared in an area of extensive ground-water extraction within the San Joaquin Valley, following surface flooding (Guacci, 1979). It is inferred that the ground-water extraction produced differential subsidence; differential subsidence resulted in tension cracks; and surface flooding produced the fissure by piping, erosion, and collapse of the walls of the fracture.

According to Schumann and others (1986), land subsidence caused by ground-water depletion has produced extensive areas of earth fissures in southern Arizona. Ground-water levels in the Arizona basins have declined as much as 330 ft (100 m) since 1923 (Boling, 1986). Wells there now pump from depths as great as 2,500 ft (760 m). Large-scale pumping of ground water in southern Arizona began about 1900 and increased in the late 1940's (Schumann and others, 1986). Ground-water depletion has caused water levels to decline as much as 460 ft (140 m), resulting in compaction of silt and clay layers, and land subsidence. Aquifer compaction occurred seasonally, during summer periods of water-level decline. Some of that compaction occurred at depths greater than 830 ft (253 m). "The temporal and spatial distribution of fissures is determined by the historical development of water resources, hydrogeologic characteristics and subsidence history of a particular basin" (Larson, p. 292, 1986).

Larson and Péwé (1986) reviewed the literature on earth fissures and listed several mechanisms related to ground-water withdrawal that have been proposed to explain the origin of fissures: localized differential compaction, hydrocompaction, horizontal seepage forces, shrinkage of dewatered sediments, and regional differential compaction. They cited recent geophysical and geodetic surveying work to support their conclusion that many fissures are caused by differential subsidence localized by buried bedrock hills or fault scarps. Their own work in northeastern Phoenix, Arizona, showed that an earth fissure there was spatially associated with a convex-upward gravity anomaly. This gravity anomaly was interpreted to have at least 100 ft (30 m) of relief and to be buried 150 ft (45 m) deep, a depth comparable to the original water level in the area.

Localized differential subsidence across the Picacho fault was caused by differential compaction due to unequal water-level declines across a preexisting fault (Jachens and Holzer,

1979). Surface faulting caused by ground-water withdrawal occurred 12 years after fissuring began, which suggests that differential compaction may have produced the tension that caused fissuring (Holzer and others, 1979; Jachens and Holzer, 1979).

Fissures form at points of maximum horizontal tensile stress near maximum convex-upward curvature of the subsidence profile (Larson, 1986). Fissures may be localized in three geologic settings: (1) buried bedrock hills; (2) the hinge line of subsiding areas; and (3) buried faults (Larson and Péwé, 1986). According to a study by Jachens and Holzer (1979), earth fissures in alluvium near exposed bedrock were spatially associated with local gravity and magnetic anomalies ranging from local highs to convex-upward changes in slope. Most bedrock irregularities were at depths less than 820 ft (250 m). However, irregularities were not detected beneath fissures that were more than 1.2 mi (2 km) from bedrock outcrops (Jachens and Holzer, 1979). Differential compaction of unconsolidated alluvium over bedrock highs was the dominant source of horizontal tension that caused earth fissures in Picacho basin, Arizona (Jachens and Holzer, 1979, 1982). Withdrawing ground water from the unconsolidated alluvium caused the differential compaction (Jachens and Holzer, 1982).

Larson and Péwé (1986) discussed another potential setting for fissuring: near the hinge line of subsidence, the inferred boundary between subsiding and stable areas. The zone is dependent on a critical depth to bedrock related to the original ground-water level prior to pumping. In the Phoenix area this is about 150 to 250 ft (45 to 75 m). Little or no compaction should occur where the thickness of alluvial cover is less than the original depth to ground water.

Rough volume estimates based on observed dimensions of the crack at the Pixley fissure indicated that the crack could accommodate the volume of surface material lost from the fissure at the surface (Guacci, 1979). Persistent crack width with depth was consistent with tensional cracking generated by maximum convex-upward curvature near the edge of the subsidence bowl. Cross-sectional areas of unfilled, upper parts of fissures in arid areas commonly exceed 37.5 ft^2 (3.5 m^2). If the average width of a fissure is 1 inch (2.5 cm), a depth of 450 ft (140 m) is estimated (Holzer, 1976).

Some fissures have formed in areas where no substantial ground-water withdrawal has occurred. In this regard they are similar to the fissures in the Fort Hancock study area. The Picacho fissure formed on September 11 or 12, 1927, 3 mi (4.8 km) southeast of Picacho, Arizona, after a severe rainstorm (Leonard, 1929). Initially, the fissure was about 1,000 ft (300 m) long; its greatest measurable depth was 15 ft (4.6 m). No vertical displacement was visible at the outset. The fissure was attributed to uneven settling of basin-fill material, which was intensified by seismic shock of an earthquake that occurred on the evening of September 11, 1927, somewhere in the southwestern United States or northern Mexico about 200 mi (320 km) from the fissure. However, "no profound tectonic disturbance occurred in the Picacho area" (Leonard, 1929, p. 774).

Other fissures have formed either in areas where ground-water pumping has not been extensive (Robinson and Peterson, 1962), or before ground-water pumping began (Bull, 1972). Fissures in Black Canyon, Arizona, appeared as early as 1936. Near Sells, Arizona, a fissure 0.5 to 0.75 mi (0.8 to 1.2 km) long was first observed in the early 1950's. It intersected local drainage at right angles. At the time, ground water was not used extensively for irrigation. Bull (1972) described cracks that formed in alluvial fans prior to irrigation. He attributed their formation to hydrocompaction of moisture-deficient deposits. Water flowing across the surface of the fans wetted the deposits adjacent to the channels, causing subsidence and cracking parallel to the channels. These reports of naturally occurring fissures indicate that they can form as a result of natural geomorphic processes in arid desert basins.

CONCLUSIONS

The Fort Hancock study area is located in the Hueco Bolson, within the drainage basins of Alamo and Camp Rice Arroyos. The arroyos have incised to their current levels by adjusting to base-level changes caused by downcutting on the Rio Grande and by surface rupture events where the Campo Grande fault crosses the arroyo channels. The arroyos are at their lowest point of

incision upstream from the fault where the Fort Hancock Formation crops out in the floors of stream channels. There are no thick packages of alluvium underlying the arroyo channels or filling the arroyo valleys. The recent geomorphic history of the arroyos has been dominated by continual downcutting interrupted by short periods of alluviation. The most recent period of alluviation ended 400 to 1,300 yr ago. At present, nickpoints in alluvium are advancing headward as the sediments are episodically removed during infrequent runoff events.

Rates of headcut retreat in alluvial fill vary by more than two orders of magnitude and depend upon the time span involved in the calculation. The rate of headcut retreat varies from 1.6 inches/yr to 5.2 ft/yr (0.04 to 1.6 m/yr) for periods of 400 to 1,330 yr. Historical rates, calculated for the 44-yr period between 1941 and 1985, are much greater, ranging from 7.2 to 23 ft/yr (2.2 to 7.0 m/yr). These rates apply only to the removal of unconsolidated alluvium within the incised arroyo channels. They do not represent rates of expansion of the drainage network upslope onto the low-relief surface of the study area. Evidence from aerial photointerpretation indicates that headcut retreat on the strongly cemented calcrete that underlies the study area is much slower than in the alluvial fill. Some headcuts in valley-side gullies did not retreat by a measurable amount (50 ft [15 m]) during the 44-yr period examined, whereas some headcuts in alluvium in adjacent gullies retreated, on average, 490 ft (150 m). These results indicate that the calcrete inhibits headcut retreat, especially where the calcrete is a strongly cemented, laminated sand.

The strata underlying the study area and cropping out locally are the Tertiary Fort Hancock and Tertiary-Quaternary Camp Rice Formations and younger Quaternary strata. The older formations are composed primarily of interbedded sand, silt, and clay, with local concentrations of gravel. The younger Quaternary sediments have less clay and more gravel than the two older formations. At most outcrops the lower contact of the Quaternary alluvium is an eroded surface overlain by gravel. The younger Quaternary strata can be subdivided into four units: a basal gravel, a middle sand, a strongly cemented upper sand or gravel (Stage III–IV calcrete), and an uppermost layer (locally absent) of silty, clayey sand. The calcrete underlies the study area mostly at depths

less than 1 ft (30 cm). Locally it has been eroded by streams and is cut out by coarse-grained, sandy gravel deposits.

The calcrete is interpreted to be the upper surface of the Madden Gravel, a remnant of a formerly continuous surface developed before the arroyos incised to their current levels. Stage III–IV calcretes typically require at least 25,000 to 75,000 yr to develop the laminated character shown by this calcrete.

Pedologic data indicate that the Quaternary strata overlying the calcrete accumulated during the last 7,500 yr. The sandy strata that have been radiocarbon-dated range in age from 7,510±100 yr B.P. to 1,440±80 yr B.P. Accretion rates for these sediments appear to have slowed considerably, from 2.1 mm/yr to 0.2 mm/yr, after about 7,000 yr ago. This slowdown may be a result of a shift toward warmer and drier climatic conditions that occurred about 8,000 yr ago. Archeological evidence suggests that parts of the surface in the study area have been relatively stable for about the last 900 yr.

Short-term (14 months) erosion monitoring has shown that most sediment transport is caused by surface runoff following intense rainfall events. In the periods between extreme (25-yr recurrence interval) rainfall events, very little sediment is moved. Eolian transport occurs where sand dunes are present, but aerial photointerpretation showed that individual dunes changed little between 1941 and 1985. Most environments that were monitored during the observation period showed 0.25 inch (0.1 cm) or less of net erosion or deposition.

The surface of the study area is composed primarily of low-relief interfluves and drainageways of ephemeral streams. These and other landforms at the study area are the products of long-term operation of geomorphic processes. Gravel-covered topographic highs and uplands probably represent coarse-grained channel deposits of the younger Quaternary alluvium that are relatively resistant to erosion and consequently have higher local relief than the sandier, more erodible sediments around them. The dunes that cover the southwest corner of the study area have been largely unchanged since at least 1941. Terraces and floodplains are formed by downcutting and alluviation along the incised reaches of arroyos. Roads crossing the study area act as manmade

streams during runoff events, diverting flow from natural channels and possibly enhancing downcutting in ephemeral stream channels over long periods of time.

Three surface fissures in the study area formed as a result of surface collapse and piping along preexisting tension fractures. The surface-collapse features are aligned in discontinuous, curvilinear segments that overlap locally. All three surface fissures are in local topographic lows, which indicates that concentrated overland flow is an essential component in their development. A relict fracture, with no surface fissure above it, has been exposed in a 20-ft (6-m) deep trench at the study area. It is not in a topographic low now, but may have been in the past. The surface-collapse features that developed over it have been removed by subsequent erosion and deposition.

Tension fractures are typically 0.8 to 1.6 inches (2 to 4 cm) wide where they have not been widened by erosion or slumping. Mirror-image symmetry of the opposite walls of the fractures is common. The fractures extend at least 20 ft (6 m) deep below the ground surface. Internal clay laminae within the fracture-filling sediment represent multiple filling events and may be evidence of more than one episode of fracture opening.

The source of tensional stress that formed the tension fractures is unknown. Similar fractures in similar settings in Arizona and California have been attributed to differential compaction of unconsolidated sediments over bedrock irregularities. Compaction is commonly caused by withdrawal of ground water. However, the water table in the study area is much deeper than in other areas where fissures have been studied, and no significant drawdown has occurred in the study area. Furthermore, bedrock irregularities beneath the study area are buried deeper and have less local relief than those reported at other fissure sites.

Fissures are present in other basins in the vicinity of the study area where ground water withdrawal has not occurred as it has in Arizona and California. In addition, fissures have formed prior to inception of ground-water withdrawal in some basins. Thus, fissure development appears to be a natural geomorphic phenomenon in arid desert basins.

ACKNOWLEDGMENTS

REFERENCES

Akhter, M. S., Dutton, A. R., Kim, J. H., and Brion, L. M., 1990, Surface-water hydrology of proposed Texas low-level radioactive waste isolation site: The University of Texas at Austin, Bureau of Economic Geology, report prepared for the Texas Low-Level Radioactive Waste Disposal Authority under Interagency Contract Number 90-008 IAC(90-91) 0268.

Albritton, C. C., Jr., and Smith, J. R., Jr., 1965, Geology of the Sierra Blanca area, Hudspeth County, Texas: U.S. Geological Survey Professional Paper 479, 131 p.

Antevs, Ernst, 1952, Arroyo-cutting and filling: Journal of Geology, v. 60, p. 375–385.

Baker, C. L., 1927, Exploratory geology of a part of southwestern Trans-Pecos Texas: University of Texas, Austin, Bulletin 2745, 70 p.

Baumgardner, R. W., Jr., 1987, Morphometric studies of subhumid and semiarid drainage basins, Texas Panhandle and northeastern New Mexico: The University of Texas at Austin, Bureau of Economic Geology Report of Investigations No. 163, 68 p.

Bell, J. W., 1981, Subsidence in Las Vegas valley: Mackay School of Mines, University of Nevada, Reno, Bureau of Mines and Geology Bulletin 95, 84 p.

Boling, J. K., 1986, Earth-fissure movements in south-central Arizona, U.S.A., in Johnson, A. I., Carbognin, Laura, and Ubertini, L., (eds.), Land subsidence: Proceedings of the Third International Symposium on Land Subsidence, Venice, Italy, March 19–25, 1984, IAHS-AIHS, International Association of Hydrological Sciences Publication No. 151, p. 757–766.

Bouwer, Herman, 1977, Land subsidence and cracking due to ground-water depletion: Ground Water, v. 15, no. 5, p. 358–364.

Branson, F. A., 1985, Vegetation changes in western rangelands: Society for Range Management, Range Monograph No. 2, 76 p.

Bryan, Kirk, 1928, Historic evidence on changes in the channel of the Rio Puerco, a tributary of the Rio Grande in New Mexico: Journal of Geology, v. 36, p. 265–282.

Bryant, V. M., Jr., and Holloway, R. G., 1985, A Late-Quaternary paleoenvironmental record of Texas: an overview of the pollen evidence, in Bryant, V. M., Jr., and Holloway, R. G., (eds.), Pollen records of Late-Quaternary North American sediments: Dallas, Texas, American Association of Stratigraphic Palynologists, p. 39–70.

Bull, W. B., 1972, Prehistoric near-surface subsidence cracks in western Fresno County, California: U.S. Geological Survey Professional Paper 437-C, 85 p.

Collins, E. W., and Raney, J. A., 1990, Description and Quaternary history of the Campo Grande Fault of the Hueco Basin, Hudspeth and El Paso Counties, Trans-Pecos Texas: The University of Texas at Austin, Bureau of Economic Geology, report prepared for the Texas Low-Level Radioactive Waste Disposal Authority under Interagency Contract Number 90-008 IAC(90-91) 0268, 69 p.

Cooke, R. U., and Reeves, R. W., 1976, Arroyos and environmental change in the American Southwest: Oxford, Clarendon Press, 213 p.

Cooke, Ronald U., and Warren, Andrew, 1973, Geomorphology in deserts: Berkeley, California, University of California Press, 374 p.

Direccion General de Geografia, 1982, Carta Geologica San Antonio el Bravo, Estados Unidos Mexicanos, Map 13-5, scale 1:250,000.

Freeman, C. E., 1972, Pollen study of some Holocene alluvial deposits in Dona Ana County, southern New Mexico: Texas Journal of Science, v. 24, no. 2, p. 203–220.

Gardner, J. L., 1951, Vegetation of the creosotebush area of the Rio Grande Valley in New Mexico: Ecological Monographs, no. 21, p. 379–403.

Gerald, R. E., 1988, Report on an intensive archeological survey of the proposed Hudspeth County low-level radioactive waste disposal site, Hudspeth County, Texas: contract report prepared for the Texas Low-Level Radioactive Waste Disposal Authority, Austin, Texas, 45 p.

Gile, L. H., Hawley, J. W., and Grossman, R. B., 1981, Soils and geomorphology in the Basin and Range area of southern New Mexico—Guidebook to the desert project: New Mexico Bureau of Mines and Mineral Resources, Memoir 39, 222 p.

Goetz, L. K., 1977, Quaternary faulting in Salt Basin Graben, West Texas: The University of Texas at Austin, Master's thesis, 136 p.

——————— 1985, Giant polygonal desiccation cracks in Wildhorse Flat, West Texas—revisited, in Dickerson, P. W., and Muehlberger, W. R., (eds.), Structure and tectonics of Trans-Pecos Texas: West Texas Geological Society, Publication 85-81, p. 235–238.

Gregory, K. J., and Gardiner, V., 1975, Drainage density and climate: Zeitschrift fur Geomorphologie N. F., v. 19, no. 3, p. 287–298.

Guacci, Gary, 1979, The Pixley fissure, San Joaquin Valley, California, in Saxena, S. K. (ed.), Evaluation and prediction of subsidence: International Conference on Evaluation and

Prediction of Subsidence, Pensacola Beach, Florida, January 1978, American Society of Civil Engineers, p. 303–319.

Gustavson, T. C., 1990, Sedimentary facies, depositional environments, and paleosols of the upper Tertiary Fort Hancock Formation and the Tertiary- Quaternary Camp Rice Formation, Hueco Bolson, West Texas: Bureau of Economic Geology, The University of Texas at Austin, report prepared for the Texas Low-Level Radioactive Waste Disposal Authority under Interagency Contract Number 90-008 IAC(90-91) 0268.

Haas, Herbert, Holliday, Vance, and Stuckenrath, Robert, 1986, Dating of Holocene stratigraphy with soluble and insoluble organic fractions at the Lubbock Lake Archeological Site, Texas: an ideal case study: Radiocarbon, v. 28, no. 2A, p. 473–485.

Haenggi, W. T., 1966, Geology of El Cuervo area, northeastern Chihuahua, Mexico: The University of Texas at Austin, Ph.D. dissertation, 403 p.

Hall, S. A., 1985, Quaternary pollen analysis and vegetational history of the Southwest, *in* Bryant, V. M., Jr., and Holloway, R. G., (eds.), Pollen records of Late-Quaternary North American sediments: Dallas, Texas, American Association of Stratigraphic Palynologists, p. 95–123.

Hastings, J. R., and Turner, R. M., 1965, The changing mile: Tucson, Arizona, University of Arizona Press, 317 p.

Henry, C. D., Gluck, J. K., and Bockoven, N. T., compilers, 1985, Tectonic map of the Basin and Range province of Texas and adjacent Mexico: The University of Texas at Austin, Bureau of Economic Geology, Miscellaneous Map No. 36, scale 1:500,000.

Hereford, Richard, 1987, Sediment-yield history of a small basin in southern Utah, 1937–1976: Implications for land management and geomorphology: Geology, v. 15, no. 10, p. 954–957.

Hershfield, D. M., 1961, Rainfall frequency atlas of the United States: U.S. Department of Commerce, U.S. Weather Bureau, Technical Paper No. 40, 115 p.

Holzer, T. L., 1977, Ground failure in areas of subsidence due to ground-water decline in the United States, *in* Land subsidence symposium: International Association of Hydrological Sciences, Publication No. 121, Proceedings of the Second International Symposium, Anaheim, California, Dec. 13–17, 1976, p. 423–233.

Holzer, T. L., Davis, S. N., and Lofgren, B. E., 1979, Faulting caused by groundwater extraction in southcentral Arizona: Journal of Geophysical Research, v. 84, no. B2, p. 603–612.

Holzer, T. L., and Pampeyan, E. H., 1981, Earth fissures and localized differential subsidence: Water Resources Research, v. 17, no. 1, p. 223–227.

Horowitz, A., Gerald, R. E., and Chaiffetz, M. S., 1981, Preliminary paleoenvironmental implications of pollen analyzed from Archaic, Formative, and Historic sites near El Paso, Texas: The Texas Journal of Science, v. 33, no. 1, p. 61–72.

Horton, R. E., 1932, Drainage basin characteristics: American Geophysical Union, Transactions, v. 13, p. 350–361.

Humphrey, R. R., and Mehrhoff, L. A., 1958, Vegetation changes on Arizona grassland ranges: Ecology, v. 39, p. 720–726.

Jachens, R. C., and Holzer, T. L., 1979, Geophysical investigations of ground failure related to ground-water withdrawal—Picacho Basin, Arizona: Ground Water, v. 17, no. 6, p. 574–585.

———————— 1982, Differential compaction mechanism for earth fissures near Casa Grande, Arizona: Geological Society of America Bulletin, v. 93, no. 10, p. 998–1012.

Keller, R. G., 1990, Gravity Survey: The University of Texas at El Paso, Department of Geosciences, report prepared for the Texas Low-Level Radioactive Waste Disposal Authority under Interagency Contract Number 90-008 IAC(90-91) 0268.

Larson, M. K., 1986, Potential for subsidence fissuring in the Phoenix, Arizona U.S.A. area, in Johnson, A. I., Carbognin, Laura, and Ubertini, L., (eds.), Land subsidence: Proceedings of the Third International Symposium on Land Subsidence, Venice, Italy, March 19–25, 1984, IAHS-AIHS, International Association of Hydrological Sciences Publication No. 151, p. 291–299.

Larson, M. K., and Péwé, T. L., 1986, Origin of land subsidence and earth fissuring, northeast Phoenix, Arizona: Association of Engineering Geologists Bulletin, v. 23, no. 2, p. 139–165.

Leonard, R. J., 1929, An earth fissure in southern Arizona: Journal of Geology, v. 37, no. 8, p. 765–774.

Linsley, R. K., Jr., Kohler, M. A., and Paulhus, J. L., 1949, Applied hydrology: New York, McGraw-Hill, p. 59–125.

Long, C. A., and Killingley, C. A., 1983, The badgers of the world: Springfield, Illinois, Charles C. Thomas, 404 p.

Machette, M. N., 1985, Calcic soils of the southwestern United States, in Weide, D. L. (ed), Soils and Quaternary geology of the southwestern United States, Geological Society of America Special Paper 203, p. 1–21.

Mark, D. M., 1974, Line intersection method for estimating drainage density: Geology, v. 2, no. 5, p. 235–236.

Markgraf, Vera, Bradbury, J. P., Forester, R. M., Singh, G., and Sternberg, R. S., 1984, San Agustin Plains, New Mexico: Age and paleoenvironmental potential reassessed: Quaternary Research, v. 22, p. 336–343.

McFadden, L. D., and Tinsley, J. C., 1985, Rate and depth of pedogenic-carbonate accumulation in soils: Formulation and testing of a compartment model, in Weide, D. L. (ed.), Soils and Quaternary geology of the Southwestern United States, Geological Society of America Special Paper 203, p. 23–41.

Metcalf, A. L., 1984, Distribution of land snails of the San Andres and Organ Mountains, southern New Mexico: The Southwestern Naturalist, v. 29, no. 1, p. 35–44.

Meteorology Research, Inc., 1979, Instruction manual IM-78, tipping bucket rain gauge: MRI, Altadena, California, 29 p.

Morton, D. M., 1977, Surface deformation in part of the San Jacinto Valley, southern California: U.S. Geological Survey Journal of Research, v. 5, no. 1, p. 117–124.

Mullican, W. F., III, and Senger, R. K., 1990, Hydrologic characterization of ground-water resources in south-central Hudspeth County, Texas: The University of Texas at Austin, Bureau of Economic Geology, report prepared for the Texas Low-Level Radioactive Waste Disposal Authority under Interagency Contract Number 90-008 IAC(90-91) 0268.

Parker, G. G., 1963, Piping, a geomorphic agent in landform development of the drylands: International Association of Scientific Hydrology, Publication 65, p. 103–113.

Phillips, J. D., Dean, D. F., and Riherd, P. S., 1986, Preliminary seismic reflection study of the Fort Hancock area in Hudspeth County, Texas: University of Texas at Austin, Institute for Geophysics, final report prepared for the Texas Low-Level Radioactive Waste Disposal Authority under contract number IAC(86-87)-0994, UTIG Technical Report TR-45, 44 p.

Reeves, C. C., Jr., 1976, Caliche—origin, classification, morphology and use: Lubbock, Texas, Estacado Books, 233 p.

Reid, Ian, and Frostick, Lynne E., 1989, Channel form, flows and sediments in deserts, in Thomas, D. S. G. (ed.), Arid zone geomorphology: New York, Halsted Press, p. 117–135.

Ritter, D. F., 1978, Process geomorphology: Dubuque, Iowa, William C. Brown, 603 p.

Robinson, G. M., and Peterson, D. E., 1962, Notes on earth fissures in southern Arizona: U.S. Geological Survey Circular 466, 7 p.

Satterwhite, M. B., and Ehlen, Judy, 1982, Landform-vegetation relationships in the northern Chihuahuan Desert, in Yaalon, D. H., (ed.), Aridic soils and geomorphologic processes: Proceedings, International Conference of the International Society of Soil Science, Jerusalem, Israel, March 29–April 4, 1981, Catena Supplement 1, p. 195–209.

Scanlon, B. R., 1990, Unsaturated flow along preferential pathways in the Chihuahuan Desert of Texas: The University of Texas at Austin, Bureau of Economic Geology, report prepared for the Texas Low-Level Radioactive Waste Disposal Authority under Interagency Contract Number 90-008 IAC(90-91) 0268.

Schumann, H. H., Cripe, L. S., and Laney, R. L., 1986, Land subsidence and earth fissures caused by groundwater depletion in southern Arizona, U.S.A., *in* Johnson, A. I., Carbognin, Laura, and Ubertini, L., (eds.), Land subsidence: Proceedings of the Third International Symposium on Land Subsidence, Venice, Italy, March 19–25, 1984, IAHS-AIHS, International Association of Hydrological Sciences Publication No. 151, p. 841–851.

Sellards, E. H., 1932, The Valentine, Texas, earthquake: University of Texas, Austin, Bulletin 3201, p. 113–138.

Sergent, Hauskins, and Beckwith, Consulting Geotechnical Engineers, 1989, Preliminary geologic and hydrologic evaluation of the Fort Hancock Site (NTP-S34), Hudspeth County, Texas, for the disposal of Low-Level Radioactive Waste: prepared for Hudspeth County, Texas, Hudspeth County Conservation and Reclamation District No. 1, Hudspeth County Underground Water Conservation District No. 1, El Paso County, Texas, SHB Job No. 388-4008B, v. 1 and 2.

Slaff, Steven, 1989, Patterns of earth-fissure development: examples from Picacho Basin, Pinal County, Arizona: Arizona Geology, v. 19, no. 3, p. 4–5.

Underwood, J. R., Jr., and DeFord, R. K., 1969, Large-scale desiccation fissures in alluvium, Trans-Pecos Texas and northern Chihuahua: Geological Society of America, Abstracts with Programs, v. 1, pt. 2, p. 31.

——————— 1975, Large-scale desiccation fissures in alluvium, Eagle Mountain area, *in* Geology of the Eagle Mountains and vicinity, Trans-Pecos Texas: Society of Economic Paleontologists and Mineralogists, Permian Basin Section Guidebook, Publication 75-15, p. 135–139.

Van Devender, T. R., and Spaulding, W. G., 1979, Development of vegetation and climate in the Southwestern United States: Science, v. 204, p. 701–710.

White, S. E., and Valastro, Salvatore, 1984, Pleistocene glaciation of Volcano Ajusco, Central Mexico, and comparison with the standard Mexican glacial sequence: Quaternary Research, v. 21, p. 21–35.

York, J. C., and Dick-Peddie, W. A., 1969, Vegetation changes in southern New Mexico during the past hundred years, *in* McGinnies, W. G., and Goldman, B. J. (eds.), Arid lands in perspective: Tucson, Arizona, University of Arizona Press, p. 155–566.
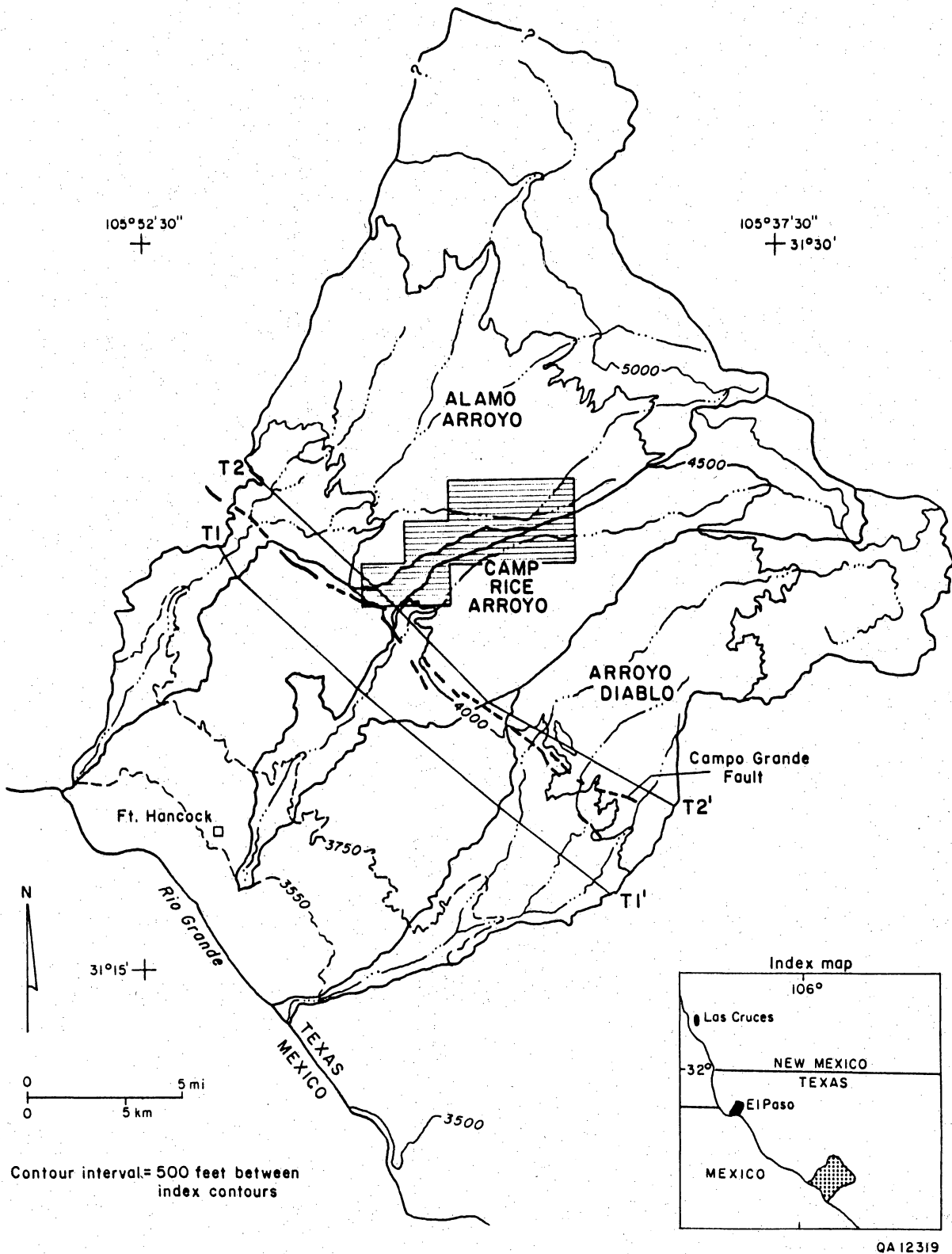
Figure 1. Map of major arroyo basins near Fort Hancock study area (shaded area), Hudspeth County, Texas. Cross-sections T1–T1′ and T2–T2′ are shown in figure 9.
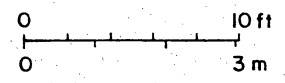
69
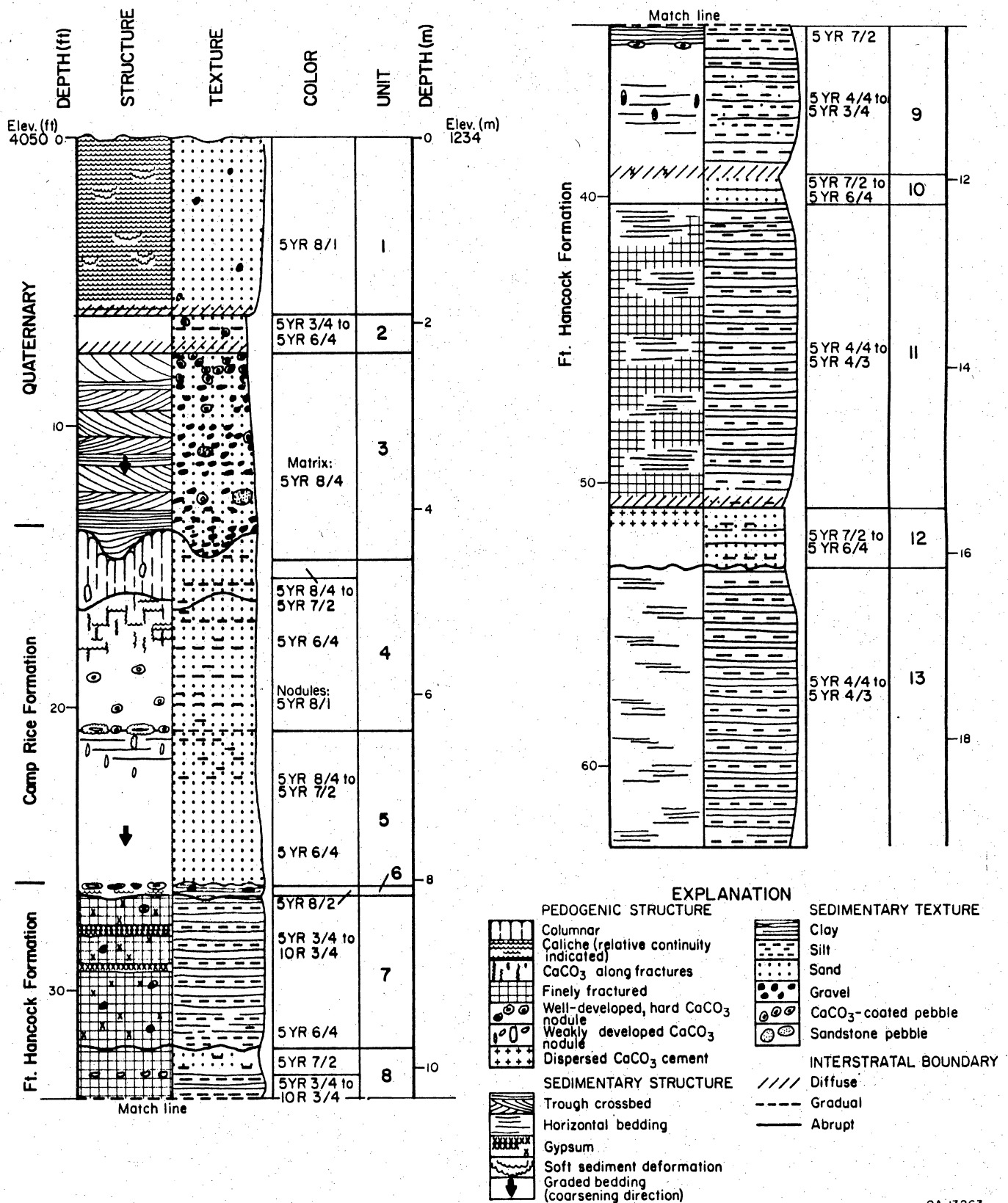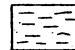
Figure 2. Measured section along valley wall of Camp Rice Arroyo near study area. The right-hand side of the texture column represents the weathering profile in outcrop: overhanging, recessive, convex, and concave.

70

Figure 3. General view of southeast wall of trench 3 at fissure 1. See figure 19 for location of trench.
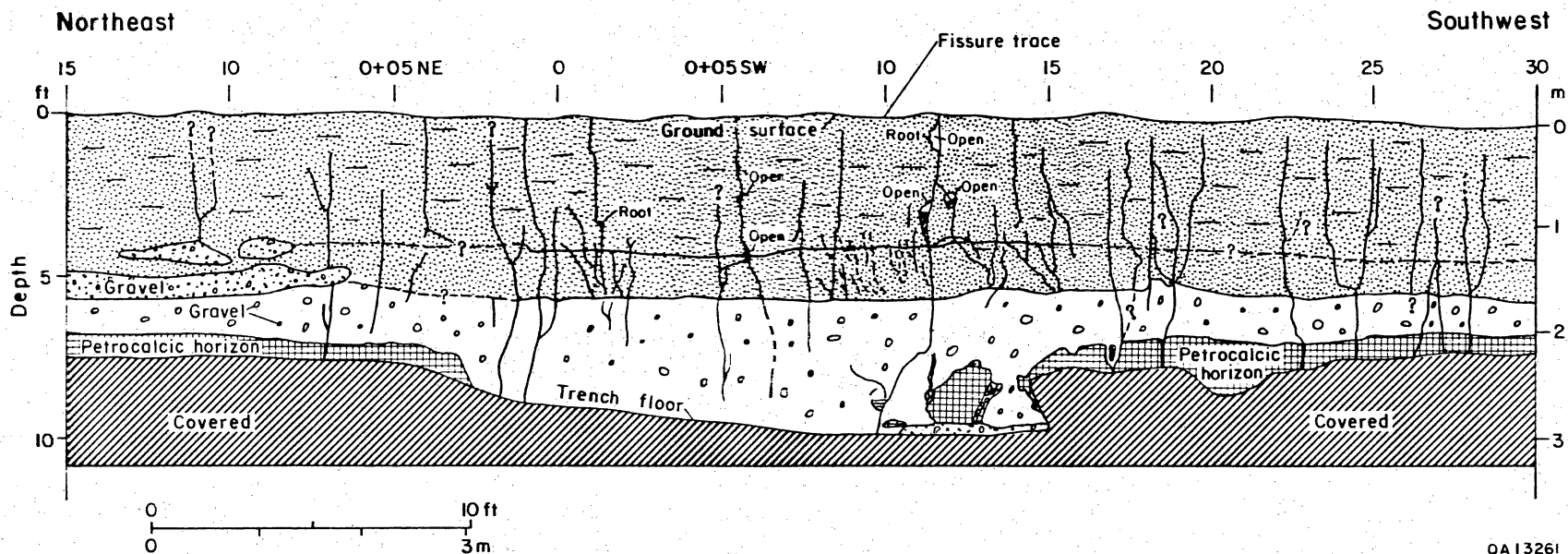
Figure 4. General view of southeast wall of trench 4 at fissure 1. Detailed sedimentary data are not shown in order to emphasize fractures. No fissure is visible here, but its interpolated position between adjacent collapse features is shown. The arbitrary numbering scheme for trench logging is shown in 5-ft intervals at top of figure. See figure 5 for sedimentologic details and figure 19 for location of trench.
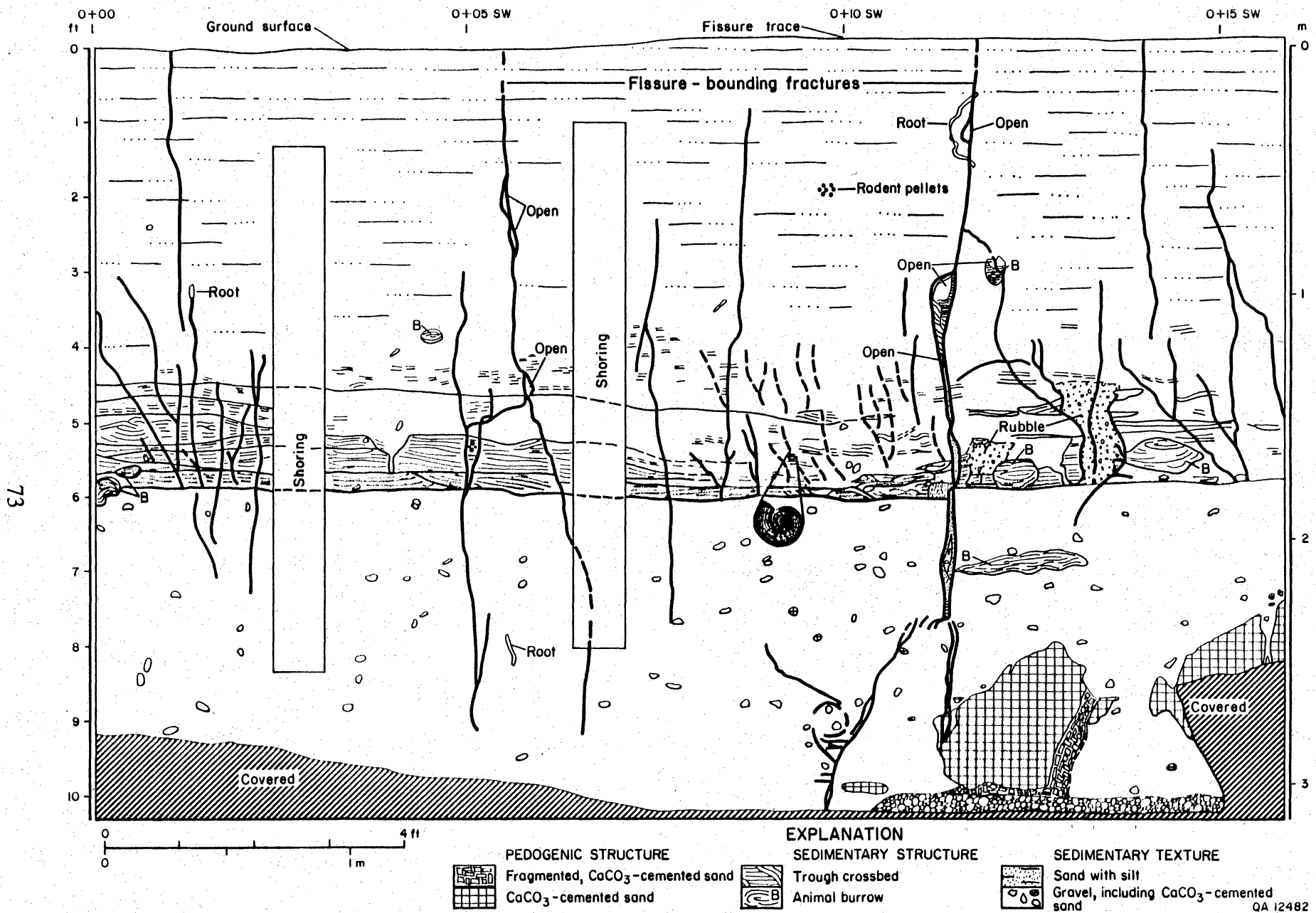
Figure 5. Detail map of southeast wall of trench 4 at fissure 1. See figure 19 for location of trench. Snail shown is *Hawaiia neomexicana*. Actual size of snail is 0.06 inch (1.5 mm) in diameter.
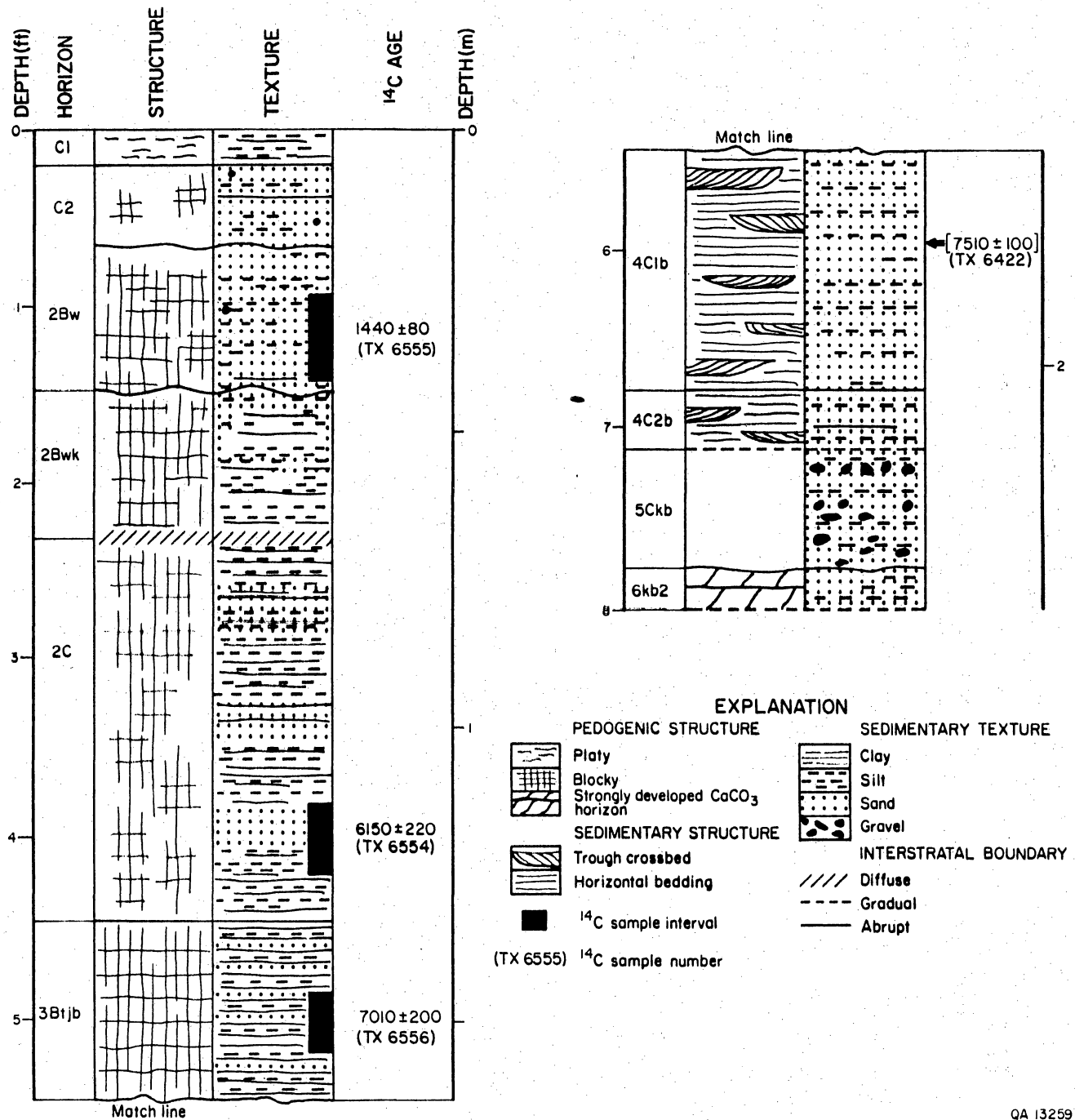
Figure 6. Strata with ¹⁴C dates near fissure 1. Stratigraphic column was described at 1+05 SW in trench 4, about 95 ft (29 m) south of the trace of the fissure. All but the oldest radiocarbon-dated samples were collected there (fig. 19). Oldest sample (TX 6422) was collected 22 inches (55 cm) above the petrocalcic horizon (6kb2), at a depth of 8.3 ft (254 cm), in trench 5 (fig. 19). Horizon 6kb2 corresponds to the Madden Gravel. Horizon designations and structural descriptions are from Sergent, Hauskins and Beckwith (1989, their table 3.4c).
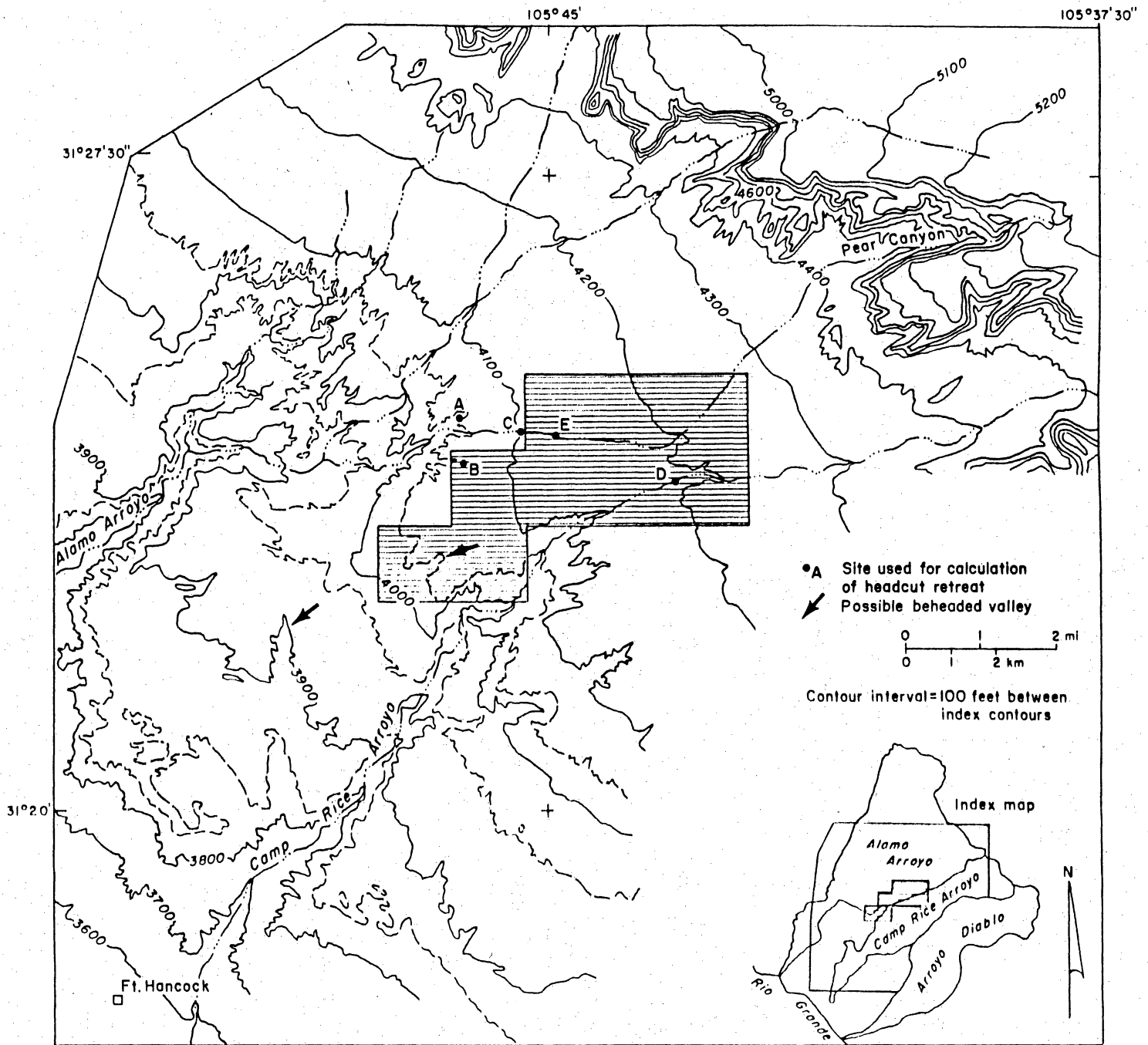
Figure 7. Map of vicinity of study area, showing locations used for calculating headcut retreat in gullies and arroyos. Shaded area is study area.

75
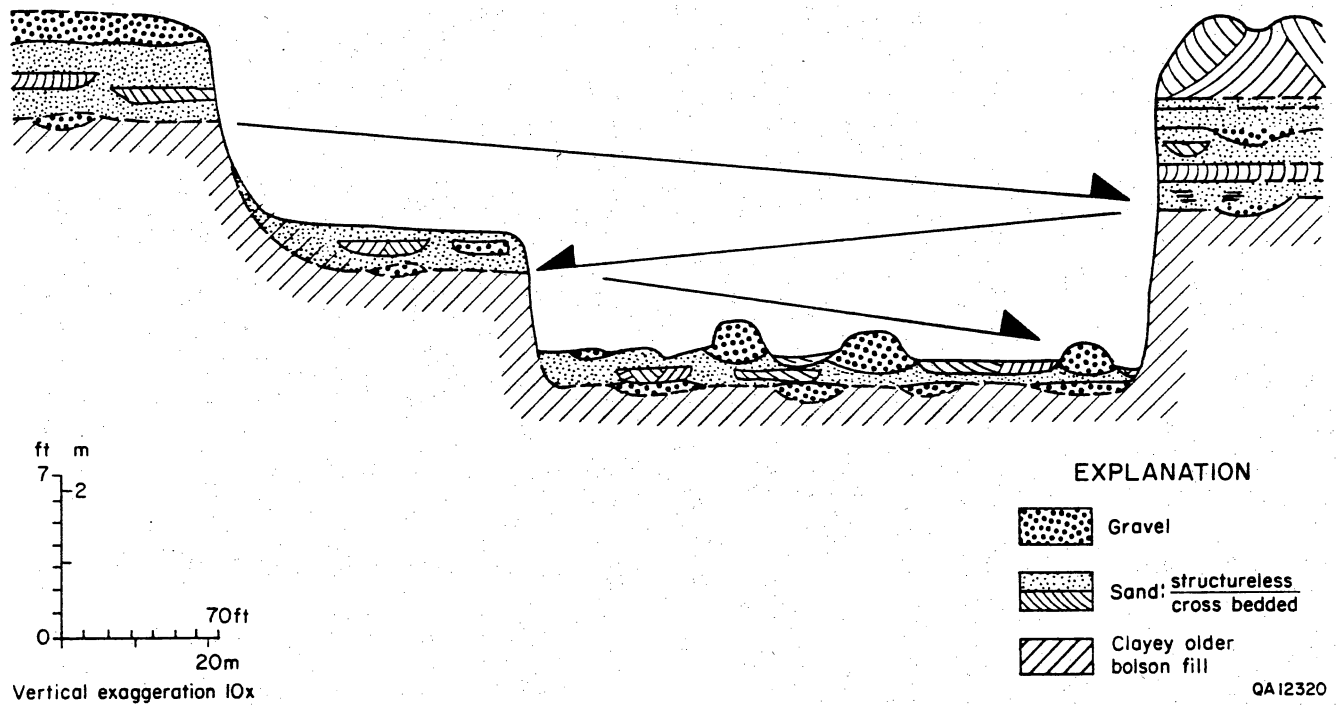
Figure 8. Terraces on Alamo Arroyo, 0.5 mi (0.8 km) upstream from Campo Grande fault. Terrace heights and bases of former channels alternate across the arroyo, indicating continual downcutting by the stream as it meandered across its valley. Arrows indicate direction of lateral movement by meandering stream during incision.
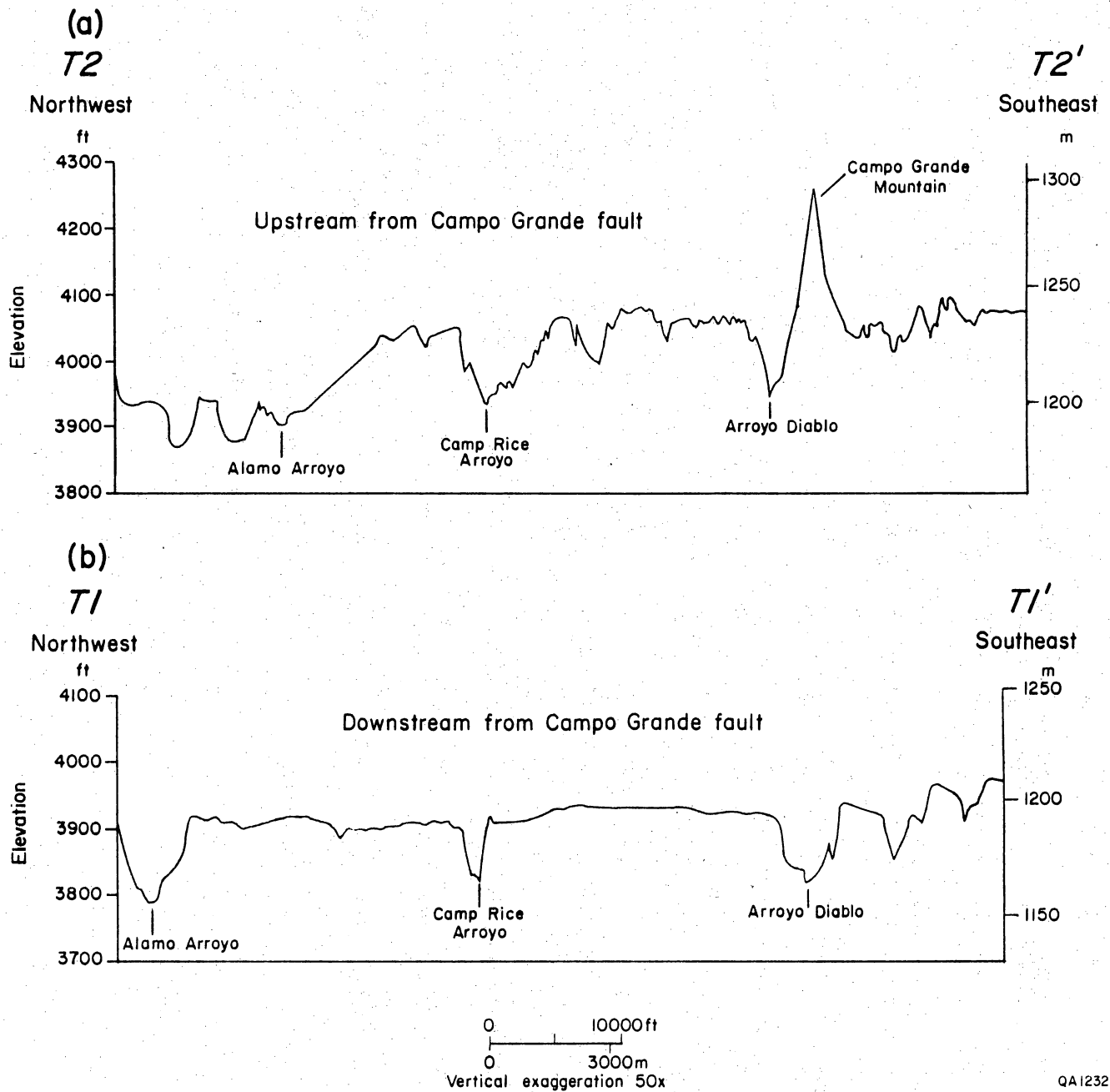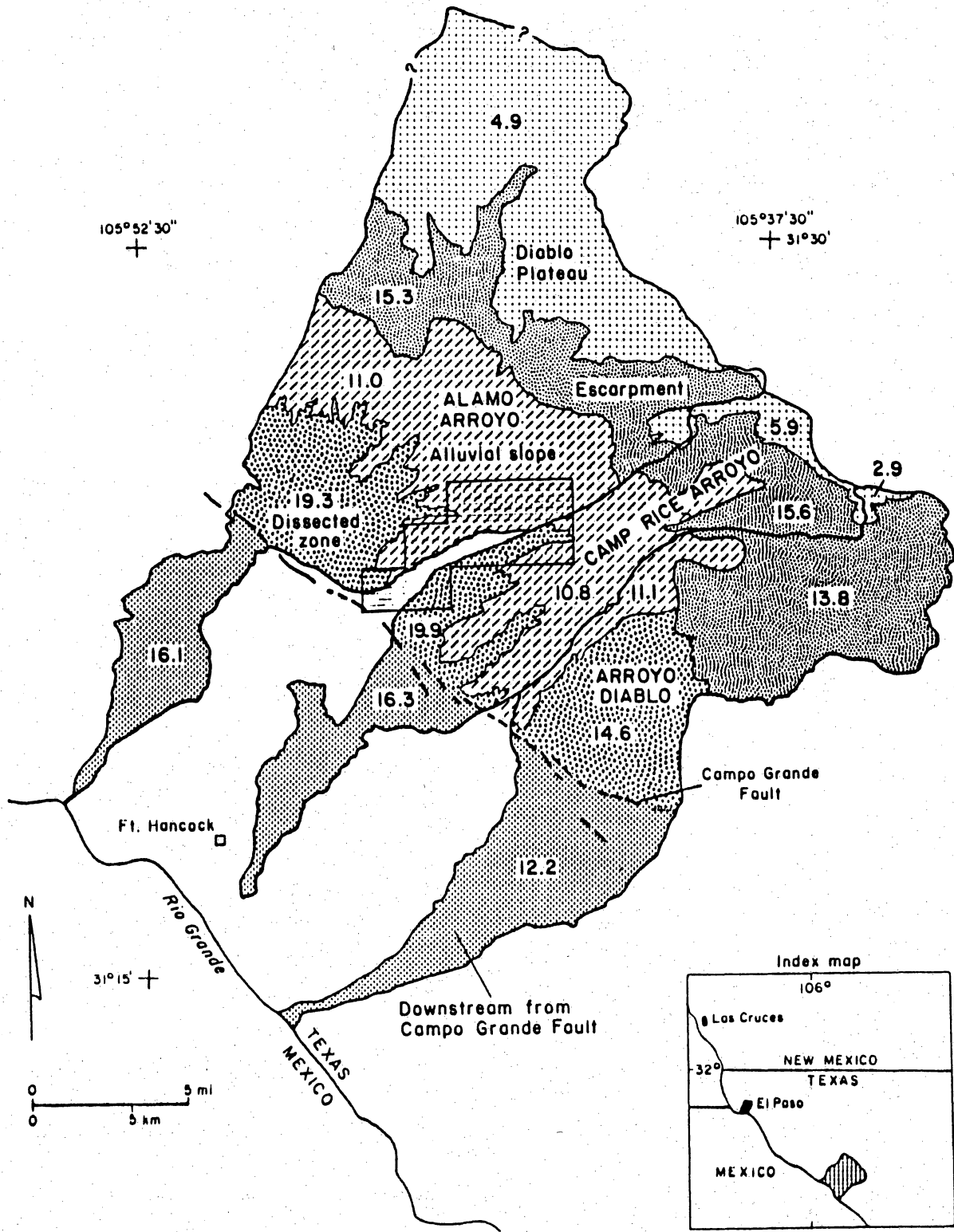
Figure 9. Transverse topographic profiles across major arroyo basins (a) upstream and (b) downstream from the Campo Grande fault. Location of profiles shown in figure 1.

Figure 10. Geomorphic zones in major arroyo basins, with values of drainage density (mi/mi^2) shown.

78
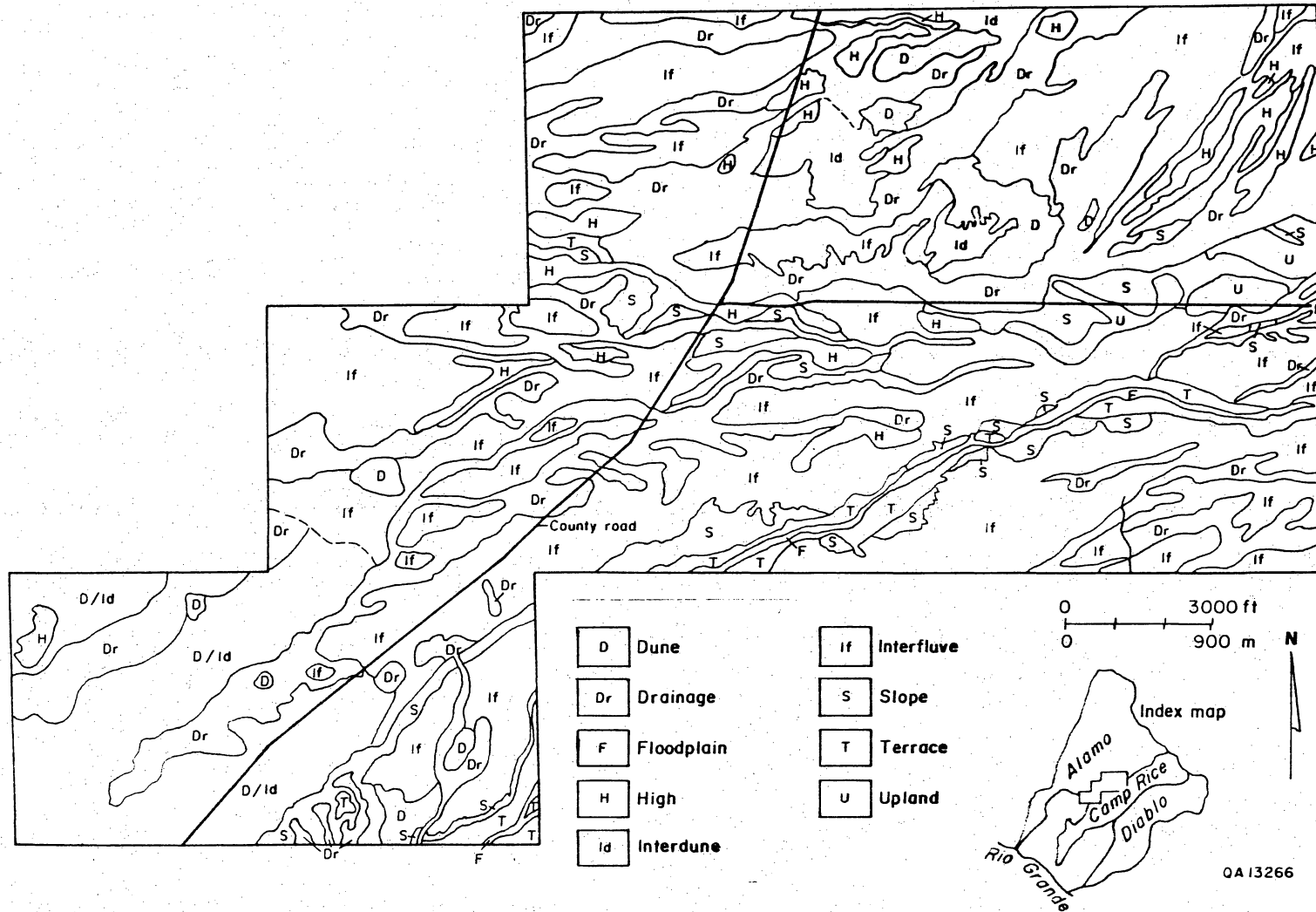
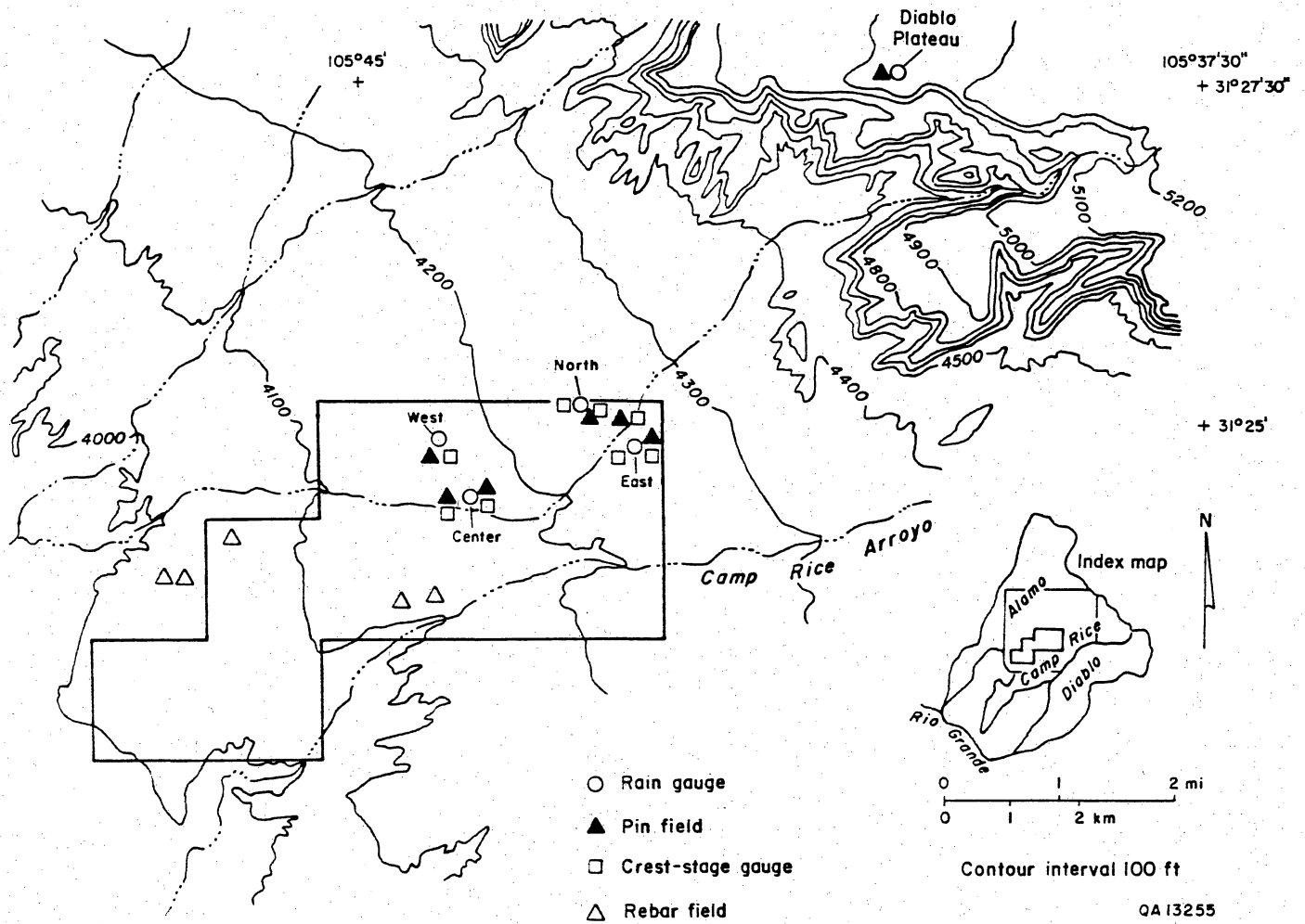**Figure 11.** Map of landforms in study area (fig. 7).

Figure 12. Map of erosion pin fields and rain gauges in study area. Center, Diablo Plateau, East, and West gauges were installed in July 1988. North gauge was installed in June 1988.
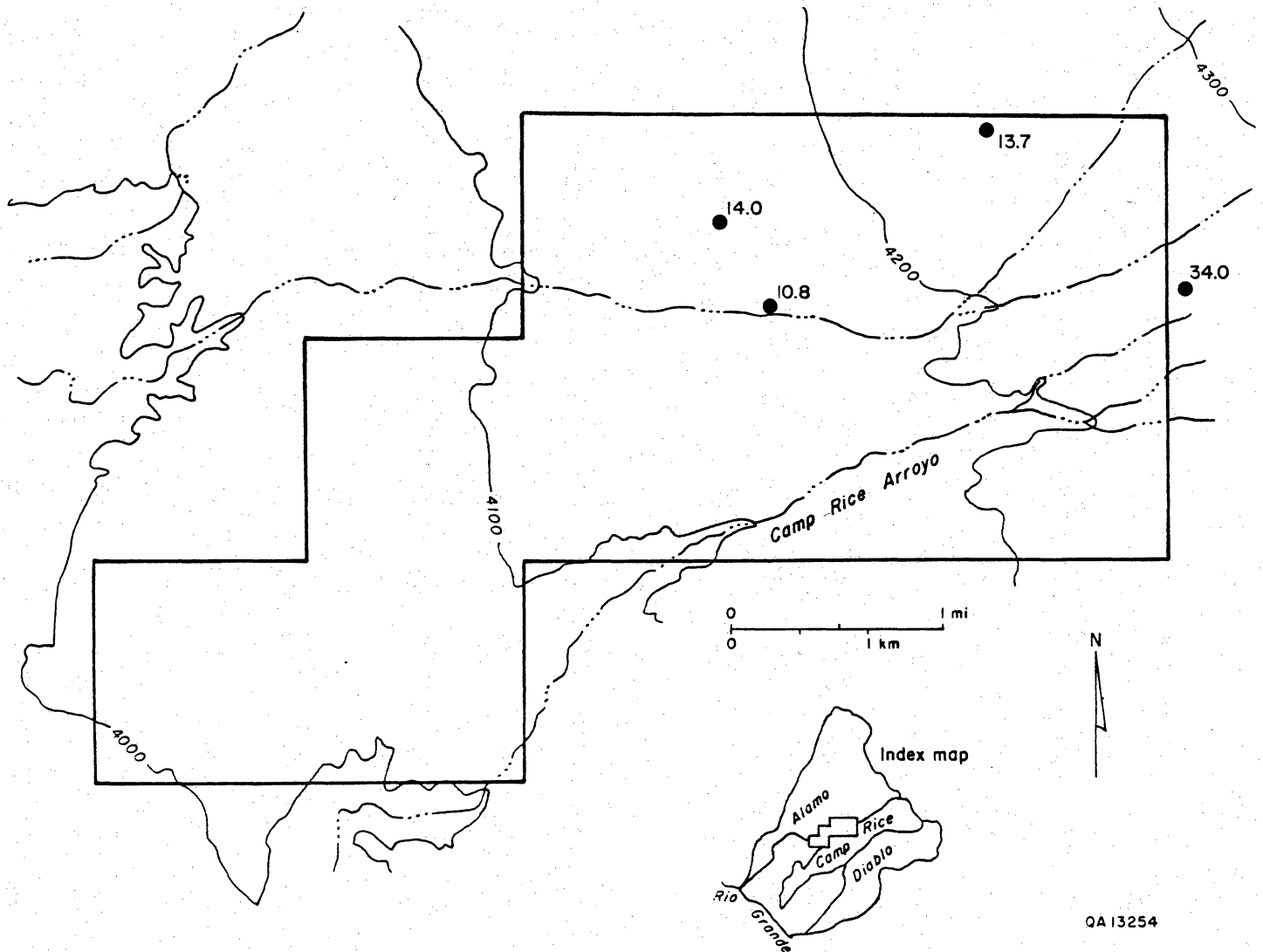
Figure 13. Maximum 0.5-hr rainfall amount (in mm) recorded at rain gauges in study area on July 29, 1988. No data are available for rain gauge on Diablo Plateau for this date. The East rain gauge was moved on August 10, 1988, to the location shown on figure 12.
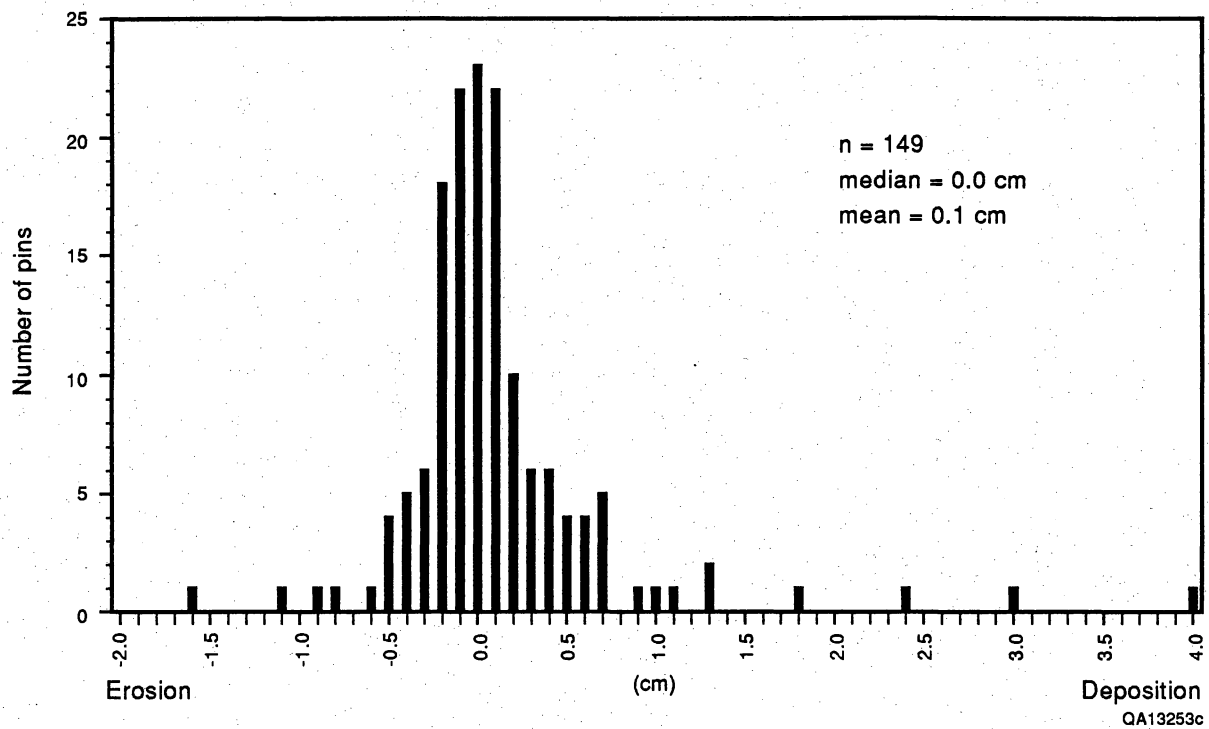
Figure 14. Graph of cumulative erosion and deposition at erosion pins. Highest values are for deposition, but mean and median values are near zero. Most measurements larger than |0.02 inch| (|0.5|) mm occurred within a month following the most intense rainfall events.
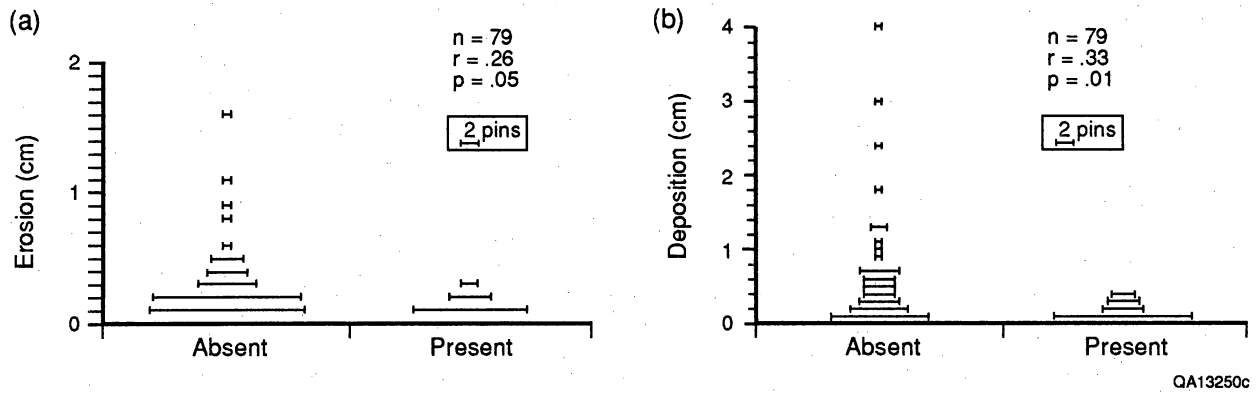
Figure 15. Erosion and deposition versus lichen crust. (a) Erosion versus lichen crust. (b) Deposition versus lichen crust. Both erosion and deposition are positively correlated with absence of lichen crust, indicating that the crust is usually found on a stable surface.
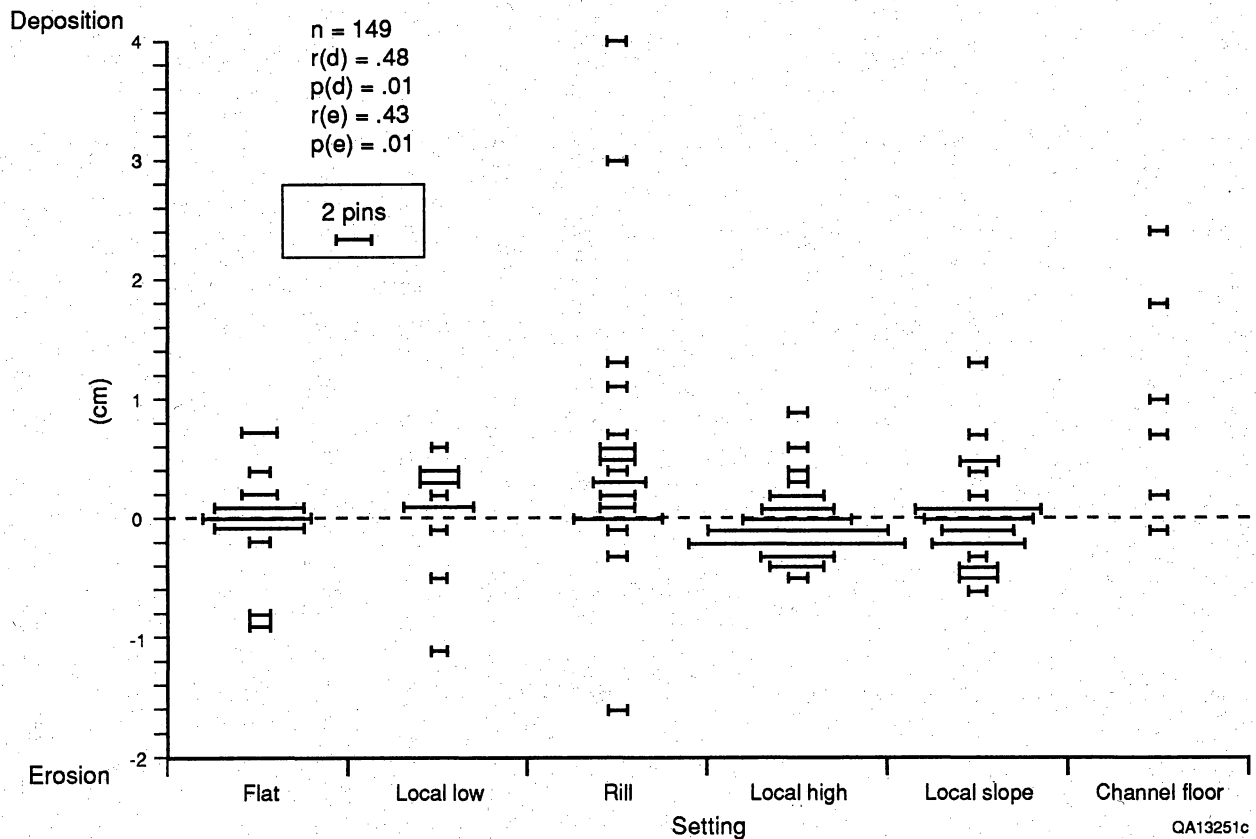
Figure 16. Deposition and erosion versus local settings of erosion pins. Highest values for deposition occur in rills and on channel floors. Highest values of erosion occur in rills, local lows, and on flat areas. Apparently, rills are the most active zones of sediment movement, undergoing both erosion and deposition locally, although net change during the monitoring period was generally negligible. Correlation coefficient for linear regression of deposition versus setting, r(d), is the highest in this study, and is significant at the p(d) = .01 level. For erosion versus setting, the correlation coefficient, r(e), is equally significant, p(e) = .01.
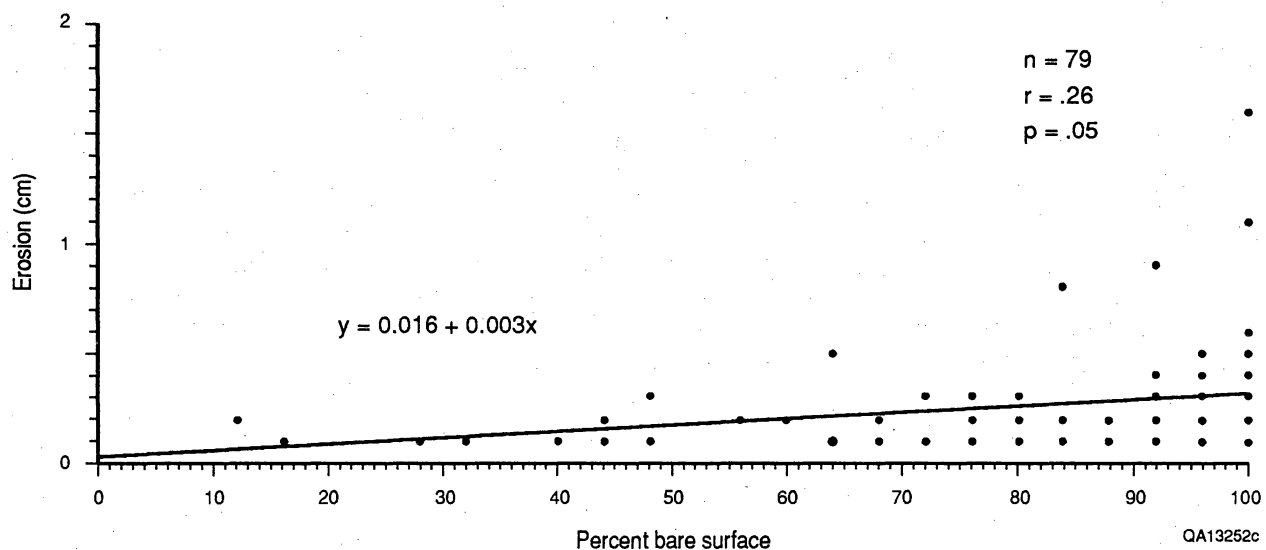
Figure 17. Erosion versus percent bare surface at erosion pins. Whereas erosion is positively correlated with percent bare surface, the correlation coefficient is low (r = .26) and significant at the .05 level.
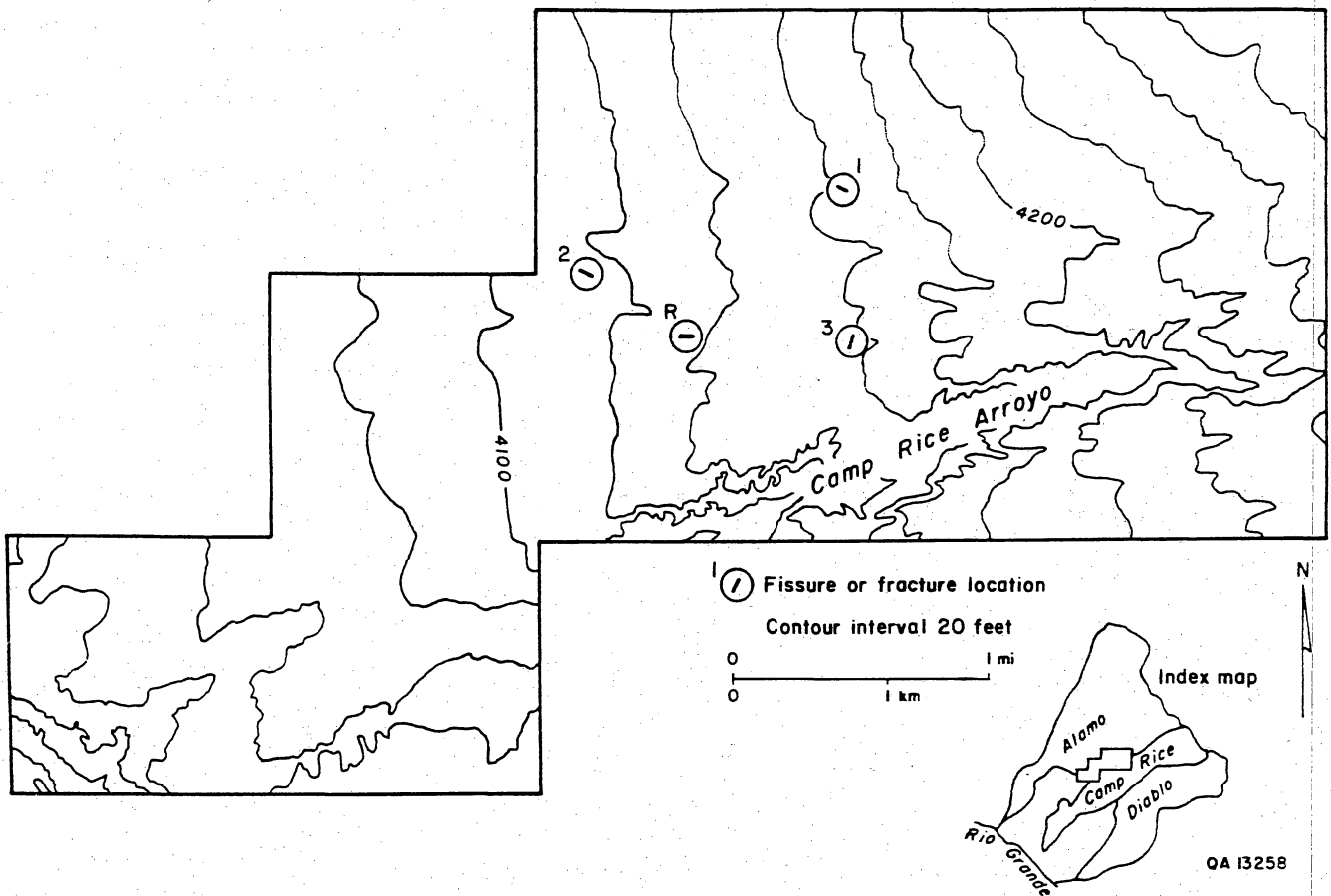
Figure 18. Map of fissures and fracture at study area (fig. 7). Fissure numbers are referred to in the text. Line within each circle represents orientation of that feature. Orientations are as follows: fissure 1 = N55°W, fissure 2 = N50°W, fissure 3 = N20°E, relict fracture = N85°E. Length is not to scale. Fracture marked with R is relict; no surface-collapse features are present at the surface there. This fracture was exposed in a 20-ft (6-m) deep trench.
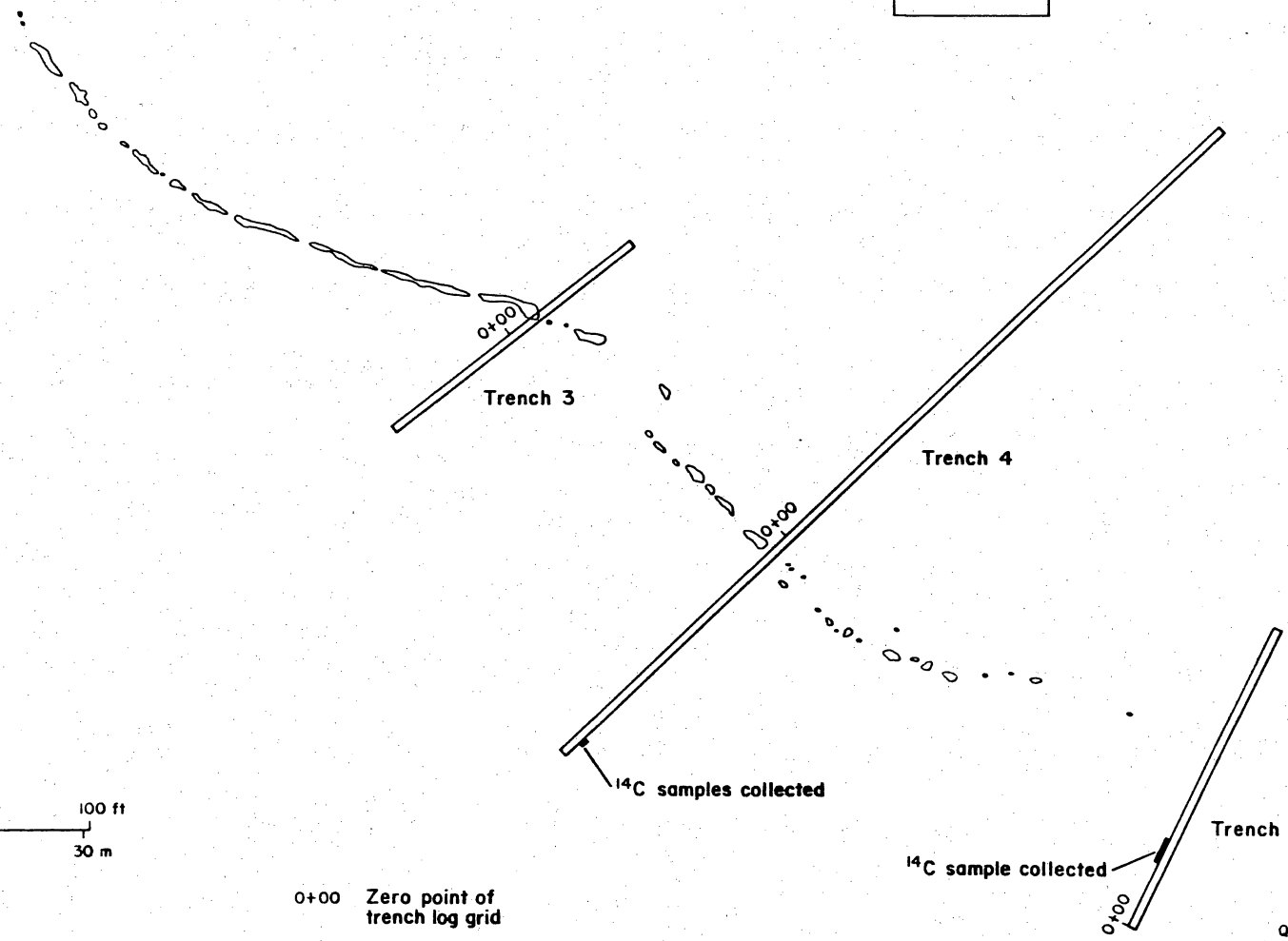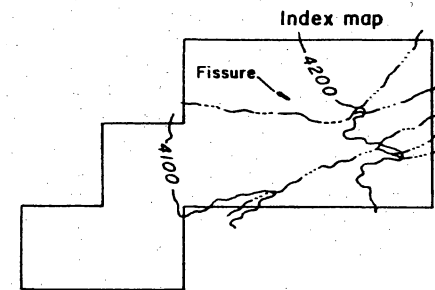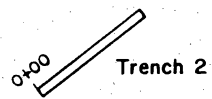
Figure 19. Map of fissure 1 and trenches. Trench 1, about 100 ft (30 m) northwest of trench 2, is not shown. Inset map derived from figure 18. After Sergent, Hauskins and Beckwith (1989, their fig. 7.1).
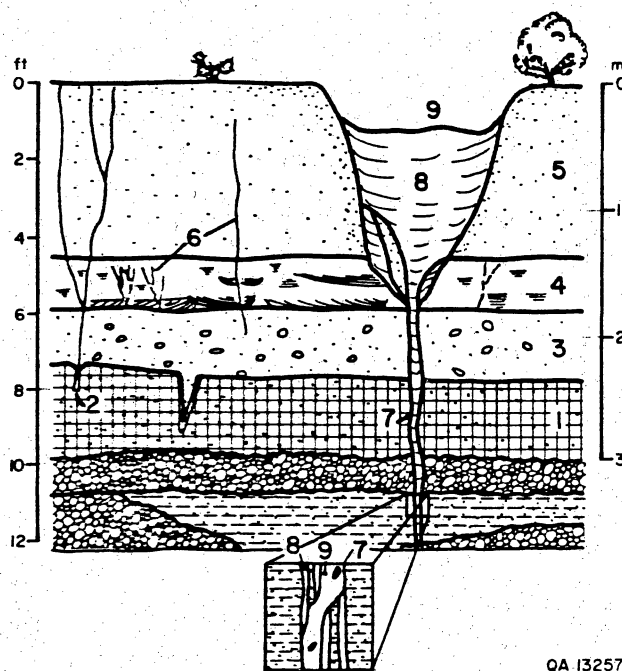
Figure 20. Schematic cross section of fissure 1. 1 = Stage III to IV petrocalcic horizon; 2 = fracture in petrocalcic horizon; 3 = poorly sorted, massive gravelly sand; 4 = crossbedded sand; 5 = structureless silty sand; 6 = fractures; 7 = tension fracture, precursor to fissure; 8 = sediment-filling surface-collapse feature and (inset) fracture; 9 = evidence of continued collapse. Subsidence at surface and (inset) sediment filling between walls of original fracture and older fracture fill.
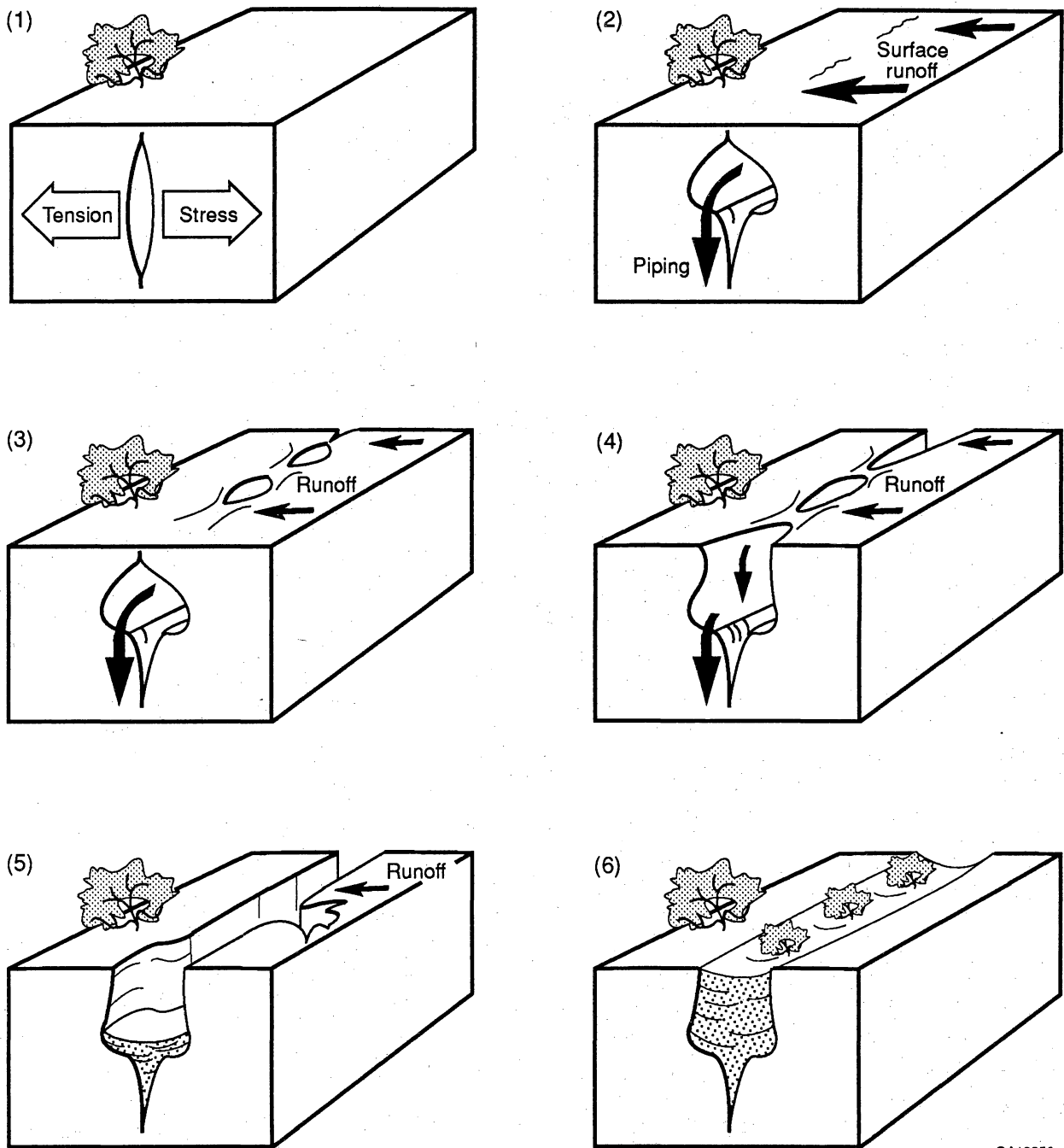
Figure 21. Block diagrams depicting fissure evolution. 1 = Tensional stress induces fracturing; 2 = runoff enters surface fracture, widening it by erosion; water moves laterally along the fracture, eroding a soil pipe, and moves downward into the fracture; 3 = surface fractures are enlarged by erosion, surface-collapse features form; 4 = surface-collapse features capture more runoff and erode laterally; 5 = surface-collapse features coalesce, forming a linear fissure, and fracture fills with sediment; 6 = fracture and fissure fill with sediment. Vegetation along the fissure trace is more vigorous due to greater availability of water. After Larson and Péwé (1986, their fig. 7).

89
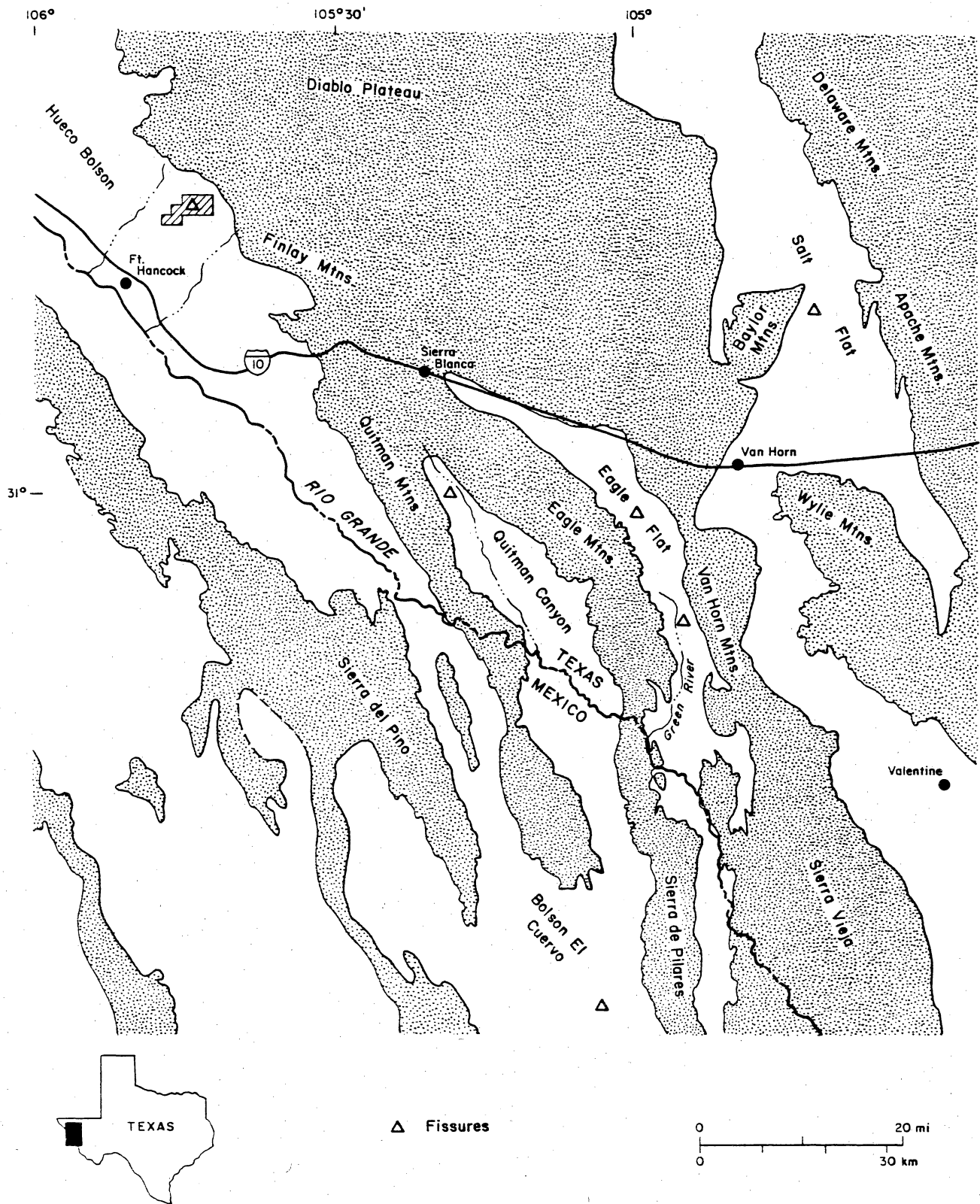
Figure 22. Map of fissures in region of the study area that have been reported in the literature. The boundary between basins and bedrock outcrops (stippled) is generalized from Direccion General de Geografia (1982) and Henry and others (1985).

90

Table 1. Average interstratal accretion rates of Quaternary sediments at the Hudspeth County study area.*

Depth[†] (cm)	Depth difference	^{14}C age (yr B.P.)	Age difference	Accretion rate (mm/yr)	Location
0		0			
	34		1,440	0.24	
34		1,440±80			Tr[‡] 4, 1+05 SW
	85		4,710	0.18	
119		6,150±220			Tr 4, 1+05 SW
	31		860	0.36	
150		7,010±200			Tr 4, 1+05 SW
	104		500	2.08	
254		7,510±100			Tr 5, 0+22 to 0+32 NE

*The rate for each sample is calculated by first subtracting the ages and depths from two adjacent samples. The difference in depths is then divided by the difference in ages. The rate represents the average annual rate of sedimentation between the centers of two samples. The rate after 7,010±200 yr B.P. is much lower than the rate before that time. For location of sampling sites see figure 19.

[†] Depth to center of sampled interval. See figure 6 for thickness of sample.

[‡] Tr = Trench

Table 2. Values of drainage density (mi/mi^2) for geomorphic zones in arroyo drainage basins.*

Geomorphic zone of arroyo basin

Arroyo name	Downstream from fault	Dissected zone	Alluvial slope	Escarpment	Diablo Plateau
Alamo	16.1	19.3	11.0	15.3	4.9
Camp Rice	16.3	19.9	10.8	15.6	5.9
Diablo	12.2	14.6	11.1	13.8	2.9

*Geomorphic zones are listed in order proceeding upstream from the basin mouth to the Diablo Plateau. See figure 10 for boundaries between geomorphic zones.

Table 3. Vegetation and surface sediment on landforms in study area.*

Landform	Creosote	Mesquite	Tarbush	Yucca/ cactus	Grass/ forbs	Other	Surface sediment Gravel	Sand
Dunes	10–45	40–70	5–10	1–10	5–10	10	0–50	50–90
Drainage	0–95	0–20	5–80	5	0–90	≤5	0–70	≤90
Floodplain	—	—	—	—	—	—	—	—
High, topo.	90	5	—	—	—	5	40–90	10–60
Interdune	75–90	~20	—	—	5–10	10	5–80	20–90
Interfluve	50–95	1–30	5–10	5	2–10	5	1–80	20–90
Slope	~90	1–5	—	5	5	—	20–40	60–80
Terrace	≤90	0–20	—	—	—	—	0–70	≤90
Upland	~80	~10	—	≤5	≤5	≤10	70–95	5–30

*Numbers represent percent of total for components listed as determined by visual estimate. These components do not represent all vegetation types or grain sizes present. A dash indicates that no observation is available for that item.

93

Table 4. Maximum rainfall events at each gauge in study area for July 15, 1988, through December 31, 1989, and the corresponding recurrence interval.*

Gauge location	Rainfall lasting 0.5 hr			Rainfall lasting 1 hr			Rainfall lasting 24 hr		
	Maximum amount (mm)	Recurrence interval (yr)[†]	Date of occurrence	Maximum amount (mm)	Recurrence interval (yr)[†]	Date of occurrence	Maximum amount (mm)	Recurrence interval (yr)[†]	Date of occurrence
Center	16.4	<2	07/19/88	23.8	2	07/19/88	24.8	<1	07/19/88
Diablo Plateau	19.2	2	08/03/89	23.4	2	08/03/89	27.2	<1	07/30/89
East	34.0	25	07/29/88	36.0	10	07/29/88	38.6	2	07/29/88
North (A&M)	28.5	10	08/12/89	33.5	5	08/12/89	37.3	<2	08/12/89
West	18.0	2	07/19/88	30.0	<5	07/19/88	30.6	1	07/19/88
El Paso[‡]				36.8	10	07/04/61	165.1	>100	07/1881
	44.5	100		55.9	100		101.6	100	

*Except for Diablo Plateau gauge, the three maxima at each gauge occurred on the same date. If the Diablo Plateau gauge had functioned during July 1988, its maxima might have been recorded then. The magnitudes of rainfall events that would have 100-yr recurrence intervals are presented for comparison.

[†] Source: Hershfield (1961), based on data through 1958.

[‡] Source: J. R. Scoggins, Texas A&M University, written communication, 1989. One-hr maximum is for 1951–1988, 24-hr maximum is for 1879–1988.

Table 5. Record of erosion pin monitoring during study.*

Date pins measured	Maximum 1-hr rainfall (mm)
07/15/88	Pins installed
08/10/88	36.0
09/13/88	19.2
01/17/89	6.0
06/04/89	7.4
08/21/89	23.4
09/26/89	17.0

*Maximum 1-hr rainfall is that recorded at one of four rain gauges (data from the North gauge were not available in the field on the days when other gauges were monitored) during the period between measurement dates. Pins were measured in January and June 1989 because 4 months had passed since the previous measurement.

Table 6. Rates of headcut retreat in gullies and arroyos determined by different methods.*

a. Radiocarbon-Dating Organic Material in Arroyos.

Location	Description of dated material	Distance (m)	Period (yr B.P.)	Rate of retreat (m/yr)
A	carbonized wood	1,320	920±70	1.3 to 1.6
B	soil organic matter	175	400±70	0.4 to 0.5
C	soil organic matter	50	1,330±60	0.04

b. Photointerpretation of Headcut Retreat Between 1941 and 1985. (Period used for calculating rates of retreat is 44 yr.)

Location	Drainage area (km²)	Distance (m)	Rate of retreat (m/yr)
A	11.9	310	7.0
B	1.9	115	2.6
C	30.9	95	2.2
D	37.8	365	8.3
E†	29.9	45	1.0
gullies	various	150 (mean)	3.4 (mean)

*See figure 7 for locations. The distance of retreat at location C is greater for the period 1941 to 1985 than for 1,330±60 yr B.P. because the present-day distance between outcrop and headcut was used at all radiocarbon sites to compute comparable rates of retreat. At location C, the dated outcrop is only 50 m downstream from the headcut, but vintage photographs document 95 m of headcut retreat between 1941 and 1985.

† Headcut at E is in a Stage IV petrocalcic horizon.

Table 7. Aerial photographs used for mapping changes in headcuts and gullies on Alamo Arroyo and Camp Rice Arroyo in study area.

Vintage	Scale
1941	1:31,680
1971*	1:16,000
1974*	1:31,400
1985	1:13,680[†]

*Partial coverage of area, no overlap. In general, Alamo Arroyo covered by 1971 vintage, Camp Rice Arroyo covered by 1974 vintage.
[†]Scale of this vintage varies. Scale shown is for the photos used in this comparison.

Table 8. Fissures reported in the Basin and Range province of West Texas and northeastern Chihuahua.*

Location	Length (m)	W/D ratio	Geologic unit	Date formed	Source
Bolson El Cuervo	—	—	Bolson deposits	pre-1965	5, 6
Eagle Flat	65	0.4	Alluvium	1927 or 1928	6, 7
Eagle Flat	—	2.7	Alluvium	1927 or 1928	6, 7
Eagle Flat	910	28	Alluvium	1927 or 1928	6, 7
Green River	740	—	Bolson deposits	pre-1927, 1959	2, 7
Quitman Canyon	4,200	0.2 to 5	Alluvium	1924	1, 7
Salt Flat	800	—	Lacustrine deposits	pre-1946	3, 4
Study area	140	0.2 to 2	Alluvium	1971–1985	this study

*Width/depth (W/D) ratio increases as the fissure is widened by erosion and filled with sediment. Higher values denote older or less active fissures.

— No measurement.

Sources: 1=Albritton and Smith (1965); 2=Baker (1927); 3=Goetz (1977); 4=Goetz (1985); 5=Haenggi (1966); 6=Underwood and DeFord (1969); and 7=Underwood and DeFord (1975).